

**METHODS FOR HIGH THROUGHPUT SINGLE CELL ANALYSIS
THROUGHOUT INTACT HUMAN BRAIN ORGANIDS**

A Dissertation
Presented to
The Academic Faculty

by

Corey Raymond Landry

In Partial Fulfillment
of the Requirements for the Degree
Doctor of Philosophy in Biomedical Engineering

Georgia Institute of Technology
Emory University
Peking University
December 2021

COPYRIGHT © 2021 BY COREY LANDRY

**METHODS FOR HIGH THROUGHPUT SINGLE CELL ANALYSIS
THROUGHOUT INTACT HUMAN BRAIN ORGANIDS**

Approved by:

Dr. Craig R. Forest, Advisor
George W. Woodruff School of
Mechanical Engineering
Georgia Institute of Technology

Dr. Matt Rowan
Department of Cell Biology
Emory University

Dr. Zhexing Wen
Departments of Psychiatry and Behavioral
Sciences, Cell Biology, and Neurology
Emory University

Dr. Yong Zhang
IDG/McGovern Institute for Brain
Research
Peking University

Dr. Alysson Muotri
Departments of Pediatrics & Cellular
Molecular Medicine
University of California, San Diego

Dr. Bilal Haider
Coulter Department of Biomedical
Engineering
Georgia Institute of Technology

Date Approved: December 7, 2021

To Meygan, my wife and best friend

ACKNOWLEDGEMENTS

A Ph.D. is invariably a long and winding journey full of challenge and excitement. Mine has been especially so. I would like to take this time to reflect and thank all of the people who helped me to get to this point. First and last, to my amazing wife, Meygan. You have been the source of so much joy, encouragement, and purpose in my life. I could write an entire thesis on how much you mean to me. You've been such an incredible best friend and I'm so excited for this next stage of our lives. Through the highs and lows, you have been a constant source of love and support. Thank you for always believing in me.

Next, I would like to thank my advisor, Dr. Craig Forest, who has been a constant support through the highs and lows of graduate school. I've learned so much from you and I'm forever grateful to you for always being in my corner. To my committee members, each of you have helped me in important ways to become the engineer and scientist that I am today. Thank you for your support, advice, and expertise along the way. To my lab mates, collaborators, family, and friends, thank you for being a constant source of help, ideas, and encouragement. It has been an incredible journey and I can't imagine going through it with a better group of people. I also could never have done any of this without the unconditional love and support of our two rescue dogs, Lucy and Winnie, who are a constant source of love and laughter.

TABLE OF CONTENTS

ACKNOWLEDGEMENTS	iv
LIST OF TABLES	viii
LIST OF FIGURES	ix
LIST OF SYMBOLS AND ABBREVIATIONS	xvi
SUMMARY	xvii
CHAPTER 1. Introduction	1
1.1 Background	1
1.1.1 Human brain organoids	1
1.1.2 Biological self-assembly of complex tissues	3
1.1.3 Intracellular electrophysiology	5
1.1.4 Steps of the whole cell patch clamp method	7
1.1.5 Automation of patch clamp electrophysiology	8
1.1.6 Morphological reconstruction of neuron structure	9
1.2 Motivation	11
1.2.1 Human brain organoids as a model system for neuroscience	11
1.2.2 Challenges of single cell experiments in intact human brain organoids	12
CHAPTER 2. Enzymatic Cleaning and Reuse of Patch Pipettes	15
2.1 Introduction	15
2.1.1 Chemical and enzymatic removal of cellular debris from pipettes	16
2.1.2 Pipette cleaning as an enabling technology	17
2.1.3 Pipette replacement as a bottleneck for automated patch clamp experiments	18
2.1.4 Methods development for patch clamp experiments	18
2.2 Methodology	19
2.2.1 Patch clamp hardware	19
2.2.2 Fully automated patcherBot software	20
2.2.3 Push-to-clean software for automated pipette cleaning	20
2.2.4 Pipette cleaning procedure	21
2.2.5 Cell culture methods	22
2.2.6 Single-blinded experimental design	23
2.2.7 Cleaning limits experimental design	25
2.2.8 Opsin screening experimental design	26
2.3 Results and Discussion	26
2.3.1 Tergazyme is superior to Alconox for pipette cleaning	26
2.3.2 Tergazyme cleaning enables over 100 patch clamp recordings with a single pipette	28

2.3.3	Tergazyme cleaning enables high throughput automated characterization of opsins	29
2.3.4	Future applications of Tergazyme pipette cleaning	30
CHAPTER 3. Patch Clamp Recordings in Intact Human Brain Organoids		34
3.1	Introduction	34
3.1.1	Patch clamp methods in human brain organoids	34
3.1.2	Electrophysiology approaches for intact tissues	36
3.1.3	Electrophysiological development in human brain organoids	39
3.1.4	Challenges for patch clamp recordings in intact human brain organoids	40
3.2	Methodology	41
3.2.1	Fixturing of intact human brain organoids for patch clamp experiments	41
3.2.2	Patch clamp methods for intact human brain organoids	42
3.2.3	Manual patch clamp methods for intact human brain organoids	44
3.2.4	Automated patch clamp methods for intact human brain organoids	44
3.3	Results and Discussion	45
3.3.1	Fixturing of intact human brain organoids for patch clamp experiments	45
3.3.2	Performance of manual and automated patch clamp in intact human brain organoids	47
3.3.3	Electrophysiological properties of intact human brain organoid cells	51
3.3.4	Challenges of interpreting data from intact human brain organoid recordings	54
CHAPTER 4. Single Cell Electrophysiology and Morphology in Intact Human Brain Organoids		57
4.1	Introduction	57
4.1.1	Limitations of blind patch clamp in intact human brain organoids	57
4.1.2	Neuronal morphology methods	58
4.1.3	Tissue clearing for imaging of intact tissues	58
4.1.4	Classification of neurons using electrophysiology and morphology	59
4.2	Methodology	60
4.2.1	Delivery of intracellular dye during patch clamp experiments	60
4.2.2	CUBIC tissue clearing of intact human brain organoids	62
4.2.3	Correlation of labelled cells with patch clamp recordings	66
4.2.4	Morphological tracing of labelled cells	69
4.2.5	Preliminary classification of organoid cells by electrophysiology and morphology	70
4.3	Results and Discussion	70
4.3.1	Yield and efficacy of detecting filled cells	70
4.3.2	Electrophysiology of labelled cells	73
4.3.3	Organoid clearing	76
4.3.4	Morphology of labelled cells	76
4.3.5	Preliminary classification of recorded cells from intact human brain organoids	77
4.3.6	Putative neurite recordings from intact human brain organoids	78
4.3.7	Challenges of interpreting data from electrophysiology and morphology in intact human brain organoids	79

CHAPTER 5. Conclusion	81
5.1 Major Contributions	81
5.2 Perspectives	82
5.2.1 The Future of Automated Patch Clamping	82
5.3 Future Directions	83
5.3.1 Improving neuronal yield in intact organoid recordings	83
5.3.2 Improving Throughput of Imaging and Reconstruction of Organoid Cells	85
5.3.3 Integrating Immunohistochemistry Methods in Single Cell Intact Organoid Experiments	85
5.3.4 Delivery and Extraction of Genetic Material for Multimodal Single Cell Studies	86
5.3.5 Longitudinal Studies of Disease and Development Using Human Brain Organoids	87
APPENDIX A. Ethical Implications of Brain Organoid Research	89
Utility of proposed work	89
APPENDIX B. Detailed Protocol for Enzymatic Pipette Cleaning	91
Materials and reagents	91
Equipment	91
REFERENCES	104

LIST OF TABLES

Table 1	Methods for patch clamp recordings in human brain organoids.	36
Table 2	Compatibility of intracellular dyes with CUBIC L/R	61

LIST OF FIGURES

- Figure 1 Biological self-assembly produces complex tissues. A) Scrambled and reassembled kidney showing micrograph showing features of complex tissue including cortex (C), medulla (M), pelvis like cavity (P), radial collecting tubes (T), and openings for radial collecting tubes into the pelvic area (O). Image modified from (P. Weiss & Taylor, 1960). B) Brain organoid (60 DIV) showing bilateral, pigmented optic cups. Scale bar is 1 mm. C) Rate of bilateral optic cup formation is high across multiple cell lines and batches of organoids. Images modified from (Gabriel et al., 2021). 3
- Figure 2 Overview of the whole cell patch clamp method. A) Schematic of the steps of a whole cell patch clamp experiment showing approaching the cell, forming a gigaseal, and rupturing the seal to form the whole cell recording configuration. Image modified from (Segev et al., 2016). B) Electrophysiology rig used to perform automated patch clamp recordings using the patcherBot. Scale bar is 10 cm. 5
- Figure 3 Morphology of single neurons. A) Composite drawing of the organization of a folium of the cerebellum drawn in three dimensions by Santiago Ramon y Cajal, based on reconstruction of neuronal morphology. Image from (Sotelo, 2003) B) Mouse pyramidal neuron being filled with dyes from whole cell pipettes at both the soma (blue) and dendrite (green). Dye filling enables the identification of dendrites for patch clamp recording of dendrites. Image from (Bert Sakmann & Stuart, 1994). C) Modern neuronal reconstruction of cortical neurons filled with dye during simultaneous patch clamp recording shows the connection between structure and function in neural networks (X. Jiang et al., 2015a). 11
- Figure 4 Literature review shows limited adoption of patch clamp experiments in human brain organoids (all methods). Vertical axis shows number of citations reported in Google Scholar for each year listed on the horizontal axis. Data was collected up to 5 November 2021. 12
- Figure 5 Challenges of organoid electrophysiology. A) Comparison of representative cells from the mouse brain (left) and a human brain organoid (right). Scale bar is 10 μm . B) Representative brightfield image of an intact human brain organoid showing large regions of opaque tissue. Scale bar is 1 mm. C) Anatomical regularity of the mouse brain enables registration of single cells from multiple 14

experiments to common coordinate system. No such anatomical regularity exists in organoids. Image from (H. Peng et al., 2021)

- Figure 6 Pipette cleaning simplifies multiple attempt automated patching. A) The Auto Swapper approach to sequential automated patch clamp experiments. Steps of the process are: robot arm (i) moves toward pipette storage rack (ii), brings pipette to filling station (iii), positions the pipette for measurement (iv), and inserts into pipette holder before beginning patch clamp attempt (v). Figure adapted from (Holst et al., 2019a). B) Schematic of pipette contamination from gigaseal formation showing membrane residue covering the interior of the pipette tip. C) Process of pipette cleaning shows simplicity of the method. After a patch clamp attempt, the pipette is moved to the cleaning bath where cleaning solution is pneumatically cycled through the tip (i). Pipette is then moved from cleaning solution to ACSF washing solution (ii) and after cycling ACSF through the tip is returned to the experimental chamber (iii). The entire process takes <1 minute. Step (ii) is optional (Landry et al., 2021). Figure is adapted from (I. Kolb et al., 2016). 17
- Figure 7 Patch clamp performance is affected by experimenter skill. In experiments using a 12 pipette multi-patching system, yield was reduced from 80% whole cell success per cell to 40% when the experimenters of different skill levels used the same system. Figure adapted from (Perin & Markram, 2013). 19
- Figure 8 Pipette cleaning methods. A) Process flow chart for traditional manual patch clamping without pipette cleaning. Removing, filling, and installing fresh pipettes takes between 60-120 s. B) Process flow chart for manual patching with automated cleaning (“push-to-clean”). Automated cleaning can be run in as little as 30 s. C) Close up images of pipette being moved from experimental chamber (left) to cleaning bath (middle) to rinse bath (right) before returning to the experimental bath to patch another cell. Scale bar is 25 mm. D) Custom experimental chamber for pipette cleaning featuring fluid inlet and outlet, inset for ground wire, and external baths for cleaning and rinsing solutions. Scale bar is 1 cm. 21
- Figure 9 Improvements to pipette cleaning. A) Each trace represents the number of whole cell recordings in HEK 293 cells as a function of number of recording attempts with a single pipette. Each trace is the average of at least 3 pipettes. Saline trace is a negative control (*i.e.*, cleaning solution replaced with extracellular solution) and 100% theoretical maximum is included for reference. Alconox trace shows performance of 2% w/v Alconox cleaning decreasing as a function of number of attempts. Tergazyme trace shows no decrease in yield for 30 attempts with 2% w/v Tergazyme. Optimized trace represents 23

2% w/v Tergazyme cleaning with optimized pipette positioning relative to the cell surface for gigasealing. Tergazyme performance is superior to Alconox (*, $P = 1.375E-5$, Kolmogorov-Smirnov test). Optimized performance is superior to Tergazyme (**, $P = 0.04368$, Kolmogorov-Smirnov test). B) Success rate of whole cell patch clamp as a function of number of cleans using 2% w/v Tergazyme shows no significant decrease in likelihood of subsequent whole cell recording (Odds ratio (OR) = 1.0067, CI: 0.97-1.04, $P = 0.69$, $n = 215$ attempts, each attempt is for $n = 7$ pipettes, except attempts 29 and 30, which are marked $n = 6$). C) Optimized indentation with Tergazyme cleaning shows no significant decrease in likelihood of subsequent whole cell recording (OR = 1.00, CI: 0.94-1.06, $P = 0.95$, $n = 124$ attempts, each attempt is for $n = 4$ pipettes).

- Figure 10 Upper limits of pipette cleaning with 2% w/v Tergazyme. A) Yield curves for individual pipettes showing cleaning for over 90 recording attempts with associated failure modes. “Success” trace shows effective pipette cleaning, “clog” trace shows reversible pipette tip clogs that cause low yield over time, and “break” trace shows experiment terminated by broken pipette tip. Theoretical maximum (100% yield) included for reference. B) Representative pipette images taken at 40× magnification for each failure mode in (A). Scale bar is 1 μm. C) Individual gigaseal resistance traces from “success” trace ($n = 122$ gigaseal attempts). D) Access resistance of cells recorded in “success” trace ($n = 101$ whole cell recordings). 25
- Figure 11 High-throughput opsin screening with pipette cleaning. A. Yield curve for a single pipette channelrhodopsin-2 (ChR-2) characterization experiment (46/51 attempts, 90% yield). B. Representative photocurrent trace (voltage clamp) in response to initial pulse of 500 ms 480 nm LED pulse recorded from transiently transfected HEK 293 cell showing large peak photocurrent response. C. Representative current response of ChR2 to rapid 10 msec pulses of 488 nm light. 32
- Figure 12 Pipettes as integrated devices. A) Schematic depicting the elements of an integrate Patch-Titrode device used to record simultaneous extracellular and intracellular activity in the mouse brain in vivo. B) Schematic showing process of mounting flexible electronics onto patch clamp pipette. Each pipette takes 20-25 minutes to fabricate C) Low (left, 500x) and high (right, 2500x) electron micrographs of pipette with mounted flexible electrodes. D) Demonstration of the Patch-Titrode in vivo recordings. Top traces are extracellular recordings from each of the three electrode sites integrated into the pipette and the lower trace shows a burst of action potentials recorded in current clamp. Figure adapted from (Hunt et al., 2019). 33

- Figure 13 Flow chart showing process and experimental yield from manual and automated patch clamp experiments in intact brain organoids. All recordings were performed on intact control organoids (lines 11C1 and C-3-1) between 80-130 DIV. 45
- Figure 14 Fixturing methods for intact human brain organoids. (A) Side-view image of a large (1-2 mm) human brain organoid resting on a layer of 1% w/v agarose. (B) Damage caused to human brain organoid by traditional fixturing method of a hard surface and a weighted harp with low clearance. (C) Modified fixturing method preserves shape of intact organoid using a high clearance weighted harp and a layer of 1% w/v agarose to minimize area change in tissue. Scale bar for (A,B,C,E, and F) is 1 mm. (D) Harp and agarose method reduces the area change in organoids compared to harp only method from $30.4 \pm 27.3\%$ to $5.6 \pm 4.5\%$ ($p = .0475$, Student's t-test, $n = 6$ organoids). (E-F) Representative shape outlines show changes in organoid area for each method (black = unfixtured, red = fixtured with traditional harp, blue = fixtured with harp and agarose). 46
- Figure 15 Patching cells on the surface of intact organoids. A) Target organoid cell on the surface of the tissue. Scale bar is $25 \mu\text{m}$. B) Representative recording of mature organoid neuron (120 DIV) recorded at the tissue surface firing multiple action potentials. 48
- Figure 16 Patch clamp recordings in intact human brain organoids. A) Representative neuron hunt resistance traces as a function of depth (gray) showing cell detection events for blind patching as changes in resistance. Arrows over black trace show potential detections before threshold is crossed. B) Representative gigaseal resistance traces (gray) as a function of time from cells in (A). Black trace shows gigaseal formation for cell shown in (A). C) Representative current clamp recordings from intact brain organoids showing different levels of action potential activity. 50
- Figure 17 Electrophysiological properties of cells in intact human brain organoids. A) Patch clamp recording rig for recording from intact human brain organoids. Inset shows intact human brain organoid held in place using the harp and agarose method. Scale bar is $100 \mu\text{m}$. B) Representative spontaneous action potentials from organoid neuron. The presence of multiple spontaneous action potentials is a sign of mature neurons. C) Representative voltage clamp recordings showing subthreshold activity in organoid neurons. Trace on the left shows an overlay of many traces, and trace on the right shows the averaged trace. D) Organoid electrophysiological properties vary with age. In recordings of 90 and 120 DIV organoids, resting membrane potential (RMP) decreased slightly in older organoids, but was not significant. Sag ratio decreased significantly in 120 DIV 52

organoids. E) Organoid electrophysiological properties vary with respect to depth of recording. In recordings performed on subsurface cells, RMP increased, but the difference was not significant. Deeper organoid cells express larger sag ratios.

- Figure 18 Action potential activity in intact organoid cells show range of developmental stages. A) Developmental stages of action potential development from human fetal brain slices (A. R. Moore et al., 2009). Major stages are passive, abortive action potentials, single action potentials, and multiple action potentials (left to right). B) Cells recorded from intact human brain organoids display these features. All recordings were made from control organoids between 90-120 DIV. C) Across age and depth groups, recordings featured primarily single action potentials, and proportion of cells firing multiple action potentials or rebound action potentials were not statistically significant. D) Representative recording of organoid neuron firing a single action potential and a rebound action potential. 56
- Figure 19 Protocol flowchart for patch clamp and morphological reconstruction using CUBIC tissue clearing. The process is can be performed in one week and is compatible with batch processing and imaging of tissues. 63
- Figure 20 Fluorescence imaging of dye filling in surface cells. A) Sequence of fluorescence images showing dye filling a single cell during patch clamp recordings starting in (i). Cell showed diffusion of dye through visible neurites, indicating successful filling (ii). Cell retained fluorescence signal following retraction of pipette (ii). B) An example of a failure to retract the pipette. This sequence of images shows a filled cell (i) being pulled away from the surface of the cell (ii, iii). The cell retained fluorescence signal briefly after retraction (iv), but was not able to be located in cleared tissue. C) Dye filling showing a patched cell (bright) surrounded by fluorescent cells that have been filled with dye, likely through gap junction coupling, indicative of astrocytes networks. D) Dye filling of a putative neuron, which shows no background dye staining. Scale bar for all images is 25 μm . 67
- Figure 21 Process of locating patched cells in cleared tissues. A) Organoid fixtured on agarose slab with weighted harp. Shape of the organoid and orientation of the harp strings are critical for locating the cell in the cleared tissue. Scale bar is 1 mm. B) Fluorescence image of patched cell in organoid from (A). Note the distinctive branching dendrite feature directly beneath the patch pipette. Scale bar is 10 μm . C) Volumetric rendering of the organoid in (A) following clearing showing a visible soma and dendrite. Scale bar is 1 mm. D) Relocated patched cell imaged at 20x magnification. Note the 69

dendritic branching pattern observed in (B) is still present. Scale bar is 20 μm .

- Figure 22 Process yields for patching, relocation, and reconstruction of single cells in intact human brain organoids. A) DIC image of whole cell patch clamp attempt on a surface organoid cell. Scale bar is 50 μm . Whole cell patch clamp yield was 39% for a total of 32 cells recorded from 15 intact human brain organoids. B) Representative slice from a confocal image stack showing localized biocytin Alexa Fluor 594 signal. Cells are manually based on gross organoid features and relative locations of cells. The yield for this process was 72%, with 23/32 total cells being identified by fluorescent signal and assigned to a patch clamp recorded based on location. C) Cell tracing was carried out on recorded and assigned cells to quantify morphological features. Cells that did not feature multiple neurites or significant branching were considered incomplete fills. 20/23 cells (87% yield) passed this stage. 71
- Figure 23 Resolving the morphology and electrophysiology of nearby neurons in intact human brain organoids. A) Neuron tracings overlaid on a maximum intensity z-projection. Scale bar is 25 μm . B) Spontaneous activity recorded in current clamp for both neurons. The blue neuron corresponds to the blue trace and the pink neuron corresponds to the pink trace. Based on the low level of spiking activity (3-5 mV), the blue cell is an immature neuron. Based on spontaneous action potentials, the pink cell is a mature neuron. C) Spontaneous activity recorded in voltage clamp for the pink and blue neurons, respectively. 72
- Figure 24 Morphology and electrophysiology of an immature organoid neuron. A) Morphology of a single organoid neuron from manual tracing in ImageJ. Inset image is a maximum intensity z-projection of the raw image stack to show the shape of the soma and proximal dendrites. Scale bar for both images is 50 μm . B) Current clamp response of the cell recorded in (A) showing strong hyperpolarization response and a single immature action potential. C) Immature rebound spike observed as the cell returns to baseline after hyperpolarization. D) Spontaneous activity recorded in current clamp showing low levels of activity in baseline signal. 75
- Figure 25 Putative neurite patch clamp recording in intact human brain organoid. A) Fluorescence image during recording showing pipette sealed onto neurite extending outward from soma. Scale bar on main image is 25 μm . Scale bar on inset is 10 μm . B) Trace of recorded neuron. Soma is shown in red and the patched neurite is labelled green and marked with an arrow. Scale bar is 50 μm . C) Spontaneous 80

activity recording in neurite showing stable baseline and complex subthreshold activity.

LIST OF SYMBOLS AND ABBREVIATIONS

hiPSCs	Human induced pluripotent stem cells
MCPH	Primary microcephaly
RPE	Retinal pigment epithelium
DIV	Days <i>in vitro</i>
BRAIN	Brain Research Through Advancing Innovative Neurotechnologies
RNA seq	Ribonucleic acid sequencing
ChR-2	Channelrhodopsin-2
DIC	Differential interference contrast
OR	Odds ratio
HEK 293T	Human embryonic kidney cells, 293T line
RMP	Resting membrane potential
CUBIC	Clear unobstructed brain imaging cocktails and computational analysis
SNT	Simple Neurite Tracer

SUMMARY

Human brain organoids, three-dimensional spheres of human induced pluripotent stem cells (hiPSCs), have become widely used as a model system to study human neurodevelopment in recent years. Specifically, the model of intact (i.e., unsliced) brain organoids could present an ideal system for studying synaptic activity, spontaneous oscillations, and connectivity of developing neuronal networks in self-assembled tissues – opening the door to previously inaccessible windows of human neurodevelopment. As a gold standard single cell method, whole cell patch clamp is a critical tool in unraveling the physiology of neural tissues. In addition to capturing the millivolt- and millisecond-scale dynamics of neuronal cells, patch clamp also provides direct physical access to single cells in intact tissues allowing for the delivery and extraction of molecules such as dyes or genes. Critically, the delivery of intracellular dyes via patch clamp recording enables multidimensional characterization of single cells, including relationships between cellular structure and function. Despite this potential, the challenges of performing single cell studies in human brain organoids are substantial and have limited progress in this field. This work addresses these problems first by developing a method for cleaning and reuse of patch clamp pipettes that increases the throughput, scalability, and reproducibility of patch clamp recordings and second by developing a suite of methods for performing patch clamp measurements in intact human brain organoids. The result of this work is a set of scalable methods for patch clamp recordings and morphological reconstruction in intact brain organoids.

CHAPTER 1. Introduction

1.1 Background

1.1.1 Human brain organoids

Human brain organoids are self-assembled tissues composed of human induced pluripotent stem cells (hiPSCs) that are rapidly becoming an essential model of human neural development and disease (M. A. Lancaster et al., 2013). The growth of this field is closely tied to the discovery of induced pluripotency in the mid-2000s (Kazutoshi Takahashi et al., 2007; Kazutoshi Takahashi & Yamanaka, 2006) and long-standing research into organogenesis and self-assembly in the field of developmental biology (P. Weiss & Taylor, 1960). The early 2010s saw rapid innovation in development of human brain organoids that recapitulated many characteristics of brain development (Cugola et al., 2016; M. a Lancaster et al., 2014; Yoshiki Sasai, 2013; Sato & Clevers, 2013; Yin et al., 2016). These early studies employed a combination of gene expression, immunohistochemistry, and electrophysiology to demonstrate that brain organoids exhibit complex developmental features associated with brain development, including cell type specialization, laminarization, and spontaneous oscillatory activity (Quadrato et al., 2017; Trujillo et al., 2018).

A key feature of human brain organoids is that they are derived from individual patients and can be generated to study specific genetic variations of neurological diseases. The potential ability of human brain organoids to provide a close approximation of *in vivo* brain tissue matching specific patient genetic conditions make this a promising model for

exploring disease mechanisms as well as screening potential therapeutics. This genetic specificity and tissue organization make human brain organoids a critical model system for the future of neuroscience.

A key goal of brain organoid research is to use this new model system to answer questions that have been confounded by limitations of other model systems such as 2D cell culture or mouse models of human diseases. Indeed, in one of the original brain organoid papers, Lancaster et al, use the example of primary microcephaly, writing (emphasis mine):

“Primary microcephaly (MCPH) is a neurodevelopmental disorder in which brain size is markedly reduced... Heretofore, MCPH pathogenesis has primarily been examined in mouse models. However, mouse mutants for several of the known genes have failed to recapitulate the severely reduced brain size seen in human patients. *Given the dramatic differences between mice and humans, methods that recapitulate paradigms of human brain development in vitro have enormous potential.*” (M. A. Lancaster et al., 2013)

While unlikely to fully recapitulate all features of human brain development, human brain organoids enable scientists to study aspects of human development that are not captured in other model systems (Yang & Ng, 2017).

Human brain organoids have already been used for real-world applications, including the development of the Zika virus vaccine in 2016 (Qian et al., 2016c; Whalley, 2016). Brain organoids allowed scientists to understand the mechanism of Zika virus infection without the need to access tissue from infected fetuses and children and the ability to rapidly generate large numbers of brain organoids enabled vaccines and treatments to be

screened for multiple complex phenotypes simultaneously (Trujillo & Muotri, 2018; Whalley, 2016). Current efforts in the field focus on demonstrating that cell types and their connections, laminar organization, network dynamics, and migratory dynamics are comparable to *in vivo* brain tissue, with the goal of performing large scale comparative studies of development and disease (Arlotta, 2018; Kelava & Lancaster, 2016a). This approach continues to drive interest in brain organoids for large scale screening work, such as “phase zero” clinical trials (C. T. Lee et al., 2017).

1.1.2 Biological self-assembly of complex tissues

A persistent question in the organoid field is how fully the genetic program and microenvironment of human brain organoids can mimic *in vivo* brain development (Velasco et al., 2019a). While this is a complex answer that will require decades of work to fully define, evidence from developmental biology and organoid characterization suggest that the power of biological self-assembly should not be underestimated (Gabriel et al., 2021; Krencik et al., 2017; Velasco et al., 2019b).

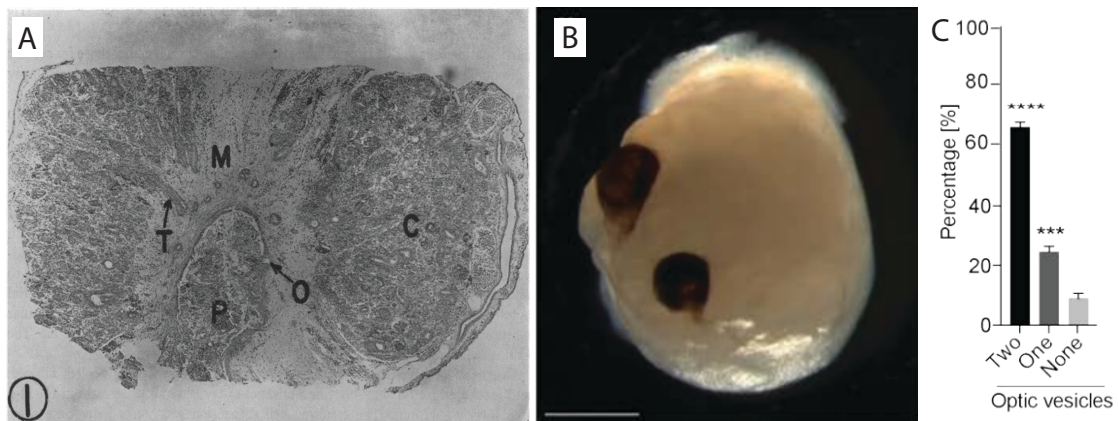


Figure 1. Biological self-assembly produces complex tissues. A) Scrambled and reassembled kidney showing micrograph showing features of complex tissue including cortex (C), medulla (M), pelvis like cavity (P), radial collecting tubes (T),

and openings for radial collecting tubes into the pelvic area (O). Image modified from (P. Weiss & Taylor, 1960). B) Brain organoid (60 DIV) showing bilateral, pigmented optic cups. Scale bar is 1 mm. C) Rate of bilateral optic cup formation is high across multiple cell lines and batches of organoids. Images modified from (Gabriel et al., 2021).

Developmental biologists like H.V. Wilson discovered in the early 20th century that single cells from sea sponges possessed the ability to regrow complex multicellular structures (Wilson, 1907). Later work with teratomas and embryoid bodies showed that mammalian cells also possess the genetic programs sufficient to generate complex three-dimensional structures and even functional organs. Consider, for example, a 1960 study by Weiss and Taylor, in which embryonic tissue samples from the kidney, skin, or liver were excised, fully dissociated, and reinjected into 8 day old chick embryos (P. Weiss & Taylor, 1960). Upon examination 9 days after injection, Weiss and Taylor found that the dissociated cells had reassembled into structures that were histologically identical to native tissue, including organs like the kidneys which display prominent laminarization and symmetry (Figure 1A). Further, these reassembled tissues appeared to be functional, with reassembled skin growing feathers several millimeters in length. They describe the organizational potential of single cells in stark terms (emphasis mine):

“Since the grafted cells, whose morphological arrangement had been completely disrupted, accomplished on a neutral test site a second organogenesis strictly corresponding to the organ from which they had been isolated, they must have *achieved their transformation from the random scrambled into the morphologically fully organized state wholly by "self-organization,"* that is, by virtue of properties residing within the isolated cell population, unaided by specific inductive instructions from without.” (P. Weiss & Taylor, 1960)

Recent developments in the brain organoid field have continued to stretch the boundaries of what has been thought possible for self-assembled tissues. In notable recent work (Figure 1B,C), Gabriel et al. reported the repeatable generation of human brain organoids with bilateral, pigmented optic cups (Gabriel et al., 2021). This work shows that brain organoids can generate complex organization such as bilateral symmetry as well as highly specialized cell types such as retinal pigment epithelium (RPE). Critically for this work, the increasing complexity of human brain organoids provides strong motivation for studying human brain organoids as intact systems using multiple single cell methods. Improving and integrating methods for single cell analysis in intact organoids can provide new insights into complex phenotypes within complex self-assembled tissues.

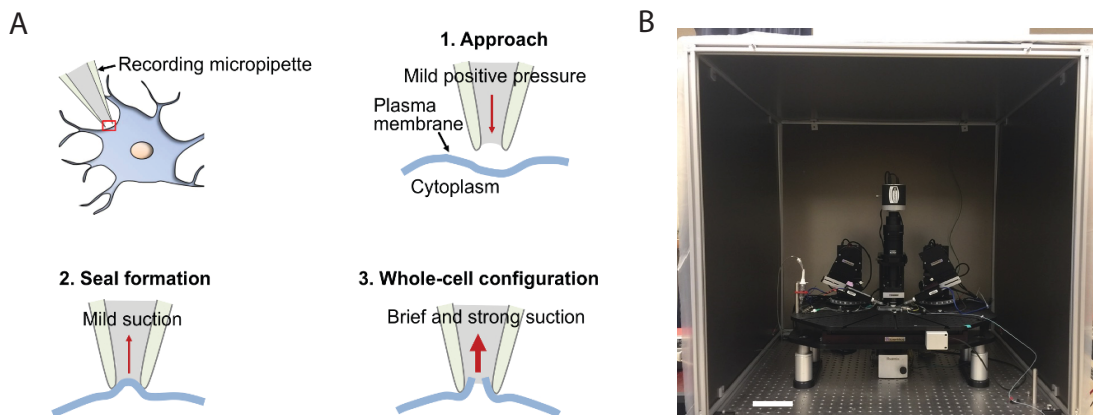


Figure 2. Overview of the whole cell patch clamp method. A) Schematic of the steps of a whole cell patch clamp experiment showing approaching the cell, forming a gigaseal, and rupturing the seal to form the whole cell recording configuration. Image modified from (Segev et al., 2016). B) Electrophysiology rig used to perform automated patch clamp recordings using the patcherBot. Scale bar is 10 cm.

1.1.3 Intracellular electrophysiology

Because neuronal tissues like the brain or brain organoids are composed of densely packed and inter-connected electrically active cells, the ability to physically access those

individual cells with an insulated electrode is a fundamental technique in neuroscience (X. Jiang et al., 2015a; Xiaolong Jiang et al., 2013; Henry Markram, 2008). Early electrophysiologists used glass capillaries, hand-pulled to a sharp tip ($< 1\mu\text{m}$ tip) over an open flame, filled with conducting fluid and a metal electrode insulated by the glass capillary (B Sakmann & Neher, 1984). This key innovation provided increased the signal-to-noise ratio of the recordings over previous metal electrodes (Hodgkin & Huxley, 1952). The ability to record single signals by impaling single cells with glass electrodes were a significant moment in the history of neuroscience, leading directly to the discovery and computational modeling of the neuronal action potential by Hodgkin and Huxley, which won the Nobel Prize in 1963 (Schwiening, 2012).

In the 1970s, Bert Sakmann and Erwin Neher further improved the signal-to-noise ratio of intracellular recordings by forming a high-resistance gigaohm seal, known as a “gigaseal” between a glass pipette tip ($1\mu\text{m}$ tip) and a patch of the cell membrane (Hamill et al., 1981). This tight physical seal between the cell membrane and the glass pipette enabled electrical activity of single cells to be recorded with millivolt and millisecond resolution (Figure 2A). This technique has become critical to a modern understanding of neuroscience and has enabled the recording of single ion channel currents and analysis of electrical signaling at synapses (H Markram et al., 1997; Neher & Sakmann, 1976). Additionally, whole cell patch clamp, a variant of the technique where the membrane patch is ruptured to record electrical signals from the “whole cell” has been widely used to study neuronal plasticity, unravel neuronal connectivity, and characterize the diversity of neuronal cell types (Kalisman et al., 2005; Zeng & Sanes, 2017). One distinguishing aspect of patch clamp in comparison to other methods is the direct physical access that it provides

to single cells in living tissues (B. R. Lee et al., 2020). This single cell access can take multiple forms and has been used to great effect in studies that classify neurons and synapses by multidimensional types (Xiaolong Jiang et al., 2015). The ability to gather morphological and electrophysiological data from the same cell while preserving its location in the tissue is critical to understanding the connectivity matrix between neurons and serves as a “ground truth” for future studies and classification schemes. Because of this, methods that simultaneously gather morphological and electrophysiological data at a large scale in the living mouse brain were a major technology goal of the Brain Research Through Advancing Innovative Neurotechnologies (BRAIN) Initiative (Bargmann & Newsome, 2014) and these methods are highly valued across different model systems.

1.1.4 Steps of the whole cell patch clamp method

Whole cell patch clamp is one of the art forms of neuroscience, involving a series of delicate steps to form a high resistance seal with a single cell in living brain tissue. These experiments are typically performed on a rig similar to the one in (Figure 2B). The general process of the experiment is below:

- 1) Identify the target cell under or target region of interest under DIC or other optics. Cells and regions that are desirable are highly specific to the given experiment and can be based on anatomy, morphology, fluorescent markers, or cell health, among other metrics. For experiments in unlabelled tissue (e.g., no cell type specific labelling) or blind (e.g., no visual selection of single cells because of tissue thickness or other constraints).
- 2) Locate the pipette under the microscope objective and position near the tissue.

- 3) Approach the cell while applying positive pressure to the tip of the pipette using a syringe, pressure controller, or mouth suction to prevent clogging of the membrane.
- 4) Approach the cell slowly, typically along the pipette axis, while monitoring the resistance of the pipette tip. An increase in resistance indicates that the pipette has made contact with the cell membrane.
- 5) Release positive pressure from the pipette to form a high resistance gigaohm seal (i.e., a gigaseal). If the seal forms slowly, apply light suction to the pipette tip using a syringe, pressure controller, or mouth suction. Apply a holding voltage of -70 mV.
- 6) Once a gigaseal has formed, rupture the patch of cell membrane by applying a short burst of suction using a syringe, pressure controller, or mouth suction. Successful break-in can be detected by capacitive transients in response to membrane test pulses.
- 7) Whole cell recordings are performed in current clamp or voltage clamp configurations, as needed for experiment.
- 8) After recording is completed, the pipette is slowly withdrawn from the cell and removed from the experimental bath. Used pipettes can be discarded and replaced or cleaned using the pipette cleaning method described in Chapter 2.

1.1.5 Automation of patch clamp electrophysiology

Although patch clamp electrophysiology is one of the foundational techniques of modern neuroscience, it is an art form that requires a tremendous amount of skill and training to perform (Neher & Sakmann, 1976). One of the goals in the Forest lab has been to reduce this art form to a series of steps that can be executed by a robot (Figure 2B). In

2012, we discovered through years of iterative development that the final steps of *in vivo* patch clamp recordings (i.e., gigasealing and break-in) in the mouse cortex can be automated and executed by a robot called the “autopatcher” (Kodandaramaiah et al., 2012). Subsequent years of iterative, trial-and-error development have extended the capabilities of the autopatcher to include such features as: navigation to target cells using two photon microscopy (Suk et al., 2017), avoidance of blood vessels and other obstacles (W. A. Stoy et al., 2017), compensation for *in vivo* brain motion (W. Stoy et al., 2020), automated cell labeling for morphology (Li et al., 2017b), robotic replacement and filling of pipettes (Holst et al., 2019b), simultaneous recordings of multiple connected neurons (Kodandaramaiah et al., 2018), identification and tracking of target cells in tissue (J. Lee et al., 2018), cleaning and reuse of pipettes (I. Kolb et al., 2016; Landry et al., 2021), and unattended operation of entire patch clamp experiments (Ilya Kolb et al., 2019; Landry et al., 2021).

1.1.6 Morphological reconstruction of neuron structure

Before the development of modern electrophysiology, the study of neuronal morphology, perhaps more than any other field, helped to shape the fundamental understanding of the brain and of the neurons and glia that compose it (Marx et al., 2012). The visionary anatomist Santiago Ramon y Cajal used his studies of neuronal morphology to develop neuron theory, the theory that the brain is composed of many single cells called neurons (Henry Markram, 2008). Cajal used techniques such as Golgi staining to prove the existence of synapses between neurons, and proposed an early version of the synaptic theory of memory in 1894 (Yuste, 2015). Cajal thought deeply about how the structure of neurons influenced their function, proposing that neuronal shape and function are linked

by the conservation of time, material, and space, a concept that continues to guide the study of connectomics (Schröter et al., 2017; Sotelo, 2003).

The study of neuronal morphology pioneered by Cajal later intersected with the study of single cell electrophysiology pioneered by Neher and Sakmann, an integration of methods that has provided a wealth of information about the structure and function of neurons (B. R. Lee et al., 2021; Henry Markram, 1997). While there are multiple techniques to combine electrophysiology and morphology, one of the most widely used is the delivery of intracellular dyes to the cell via the patch clamp pipette. Briefly, a fluorescent dye is dissolved into the pipette internal recording solution and then diffused into the cell during whole cell recording (Horikawa & Armstrong, 1988). By carefully retracting the patch pipette after recording, the cell will re-seal its membrane allowing the dye to diffuse into the fine dendritic and axonal processes (Figure 3B). The tissues are then fixed, processed, and imaged on a microscope to reveal the structure of the recorded cell (Figure 3C). By collecting data containing linked morphology and electrophysiology, neuroscientists have developed classification schemes to define the different cell types throughout the brain (Zeng & Sanes, 2017). Recent work with extracting and sequencing genetic material from single cells during these experiments have provided additional insights from this method, providing a new “ground truth” method for modern neuroscience (Berg et al., 2020; B. R. Lee et al., 2021).

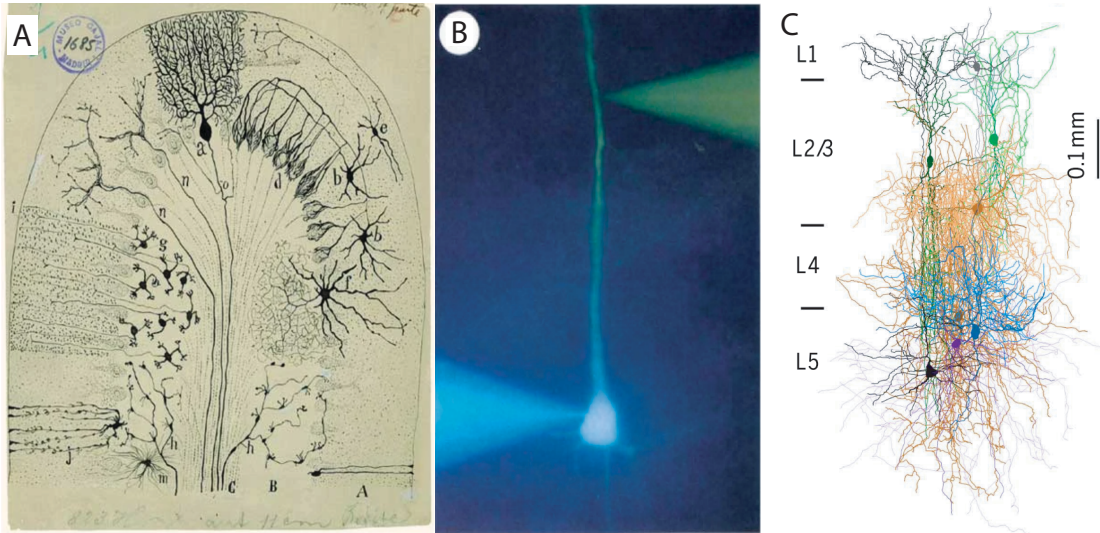


Figure 3. Morphology of single neurons. A) Composite drawing of the organization of a folium of the cerebellum drawn in three dimensions by Santiago Ramon y Cajal, based on reconstruction of neuronal morphology. Image from (Sotelo, 2003) B) Mouse pyramidal neuron being filled with dyes from whole cell pipettes at both the soma (blue) and dendrite (green). Dye filling enables the identification of dendrites for patch clamp recording of dendrites. Image from (Bert Sakmann & Stuart, 1994). C) Modern neuronal reconstruction of cortical neurons filled with dye during simultaneous patch clamp recording shows the connection between structure and function in neural networks (X. Jiang et al., 2015a).

1.2 Motivation

1.2.1 Human brain organoids as a model system for neuroscience

Human brain organoids are rapidly becoming a critical component in the effort to understand, treat, and cure neurological diseases. Organoid models are widely used to understand the complexities of human genetics and to explore the efficacy of new drugs to treat brain diseases. While many of these studies rely on methods that can study many cells at once (i.e., microscopy, genetics, and histology), as with any model system in neuroscience, there is an important place for techniques where single cells can be studied at high resolution in intact tissue using multiple methods. However, the techniques for

studying single cells in intact brain organoids are underdeveloped. This lack of methods development can be seen from literature trends as measured by Google Scholar (Figure 4). Among papers mentioning brain organoids, fewer than 10% per year mention patch clamp recordings, compared to 30% or higher for methods like immunostaining or RNA seq. Filling these methodological gaps in the field to enable new multimodal single cell studies in intact human brain organoids is the primary goal of this work.

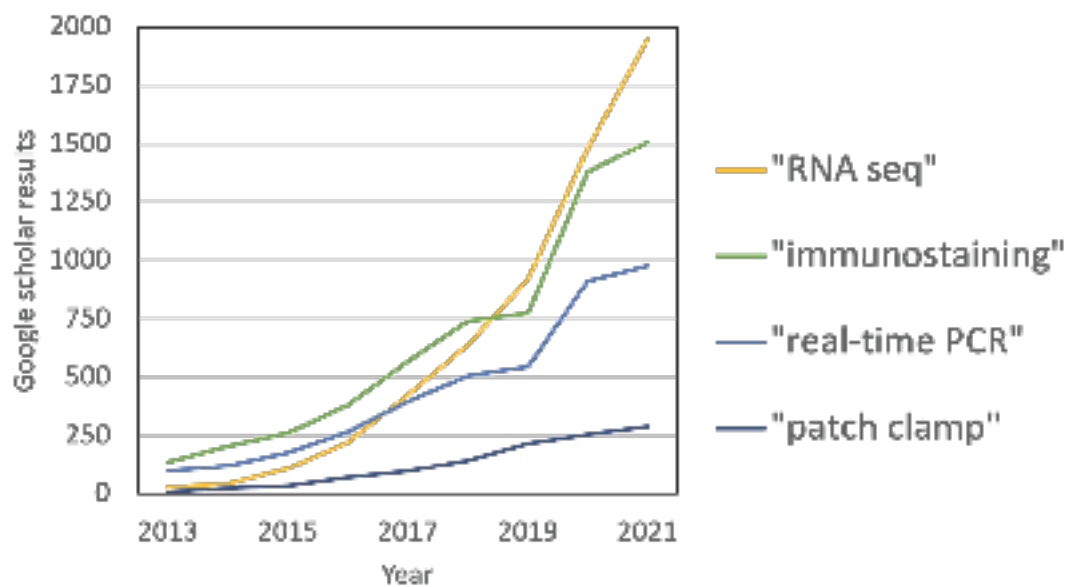


Figure 4. Literature review shows limited adoption of patch clamp experiments in human brain organoids (all methods). Vertical axis shows number of citations reported in Google Scholar for each year listed on the horizontal axis. Data was collected up to 5 November 2021.

1.2.2 Challenges of single cell experiments in intact human brain organoids

Although a primary reason for interest in brain organoids is their ability to act as a near-physiological self-organized tissue, the majority of patch clamp studies are performed in non-physiological preparations like acute slices or dissociated cultures (Kelava & Lancaster, 2016b; Otani et al., 2016; Y. Sasai et al., 2012). Because of the lack of

anatomical regularity in brain organoids, it is unlikely that these preparations reflect the intrinsic pattern of connectivity found in intact organoids. In fact, this point is debated even for acute slice methods in rodents, which are highly optimized to preserve specific types of local and/or long-range connections (Barth et al., 2016; X. Jiang et al., 2015a, 2016). This damage caused to intrinsic patterns of connectivity is one of several motivating factors for the continued development of the *in vivo* patch clamp methods in rodents and primates, despite the increased complexity of the experiment and the corresponding decrease in experimental yields (Holst et al., 2019a; W. Stoy et al., 2020). Indeed, the continued development of methods for patch clamp in intact and *in vivo* preparations have yielded crucially important data, including connections between single cell activity and brain state, as well as correlation of single cell activity with behavioral output in awake animals (Haider et al., 2013; Petersen, 2017).

To patch in intact brain organoids is a challenging proposition that has not been fully achieved in the literature. In fact, one recent publication claims that “it was technically impossible to perform the patch clamp measurements on intact aggregates (organoids)” (Renner et al., 2020). Previous attempts at patching in intact brain organoids have failed because brain organoids are large clusters (0.5-3 mm diameter) of small cells ($5.5 \pm 1.1 \mu\text{m}$ diameter) that make identification, detection, and recording of target cells challenging (Figure 5A,B) (Qian et al., 2016b). The development of methods for patching in intact brain organoids could allow measurements of single human neurons in an *in vivo*-like environment. Techniques for performing patch clamp recordings in intact organoids efficiently and combining those methods with additional single cell techniques such as morphological reconstruction will be of great interest to the broader neuroscience

community and provide “ground truth” data for this new model system. These methods are critical for generalization and standardization of single cell organoid data, enabling comparisons across preparations, ages, and organoid types, as is possible in the mouse brain (Figure 5C).

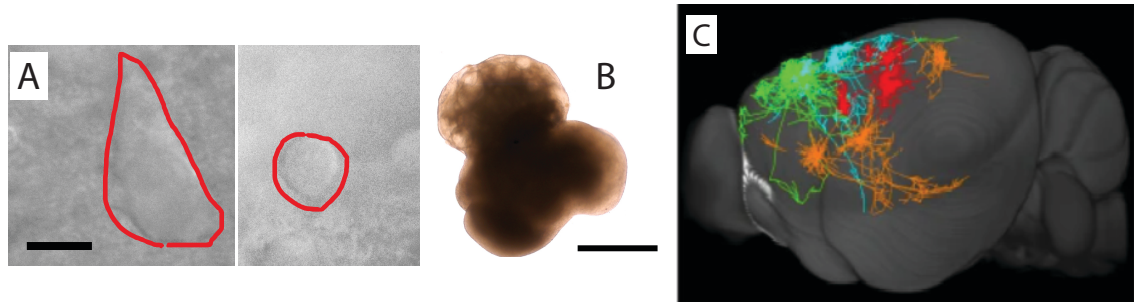


Figure 5. Challenges of organoid electrophysiology. A) Comparison of representative cells from the mouse brain (left) and a human brain organoid (right). Scale bar is 10 μm . B) Representative brightfield image of an intact human brain organoid showing large regions of opaque tissue. Scale bar is 1 mm. C) Anatomical regularity of the mouse brain enables registration of single cells from multiple experiments to common coordinate system. No such anatomical regularity exists in organoids. Image from (H. Peng et al., 2021)

CHAPTER 2. Enzymatic Cleaning and Reuse of Patch Pipettes

Portions of this chapter have been previously published (Ilya Kolb et al., 2019; Landry et al., 2021).

2.1 Introduction

Whole cell patch clamp recordings allow unprecedented access to electrical activity, neuronal morphology, and gene expression at the single cell level (Gouwens et al., 2019; X. Jiang et al., 2015a). However, because this method requires a great amount of skill and care to perform correctly, it remains one of the most difficult methods in neuroscience. A crucial step in this method is the formation of a tight, high resistance (*e.g.*, $>1 \text{ G}\Omega$) connection between the cell membrane and the glass pipette known as a gigaseal. Gigaseal formation requires a clean pipette surface and even small contaminants (*e.g.*, cell debris or dust) can disrupt this process (Hamill et al., 1981). For this reason, patch clamp experimenters need to replace glass pipettes after each recording attempt, requiring additional time and attention (*e.g.*, removal, fabrication, filling, and installation of pipettes). This delicate and highly manual process has been automated, but requires a precisely engineered, purpose-built system to accomplish these tasks, as previously demonstrated in the Forest lab (Figure 6A) (Holst et al., 2019a). This has been the ubiquitous practice in the field until the discovery of detergent-based pipette cleaning in 2016 (Figure 6B,C) (I. Kolb et al., 2016). However, for experiments requiring many patch clamp attempts or where long, fully automated experiments were desirable, detergent-based cleaning was insufficient. Therefore, in this chapter, I will discuss an improved

method for cleaning and reusing patch clamp pipettes using enzymatic detergents as well as new types of experimental design for patch clamp studies enabled by this discovery.

2.1.1 Chemical and enzymatic removal of cellular debris from pipettes

Cell membranes are composed of lipids, proteins, and carbohydrates, all of which are thought to bind to the interior of the pipette following a patch clamp attempt (I. Kolb et al., 2016). As the biochemical composition of the gigaseal is still an unsolved problem of biophysics, our work with pipette cleaning is largely empirical. The primary empirical means of testing pipette cleaning are measuring the ability of cells to form gigaseals after cleaning to determine viability of the solution. Critically, this testing process is limited by the throughput of the patch clamp method. A typical experimenter only records from 10-20 cells in a single day. With these limitations, potential cleaning solution selection has been based on existing knowledge of the biological targets of each agent. For example, bleach (sodium hypochlorite) is known to denature membrane proteins, motivating its previous use to clean planar patch clamp chips (Kao et al., 2012). Interestingly, in our hands, bleach was ineffective at cleaning traditional patch clamp pipettes, perhaps due to the formation of aggregates of denatured proteins (Winter et al., 2008). Alconox, a commercially available detergent, is known to emulsify the lipid components of the cell membrane, removing a large percentage of the cellular debris adhered to the pipette. Tergazyme, the enzymatic detergent used in these experiments, contains the detergent components of Alconox with a bacteria-derived protease, an enzyme that breaks down the protein component of the cell membrane.

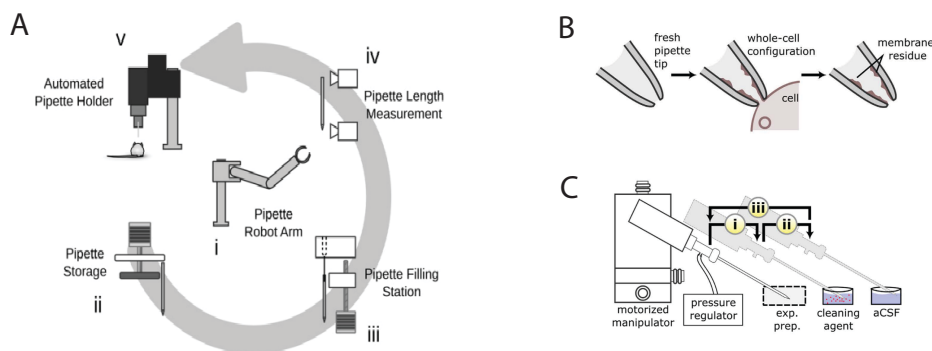


Figure 6. Pipette cleaning simplifies multiple attempt automated patching. A) The Auto Swapper approach to sequential automated patch clamp experiments. Steps of the process are: robot arm (i) moves toward pipette storage rack (ii), brings pipette to filling station (iii), positions the pipette for measurement (iv), and inserts into pipette holder before beginning patch clamp attempt (v). Figure adapted from (Holst et al., 2019a). B) Schematic of pipette contamination from gigaseal formation showing membrane residue covering the interior of the pipette tip. C) Process of pipette cleaning shows simplicity of the method. After a patch clamp attempt, the pipette is moved to the cleaning bath where cleaning solution is pneumatically cycled through the tip (i). Pipette is then moved from cleaning solution to ACSF washing solution (ii) and after cycling ACSF through the tip is returned to the experimental chamber (iii). The entire process takes <1 minute. Step (ii) is optional (Landry et al., 2021). Figure is adapted from (I. Kolb et al., 2016).

2.1.2 Pipette cleaning as an enabling technology

When the Forest laboratory initially discovered pipette cleaning in 2016, an immediate realization was that improving the efficiency of the patch clamp process enabled new types of experiments to be performed. The ability to clean and reuse pipettes enabled multiple patch clamp attempts to be fully automated in a simple procedure with only minor changes to a conventional patch clamp experimental setup. This fully autonomous patch clamp robot capable of recording dozens of cells with no human supervision was published in 2019 (Kolb *et al.*, 2016 and 2019). Further, this pipette cleaning method has been used by us, our collaborators, and other groups to make large-scale patch clamp studies (*i.e.*, single cell electrophysiology and connectomics in rodents and humans and high throughput

screening) more efficient (Peng *et al.*, 2019; Koos *et al.*, 2020) and to make complex experiments (*i.e.*, *in vivo* patch clamp) simpler (Suk *et al.*, 2017; Stoy *et al.*, 2020).

2.1.3 *Pipette replacement as a bottleneck for automated patch clamp experiments*

Despite these improvements, the original pipette cleaning protocol, which used a commercially available detergent (2% Alconox) as a cleaning solution, was only capable of achieving 10 patch clamp attempts before the ability to form high resistance seals was eliminated. For some experiments requiring long (>10 minutes) recordings or requiring solutions to be exchanged in the bath (e.g., some pharmacology experiments), this performance was sufficient. However, for applications where a high number of recordings or a long, unattended experiment was desirable, Alconox cleaning was still limited by the need to manually replace pipettes every 10 attempts, or approximately every hour.

2.1.4 *Methods development for patch clamp experiments*

The ability to control for the intrinsic variability in patch clamp pipettes and experimenter attention and skill represents a pathway towards standardization and optimization in patch clamp experimental design that has not been previously possible (Figure 7). Removing these sources of variability and increasing the throughput of the overall experiment produce more reliable patch clamp experiments and enables methods to be optimized, standardized, and shared by many laboratories. In the following, we characterize the performance of enzymatic cleaning of pipettes, demonstrate a single-blinded methods experiment to improve automated patch clamping, and show a proof of concept for automated high-throughput characterization of optogenetic proteins.

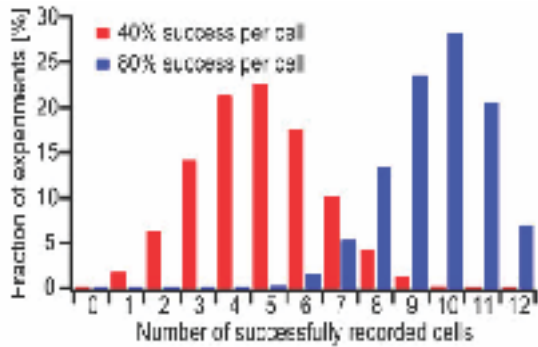


Figure 7. Patch clamp performance is affected by experimenter skill. In experiments using a 12 pipette multi-patching system, yield was reduced from 80% whole cell success per cell to 40% when the experimenters of different skill levels used the same system. Figure adapted from (Perin & Markram, 2013).

For these experiments, cultured cells (HEK 293T, ATCC) were chosen for their ease of culture and high yield in previous patch clamp experiments. From previous work, it was known that cleaning pipettes with Alconox produced similarly effective results in cultured HEK 293T cells, cultured neurons, mouse brain slices, mouse brain *in vivo*, and intact brain organoids. HEK 293T cells are an effective model system that enable the rapid testing of new methods for pipette cleaning and automated patching and continues to be used in the development of the patcherBot.

2.2 Methodology

2.2.1 Patch clamp hardware

The patcherBot system was based on a conventional electrophysiology setup (SliceScope Pro 3000, Scientifica Ltd), comprising two motorized PatchStar micromanipulators mounted on a motorized stage. Samples (cultured cells and brain slices) were imaged using a 40 × objective (LUMPLFL40XW/IR, NA 0.8, Olympus) on a motorized focus drive, illuminated under differential interference contrast (DIC) with an

infrared light-emitting diode (Scientifica), and captured with a Rolera Bolt camera (QImaging). Köhler illumination was set up and routinely checked to ensure consistent illumination. A peristaltic pump (120S/DV, Watson-Marlow) was used to perfuse cells and slices with buffer solution. Recordings were acquired using the Multiclamp 700b amplifier (Molecular Devices) and digitized to a USB-6221 OEM data acquisition board (National Instruments). Two main hardware modifications to the conventional Scientifica electrophysiology workstation to enable full automation. First, we built a custom two-channel pipette pressure controller. For each pipette, pressure was controlled by a ± 10 psi regulator (QPV1TBNEEN10P10PSGAXL, ProportionAir) using an analog (0–10 V) control signal. The control signal for each regulator was generated by a microcontroller (Arduino Uno, Arduino) via a digital-to-analog converter (MAX539, Maxim Integrated).

2.2.2 Fully automated patcherBot software

A finite state machine architecture was implemented to repeatedly patch-clamp user-selected cells. The software (written in LabVIEW, National Instruments) interfaces with MATLAB, communicates with the stage, manipulators, and pipette pressure controller with a serial interface, and communicates with the amplifier using an ActiveX interface. Further details of this software, as well as executable files can be found at autopatcher.org.

2.2.3 Push-to-clean software for automated pipette cleaning

For experiments that require manual control of the patch clamp experiment, but could still benefit from the improvements in efficiency offered by pipette cleaning a

simplified Labview program for pressure and micromanipulator control only has been developed, known as “push to clean” automation (Figure 8).

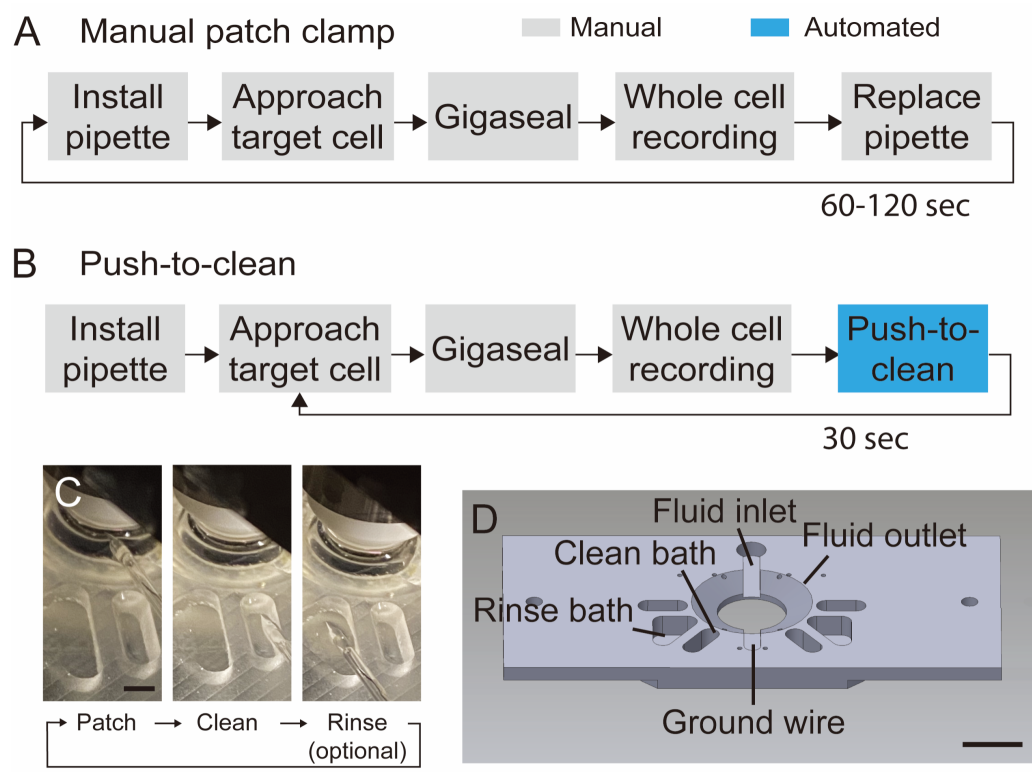


Figure 8. Pipette cleaning methods. A) Process flow chart for traditional manual patch clamping without pipette cleaning. Removing, filling, and installing fresh pipettes takes between 60-120 s. B) Process flow chart for manual patching with automated cleaning (“push-to-clean”). Automated cleaning can be run in as little as 30 s. C) Close up images of pipette being moved from experimental chamber (left) to cleaning bath (middle) to rinse bath (right) before returning to the experimental bath to patch another cell. Scale bar is 25 mm. D) Custom experimental chamber for pipette cleaning featuring fluid inlet and outlet, inset for ground wire, and external baths for cleaning and rinsing solutions. Scale bar is 1 cm.

2.2.4 Pipette cleaning procedure

Pipette cleaning is a robust, simple process involving the following steps: (1) attempt whole cell patch clamp recording, (2) retract patch clamp pipette and move towards bath containing cleaning solution, (3) with tip submerged in cleaning solution, cycle

positive and negative pressures to remove cell debris from pipette tip, (4) position pipette over new target cell for second patch clamp attempt, and (5) repeat steps 1-4 until experiment is completed or the pipette fails (*e.g.*, tip breakage, clog, evaporation of cleaning solution, or user error). This protocol, along with the hardware and software developed to support it, make it straightforward to implement pipette cleaning in any patch clamp electrophysiology experiment.

For cleaning with Tergazyme, a cleaning solution was prepared from 2% w/v Tergazyme solution in room temperature deionized water. Solution was stored in a syringe with a 0.2 μm filter and 23G needle to add to the cleaning bath milled into the experimental chamber. Because Tergazyme is an enzymatic detergent, the enzymatic component degrades over time. The manufacturer recommends making fresh solutions and using them within 8 hours for maximum efficacy.

2.2.5 Cell culture methods

Human embryonic kidney (HEK293T) cells (American Type Culture Collection, Manassas, VA) were cultured according to manufacturer's protocols. For patch-clamp recording, cells were grown on glass coverslips coated with poly-L-lysine (12 mm diameter, No.2, VWR), and used within one week of passage. Cells were only transfected for the ChR2 pilot experiment.

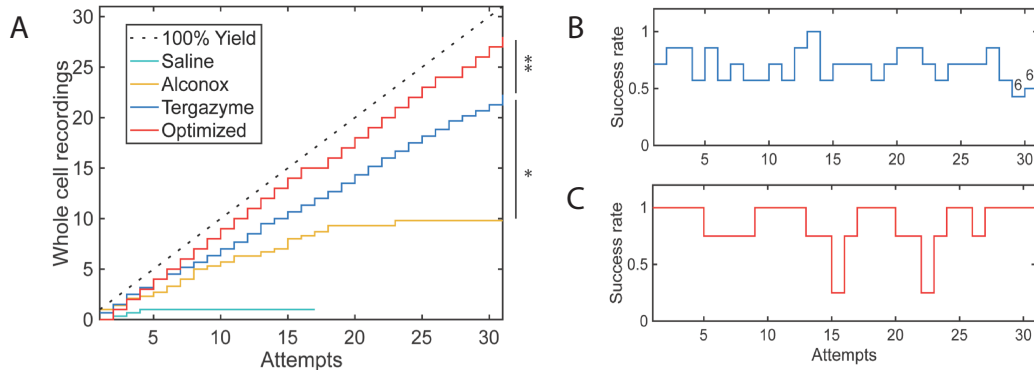


Figure 9. Improvements to pipette cleaning. A) Each trace represents the number of whole cell recordings in HEK 293 cells as a function of number of recording attempts with a single pipette. Each trace is the average of at least 3 pipettes. Saline trace is a negative control (*i.e.*, cleaning solution replaced with extracellular solution) and 100% theoretical maximum is included for reference. Alconox trace shows performance of 2% w/v Alconox cleaning decreasing as a function of number of attempts. Tergazyme trace shows no decrease in yield for 30 attempts with 2% w/v Tergazyme. Optimized trace represents 2% w/v Tergazyme cleaning with optimized pipette positioning relative to the cell surface for gigasealing. Tergazyme performance is superior to Alconox (*, $P = 1.375E-5$, Kolmogorov-Smirnov test). Optimized performance is superior to Tergazyme (**, $P = 0.04368$, Kolmogorov-Smirnov test). B) Success rate of whole cell patch clamp as a function of number of cleans using 2% w/v Tergazyme shows no significant decrease in likelihood of subsequent whole cell recording (Odds ratio (OR) = 1.0067, CI: 0.97-1.04, $P = 0.69$, $n = 215$ attempts, each attempt is for $n = 7$ pipettes, except attempts 29 and 30, which are marked $n = 6$). C) Optimized indentation with Tergazyme cleaning shows no significant decrease in likelihood of subsequent whole cell recording (OR = 1.00, CI: 0.94-1.06, $P = 0.95$, $n = 124$ attempts, each attempt is for $n = 4$ pipettes).

2.2.6 Single-blinded experimental design

A single-blinded trial design was used to compare the performance of pipette cleaning over 30 patch clamp attempts with a single pipette in HEK 293T cells (Figure 9). Briefly, borosilicate pipettes were pulled immediately prior to each experiment using a horizontal puller (P-97, Sutter Instruments) to a resistance of 5–7 M Ω . The intracellular solution was composed of (in mM): 120 KCl, 2 MgCl₂, 10 EGTA, 10 HEPES (pH: 7.2–7.3, 290–300 mOsm) and recordings were performed at room temperature with ACSF: (in

mM) 161 NaCl, 10 HEPES, 6 D-Glucose, 3 KCl, 1 MgCl₂, 1.5 CaCl₂ (pH: 7.4). While the patcherBot ran unattended, a user was monitoring progress at ~10-minute intervals to ensure that no pipettes were broken and to determine when and how a trial reached failure. 3 trials were performed for each solution (2% w/v Tergazyme, 2% w/v Alconox, and ACSF) and the experimenter was blinded to the identity of each cleaning solution. Each trial began by selecting 30 cells suitable for patching from a coverslip of HEK 293T cells and adding the cleaning solution to the cleaning dish. In cases where no gigaseals were observed over 8-10 attempt the trial was ended.

To further demonstrate the utility of blinded experimental designs using the patcherBot and Tergazyme cleaning, we experimentally validated that gigaseal probability is related to distance between the pipette and membrane. We found a strong relationship between distance and gigaseal probability which reached ~100% at a range of 1-2 μm below the cell surface (defined as the z-axis point where pipette resistance increased 0.1 M Ω from initial resistance) (W. Stoy et al., 2020). When the patcherBot was programmed to attempt gigasealing at this position, whole cell recording yield increased significantly, as shown in the “Optimized” trace of (Figure 9) ($p = 0.044$, Kolmogorov-Smirnov test).

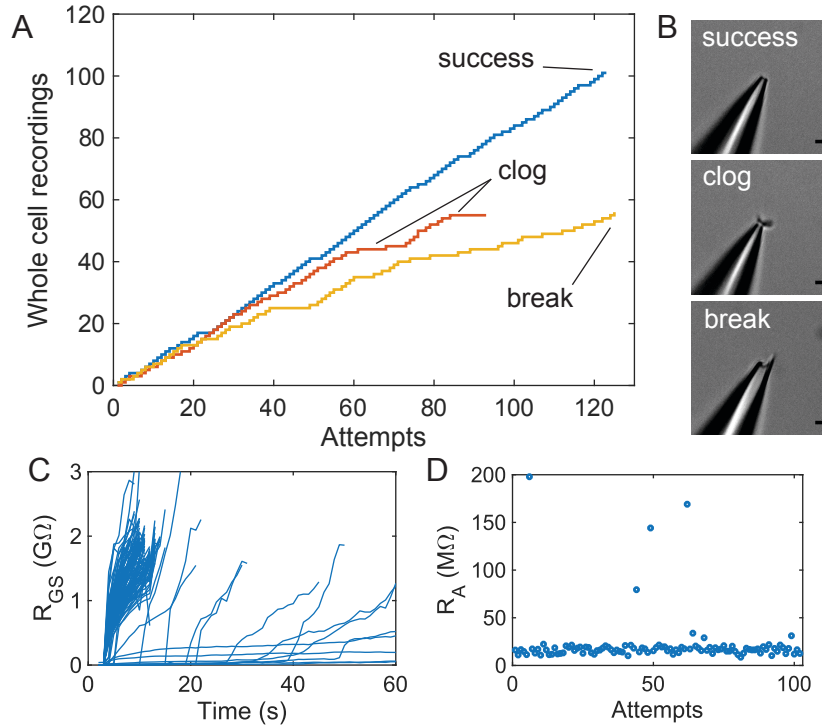


Figure 10. Upper limits of pipette cleaning with 2% w/v Tergazyme. A) Yield curves for individual pipettes showing cleaning for over 90 recording attempts with associated failure modes. “Success” trace shows effective pipette cleaning, “clog” trace shows reversible pipette tip clogs that cause low yield over time, and “break” trace shows experiment terminated by broken pipette tip. Theoretical maximum (100% yield) included for reference. B) Representative pipette images taken at 40× magnification for each failure mode in (A). Scale bar is 1 μm. C) Individual gigaseal resistance traces from “success” trace (n = 122 gigaseal attempts). D) Access resistance of cells recorded in “success” trace (n = 101 whole cell recordings).

2.2.7 Cleaning limits experimental design

In an attempt to identify the failure point of Tergazyme cleaning, a series of experiments were performed to failure in HEK 293T cells. Patching and setup were performed as in the single-blinded trial. Without swapping pipettes, the patcherBot was run continuously by replacing cells and recalibrating the software every 1-2 hours and monitoring the yield and quality of the experiment until a failure point was reached. The following failure modes were defined: 1) cleaning failure (defined as 5 or more sequential

failures to obtain a gigaseal), 2) software failure (i.e., incorrect targeting or failure to detect cell), 3) user error (i.e., fluid levels too low), and 4) pipette failure (i.e., clogging or breaking).

2.2.8 *Opsin screening experimental design*

HEK 293T cells transfected with AAV-CAG-ChR2-GFP using Lipofectamine 3000 transfection reagent. Cells were ready for patch clamp experiment 24-48 hours post-transfection. Cells were visualized using fluorescence microscopy to confirm high levels of expression of green fluorescent protein (GFP) prior to selecting cells using difference interference contrast (DIC) microscopy in the patcherBot software. While recordings were performed automatically and no human interaction with the rig was required, cells were manually stimulated by LED (COOL LED pE-100, 488 nm) to record changes in photocurrent as a function of incident light power. Optical power of the LED was measured prior to the experiment to produce a calibration curve of incident light power in the sample plane.

2.3 **Results and Discussion**

2.3.1 *Tergazyme is superior to Alconox for pipette cleaning*

Cleaning trials with ACSF produced a mean of 1 ± 1.4 whole cells over 16 attempts per trial. Cleaning trials with 2% w/v Alconox produced a mean of 9.7 ± 1.7 whole cells over 27 ± 5.7 attempts per trial. Cleaning trials with 2% w/v Tergazyme produced a mean of 22.3 ± 2.1 whole cells over 30.3 ± 0.9 attempts per trial. Differences between all groups were significant ($p < .01$, Student's t-test). For ACSF and Alconox trials, gigaseals and

whole cell recordings occurred at the beginning of the experiment, with no gigaseals or whole cells forming later in the trial (Figure 9).

There are several explanations for the failure of Alconox cleaning and the superiority of Tergazyme based on the physical and chemical processes occurring during repeated patch clamp attempts and cleaning. This data (Figure 9) supports the following model of pipette cleaning with Alconox:

- 1) After the initial patch clamp attempt, portions of the cell membrane, including lipids and proteins, are attached to the pipette interior and rim. This residual cellular debris makes the glass surface of the pipette rough and prevents close contact with successive cells.
- 2) Pipette cleaning with Alconox emulsifies the lipid component of the cell debris, uncovering the clean glass surface and enabling gigaseal formation on successive cells.
- 3) As Alconox primarily acts on lipids, protein components of the cell membrane remain bound to the pipette surface.
- 4) Over time, this protein debris builds up and fouls the pipette tip after ~15 patch clamp attempts.

Tergazyme cleaning provides the benefits of detergent-based removal of lipids and protease-based degradation and removal of proteins.

During the experiment, over 200 patch clamp attempts were made in less than 3 days of experiments. This type of experiment could not be achieved without the patcherBot and pipette cleaning. Consider the step of filling and replacing pipettes manually, as in

traditional patch clamp experiments. This task requires retracting the pipette, removing the used pipette from the holder, discarding the used pipette in a glass waste container, filling a fresh pipette with intracellular solution, installing the fresh pipette into the holder, and repositioning the pipette under the microscope objective. This is a menial, but highly attentive manual task that patch clamp experimenters perform dozens of times per day. However, this task alone can take 1-2 minutes, meaning that to replicate this experiment manually, the experimenter would spend 3-6 hours alone on the task of replacing pipettes.

2.3.2 Tergazyme cleaning enables over 100 patch clamp recordings with a single pipette

In 4 limit trials of 76.25 ± 37.58 attempts per trial, observed failure modes were pipette failures ($n = 2$) and user errors ($n = 2$), but not failure to clean the pipette (Figure 10). This suggests that trials of over 100 patch attempts are readily achievable, given the proper experimental conditions and practical optimizations. Because typical throughput for patch clamp electrophysiology experiments is in the range of 10-30 recordings per day, it is likely that pipettes only need to be replaced once per day, except in cases where pipettes are broken or clogged.

Using a single pipette cleaned with our improved 2% w/v Tergazyme cleaning solution, we achieved 102 whole cell recordings in 122 patch clamp attempts over a 13 h automated experiment. In our attempts to find the failure point of 2% w/v Tergazyme cleaning, pipette breakage or internal clogs were more likely to cause failure than an inability to clean the pipette. Internal pipette clogs are thought to form from environmental dust of particulates in pipette solution. Clogs tended to form as a function of duration of positive pressure applied and were more likely to occur over long experiments. Clogs can

be diagnosed from flat portions in the yield curve that are unlikely to result from chance. Some clogs are reversible (see representative trace in Figure 10). Pipettes can also fail after a tip breakage, which typically occurs if a target cell is missed. To determine an approximate failure point of cleaning, consider each patch clamp attempt as an independent event with a probability equal to the gigaseal recording failure rate and determine the number of cleaning attempts until the probability is less than or equal to 0.01. For example, with a gigaseal failure rate of 30% (*i.e.*, gigaseal success rate = 70%), the likelihood of a sequence of 4 failures to gigaseal has a probability of <1%.

These experiments suggest that using Tergazyme cleaning enables an entire day's worth of patch clamp experiments to be performed with a single pipette. In theory, fully automated all-day (>8 hours) experiments are possible with this technique, especially if integrated with temperature and humidity controls to maintain cell health over time. In typical cell culture and acute slice preparations, cells are maintained at room temperature in saline solutions, and typically become unhealthy and die within 3-4 hours. Further improvements in pipette materials (*i.e.*, quartz or silica) and development of storage and clog minimization techniques for cleaned pipettes could result in infinitely reusable patch clamp pipettes.

2.3.3 Tergazyme cleaning enables high throughput automated characterization of opsins

To demonstrate the ability of Tergazyme cleaning to enable a single patch clamp pipette to perform high throughput functional electrophysiology screens, we performed a pilot experiment using ChR2-transfected HEK 293T cells (Figure 11). In this experiment, the patcherBot was able to obtain whole cell recordings with photocurrent measurements

in 46/51 attempts in a total of 313 minutes of unattended operation. This represents the longest unattended operation time and highest yield recorded on the patcherBot to date in a single experiment.

There is broad applicability for techniques that improve the throughput of patch clamp studies for high content screens. These experiments range from protein engineering to drug discovery and can involve integrating measurements from many other experimental systems. Often, patch clamp-based screens are carried out by dedicated personnel whose experimental throughput is one of the limiting factors of these experimental pipelines. Often, the throughput of manual patch clamp experiments does not match the throughput of other techniques such as imaging, genomics, or proteomics (Piatkevich et al., 2018). As an example, our collaborators in the Boyden lab at MIT undertook a project to discover a red-light sensitive opsin to enable activation of neurons in deep tissues (Chuong et al., 2014). Of the many thousands of variants they characterized, only 120 variants were able to be screened by patch clamp, a critical measurement to determine opsin kinetics and photocurrent. Using the patcherBot with Tergazyme cleaning, we are currently working with the Boyden lab to screen 1000s of variants to uncover previously unknown variants to engineer near-IR sensitive opsins, selective potassium channels, and other long-desired tools for neuroscience discovery.

2.3.4 Future applications of Tergazyme pipette cleaning

Pipette cleaning with Tergazyme provides two critical improvements over manual pipette replacement and existing methods of pipette cleaning that are of interest to the electrophysiology community. First, pipette cleaning with Tergazyme increases the

throughput of patch clamp experiments by cleaning and reinserting pipettes faster than manual pipette replacement. This will enable long, unattended patch clamp experiments as well as the parallelization of patch clamp experiments. Because a cleaning-enabled automated patch clamp rig only requires a few minutes to calibrate, a single experimenter can theoretically operate multiple rigs simultaneously (N.B., I performed the initial manual patch clamp recordings in intact brain organoids while using the patcherBot to collect data in HEK 293T cells for another study). Based on a setup time of ~15 minutes per rig and an unattended operation time of 2-3 hours, a single experimenter could operate 8-12 electrophysiology rigs simultaneously.

Second, pipette cleaning removes variation in recordings associated with variability in pipette fabrication. Pipette cleaning with full automation further removes the variable of experimenter skill and attention (Figure 7). This could facilitate experiments that are more statistically powerful and efficient in their design and eliminate the differences that exist in the experimenter to experimenter, rig to rig, and lab to lab performance of patch clamp methods. Multiple laboratories implementing this technology could share standardized methods and parameters for each experimental setting, greatly enhancing the efficiency and reproducibility of patch clamp methods.

Third, pipette cleaning potentially enables the wider use of pipette-based integrated devices. Because of their unparalleled access to single cells in intact brain tissue, patch clamp pipettes have long been considered as possible platforms on which to build tools for multi-modal measurements (Hunt et al., 2019). These devices typically involve building or attaching devices such as multi-site electrodes, ring electrodes, carbon fiber electrodes, or optic fibers to the patch clamp pipette. The most successful of these devices are ones that

do not rely on bonding to the glass pipette itself, such as devices where optic fibers are integrated into the pipette holder (Ozden et al., 2013). Devices that require bonding between the glass pipette and the integrated device are considerably more challenging to implement. The fabrication of these devices, as recently detailed by the Harris and Barbic labs (Hunt et al., 2019), has been greatly improved in recent years (**Error! Reference source not found.**), but each pipette still requires time and effort to fabricate, often taking as long or longer to prepare the pipette (20-25 minutes) than a single *in vivo* single cell recording (20-30 minutes, ideally). Further, because the yield of patch clamp recordings *in vivo* is typically 50% or less, depending on target regions and preparation, a significant proportion of fabricated devices will be discarded with no useful data. The ability to clean pipettes could greatly extend the utility of these methods and reduce the associated time and cost of these challenging experiments.

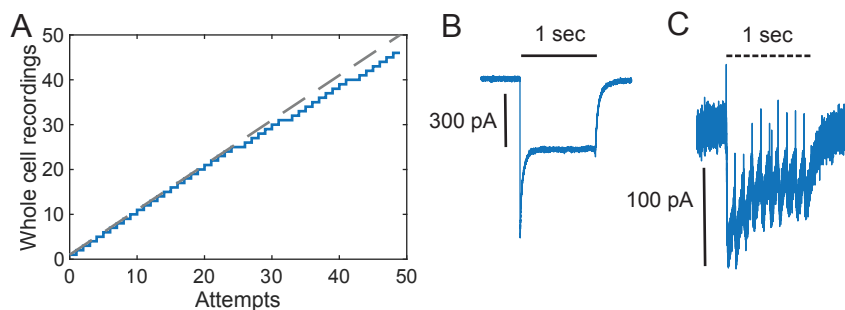


Figure 11. High-throughput opsin screening with pipette cleaning. A. Yield curve for a single pipette channelrhodopsin-2 (ChR-2) characterization experiment (46/51 attempts, 90% yield). B. Representative photocurrent trace (voltage clamp) in response to initial pulse of 500 ms 480 nm LED pulse recorded from transiently transfected HEK 293 cell showing large peak photocurrent response. C. Representative current response of ChR2 to rapid 10 msec pulses of 488 nm light.

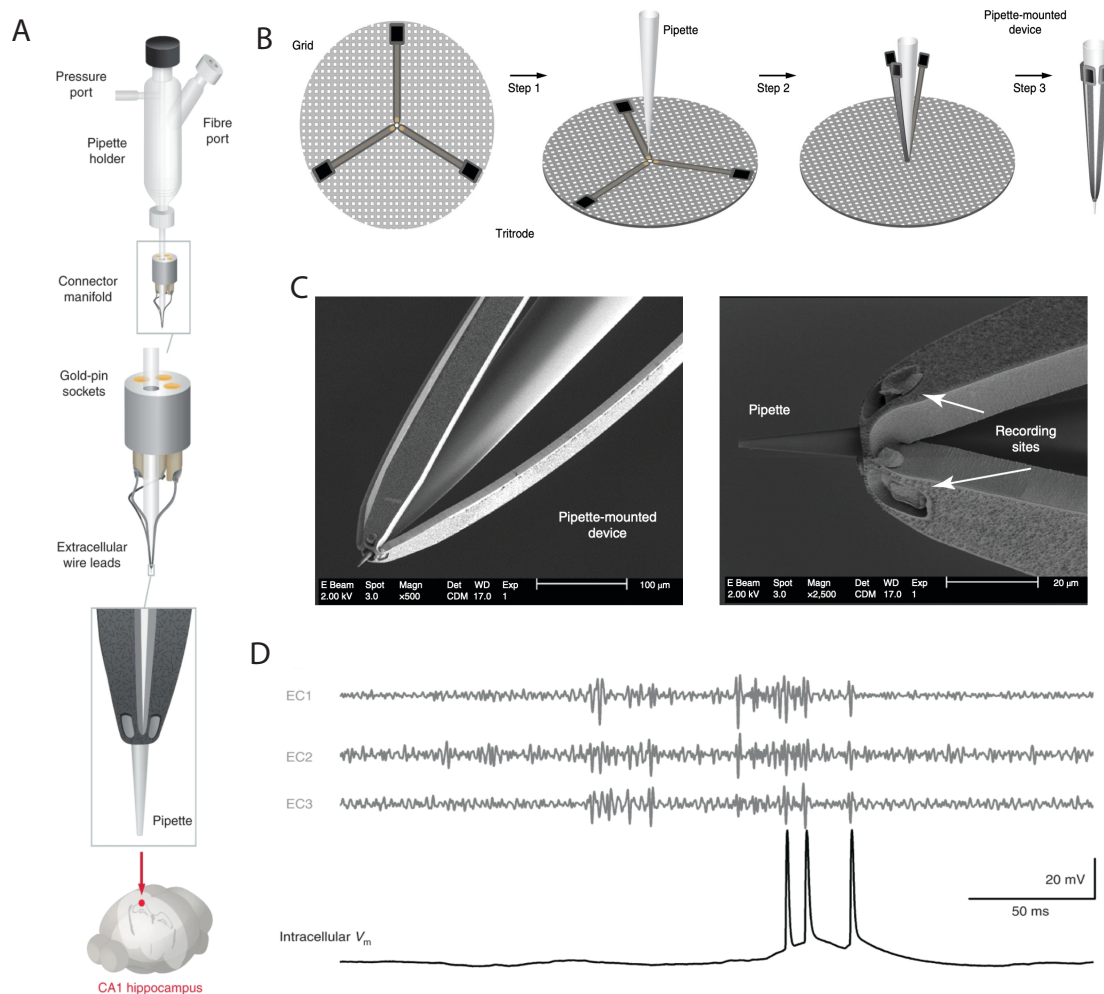


Figure 12. Pipettes as integrated devices. A) Schematic depicting the elements of an integrate Patch-Titrode device used to record simultaneous extracellular and intracellular activity in the mouse brain in vivo. B) Schematic showing process of mounting flexible electronics onto patch clamp pipette. Each pipette takes 20-25 minutes to fabricate C) Low (left, 500x) and high (right, 2500x) electron micrographs of pipette with mounted flexible electrodes. D) Demonstration of the Patch-Titrode in vivo recordings. Top traces are extracellular recordings from each of the three electrode sites integrated into the pipette and the lower trace shows a burst of action potentials recorded in current clamp. Figure adapted from (Hunt et al., 2019).

CHAPTER 3. Patch Clamp Recordings in Intact Human Brain Organoids

3.1 Introduction

Human brain organoids show complex features of human neurological development within a 3D tissue environment, but studies of single cell electrophysiology in human brain organoids offer no ability to perform these experiments in that 3D, intact organoid experimental setting. Here, I demonstrate the first known patch recordings from below the surface of an intact human brain organoid and develop methods to perform these recordings reliably using manual and automated approaches.

3.1.1 Patch clamp methods in human brain organoids

While there are many experimental methods to study human neuronal development, one of the gold standard methods is patch clamp electrophysiology (Hamill et al., 1981). Patch clamp delivers unparalleled electrical and temporal resolution and its single cell access provides researchers with the opportunity to deliver materials to cells (e.g., dyes or drugs) as well as extract cell contents (e.g., DNA, RNA, or proteins) (Cadwell et al., 2015; X. Jiang et al., 2015b). Intracellular recordings from patch clamp studies are useful to define electrophysiological cell types and form the foundation for multi-dimensional classification systems that incorporate electrophysiology, morphology, and gene expression at the single cell level (Cadwell et al., 2020; Y. Peng et al., 2019). Towards this long-term goal of scalable multi-dimensional studies of neurons in human brain organoids, we have developed a simple method for performing whole cell patch clamp recordings

throughout intact (i.e., unsliced) human brain organoids. While traditional organoid electrophysiology experiments use acute slices or dissociated cultures, these methods reduce the synaptic connectivity that develops within brain organoids and alter relevant properties such as excitability. Despite these concerns, the overwhelming majority of brain organoid studies focus on acute slices or dissociated cells, not intact organoids. In fact, groups that have attempted this method have described it as “technically impossible” (Renner et al., 2020).

While not impossible, patch clamping in intact brain organoids is challenging for several reasons: 1) intact brain organoids are thick tissues (i.e., >1 mm thick) and do not allow light to penetrate, 2) the shape of intact brain organoids is non-uniform and makes them difficult to hold in place for experiments, 3) brain organoid neurons are small (i.e., ~5 μm in diameter), and (4) the tissue is soft and more fluid than brain tissue. Despite these obstacles, the ability to study organoid electrophysiology in an intact system presents a unique model for neuroscience. Intact brain organoids maintain local- and long-range connectivity, and while it is unlikely that an organoid model will completely replicate an *in vivo* brain circuit, it is possible that certain features (e.g., preferential wiring between cell types, layers, or clonally related cells) are preserved in the genetic program and expressed in organoid tissue. Further, the random structure of brain organoids makes it unlikely that acute slices preserve a predictable percentage of local connections without damage associated with the slicing process. Acute slice procedures in the mouse brain are highly optimized to reduce this type of damage and preserve local circuits (i.e., cortical columns), but this relies the anatomical regularity of the mouse brain, which is not yet a feature of brain organoids (Barth et al., 2016; X. Jiang et al., 2016). The preservation of

these connections, along with the lack of slicing-associated cellular damage, makes the intact organoid model ideal for studying the ways that electrophysiological signaling occurs in these self-assembled *in situ* human neural circuits. While there are drawbacks to the model, including a difficulty of visually identifying cells and the need for specific types of input and activity to build more *in vivo*-like circuits, the potential for the intact brain organoid model to capture the human genetics behind specific patterns of circuit formation and synaptic activity inherent in neurological diseases shows a clear need for robust experimental methods for this system.

3.1.2 Electrophysiology approaches for intact tissues

There is a general interest in understanding the cellular and network electrophysiology of brain organoids, but the challenges associated with this new model system pose challenges for each method and have produced some creative solutions that are currently being tested throughout the field. Results, drawbacks, and technical limitations are summarized briefly Table 1.

Table 1. Methods for patch clamp recordings in human brain organoids.

Organoid preparation	Pros	Cons	Reference
Dissociated cell culture	Simple experimental design, dissociated cells retain some	Dissociated cells do not represent the connections and locations of cells in intact tissue	(Mariani et al., 2015b)

	features of 3D tissue		
Acute organoid slices	Utilizes common methods for brain slicing and patching, tissue slices show some features of intact tissue	Damage to cells and connections sustained during slicing are unpredictable	(Birey et al., 2017b)
Intact organoids	Cells exist within intact self-assembled networks and tissue microenvironment	Lack of methods, difficulty holding tissue in place, lack of visual access to sub-surface cells	(Mariani et al., 2015a; Renner et al., 2020)

As previously discussed, patch clamp methods are underutilized in the literature when compared to other single cell techniques, especially genetics. However, there is a base of researchers using dissociated cells and acute slices from human brain organoids. These researchers have developed recording solutions and protocols specific to organoid cells that can be easily transferred to studies with intact systems (Birey et al., 2017a; Mariani et al., 2015b; Qian et al., 2016a; Renner et al., 2020). Because the methods

described here can be performed blind, there is no additional need for optics to visually guide patching, decreasing the barrier to adopting this technology.

Another potential method is to record extracellular activity using multiple electrode arrays (MEAs). These extracellular electrodes take different forms and can be inserted into the tissue as an array or exposed to the organoid surface as a planar electrode array (Quadrato et al., 2017; Trujillo et al., 2019). These techniques produce recordings that are representative of local field potentials and cover large sections of the tissue, but are difficult to position and offer limited flexibility when integrating with other techniques. Additionally, some of these techniques rely on slicing the organoids to reveal a flat plane of cells for better contact with electrodes. Notably, well plate-based MEA systems, such as those manufactured by Axion Biosystems, are compatible with optogenetic stimulation of samples, which could provide a powerful tool for activation and inhibition of specific organoid cell types (Trujillo et al., 2019).

Multisite silicon probes are a similarly promising option for measuring extracellular activity. Rather than placing the organoid on top of the electrode, the electrode is inserted into the tissue using a micromanipulator, similarly to patch clamp recordings (Quadrato et al., 2017). These electrodes are useful in that they can be positioned nearby other electrodes or cells of interest and can offer higher resolution single unit recordings. However, the size of the electrode itself may cause damage to the tissue.

Optical techniques to measure cell activity such as calcium imaging and voltage imaging have potential to be applied broadly to intact human brain organoids. These methods enable recording signals from many neurons simultaneously and can be used for

chronic studies of electrophysiological development (Renner et al., 2020; Trujillo et al., 2019). However, dyes used for imaging may be toxic to some cells and systems to control the expression of exogenous proteins in brain organoids is still under development. Further, because of the three-dimensional nature of intact human brain organoids, care must be taken to avoid interference from out-of-plane light.

Finally, mesh electronics have recently been tested in intact human brain organoids to record electrical signals during development. These methods rely on a flexible net of electrodes being embedded into the tissue at the early stages of organoid generation (Floch et al., 2021). The flexible electrodes are capable of stretching as the tissue grows and could, in theory, provide a chronic system for recording the development of network activity. This nascent technology has faced challenges with implementation in existing model systems based on the insertion of electrodes, among other technical challenges (Duan et al., 2013), but seem ideally suited to intact brain organoid models.

3.1.3 Electrophysiological development in human brain organoids

Whether human brain organoids can fully recapitulate the complex electrical network present in the human brain is unsure, but it is likely that the organoid systems will accurately capture specific pieces of the complexity of the brain. One notable challenge is that neural circuits develop based upon activity and sensory input. That activity shapes the formation of synapses, maturation of neurons, and gene expression. Because brain organoids develop according to self-assembly with no physiological sensory input, it is likely that their networks develop along different pathways than *in vivo* brains. Additionally, different regions of the organoid may develop at different rates, leading to

different levels of gene expression, especially those controlling the amount and location of ion channels. Despite these challenges and limitations, promising results suggest that brain organoid cells and circuits appear to develop similarly enough to *in vivo* brains to generate and test hypotheses about the nature of human brain development (Quadrato et al., 2017; Trujillo et al., 2019; Velasco et al., 2019b).

3.1.4 Challenges for patch clamp recordings in intact human brain organoids

Brain organoids represent a significant improvement over two-dimensional hiPSC culture systems for a range of experiments, including cell migration, tissue laminarization, and gene expression studies (Birey et al., 2017b; Matsui et al., 2018; Oliveira et al., 2019). The presence of functional synapses, a range of cell types, and oscillatory electrical activity suggest that brain organoids are also a potentially useful model for patch clamp electrophysiology. However, the overwhelming majority of brain organoid studies focus on acute slices or dissociated cells, not intact organoids (Mariani et al., 2015c; Qian et al., 2016b). This is presumably for several reasons. First, intact brain organoids are thick tissues (i.e., >1 mm thick) and light does not penetrate the tissue for visual tracking of pipettes and neurons. Second, intact brain organoids are roughly spherical aggregates that are difficult to hold in place for experiments. Third, brain organoid neurons are significantly smaller than neurons commonly used for patch clamp studies (e.g., brain organoid neuron diameter = $5.5 \pm 1.1 \mu\text{m}$, mouse V1 pyramidal cell diameter = $15.6 \pm 0.27 \mu\text{m}$, $p < 0.0001$, Student's t-test) and the tissue is more fluid than mouse brain tissue (i.e., cells move away from pipettes more quickly than in mouse brain tissue) (Renner et al., 2020). Despite these obstacles, the ability to study organoid electrophysiology in an intact system presents a unique model for neuroscience. Intact brain organoids maintain all

local and long-range connectivity, and while it is unlikely that an organoid model will completely replicate an *in vivo* brain circuit, it is possible that certain important features like synapse formation are preserved in the genetic program and expressed in a three-dimensional tissue (Goda & Davis, 2003; Ransohoff & Stevens, 2011). The random structure of brain organoids makes it unlikely that acute slices preserve a predictable percentage of local circuits without damage associated with the slicing process (Qian et al., 2016b). Acute slice procedures in the mouse brain are highly optimized to reduce this type of damage and preserve local circuits (i.e., cortical columns) as well as individual dendritic arbors and axonal projections, but this relies on the anatomical regularity of the mouse brain, which is not yet a feature of brain organoids (M. A. Lancaster et al., 2017). The preservation of these connections, along with the lack of slicing-associated cellular damage, makes the intact organoid preparation ideal for studying the ways that electrophysiological signaling occurs in these self-assembled *in situ* human neural circuits. While there are drawbacks to the model, including a difficulty of visually identifying cells and the need for specific types of input and activity to build an *in vivo*-like circuit, the ability of the intact brain organoid preparation to capture the human genetics behind specific patterns of circuit formation and synaptic activity inherent in neurological diseases shows a clear need for robust experimental methods for this experimental preparation.

3.2 Methodology

3.2.1 Fixturing of intact human brain organoids for patch clamp experiments

Intact organoids were transported from the rotating bioreactor or well plate using a wide Pasteur pipette and placed in the experimental chamber containing extracellular

solution with no perfusion. If the organoid is large (i.e., > 1 mm diameter), it requires an agarose support to prevent damage from the weighted harp. Briefly, a 1% agarose solution in extracellular solution was prepared and kept in liquid form (~40 °C). Melted agarose was poured onto a cooled block using a cylindrical tube to maintain shape. After ~5 seconds of cooling, a brain organoid was placed onto the surface of the agarose solution and the entire assembly was rapidly cooled using a metal clamp at ~0 °C. The disk of solidified agarose containing the brain organoid was then transported to the experimental chamber. The agarose disk can then be held in place by a weighted harp. To test whether the organoid is secure, perfusion of the chamber was initiated, and the organoid was monitored to observe any possible movement of the tissue under the weighted harp.

To evaluate different fixturing methods, intact human brain organoids of varying sizes were imaged from either a top-down or a side-view imaging system. Top-down images were obtained using a EVOS XL Core microscope (ThermoFisher Scientific) equipped with 4x, 10x, and 20x objectives under brightfield imaging conditions (**Fig. 6D-F**). Side-view images were obtained with a USB camera mounted to a glass-sided chamber (Microsquisher, CellScale) (**Fig. 6A-C**). To measure the amount of tissue disruption caused by each fixturing method, organoids were imaged at multiple stages: 1) before fixturing, 2) partially embedded in agarose disk, 3) partially embedded in agarose disk with weighted harp, 4)

3.2.2 *Patch clamp methods for intact human brain organoids*

Both manual and robotic systems were based on commercially available patch clamp electrophysiology rig (SliceScope Pro 3000, Scientifica Ltd). The rig features two

motorized PatchStar micromanipulators (Scientifica, Ltd.) mounted on a motorized stage. Differential interference contrast (DIC) optics included a 40x objective (LUMPLFL40XW/IR, NA 0.8, Olympus), an infrared light-emitting diode (Scientifica), and a Rolera Bolt camera (QImaging). Perfusion of the sample was accomplished with a peristaltic pump (120S/DV, Watson-Marlow) and a vacuum system (Vacuubrand 1C). Recordings were acquired using a Multiclamp 700B amplifier (Molecular Devices) and digitized using a USB-6221 data acquisition board (National Instruments). For automated recordings, we used a two-channel pressure control system that has been described in detail elsewhere (Kodandaramaiah et al., 2016; Ilya Kolb et al., 2019).

Experiments were performed based on previous methods for brain organoid patching and automated patch clamping *in vivo* and in brain slices (Ilya Kolb et al., 2019; Qian et al., 2016b; W. A. Stoy et al., 2017). Briefly, pipettes were pulled to 5-10 M Ω on a horizontal puller (P-97, Sutter Instruments) and filled with (in mM): 135 K-gluconate, 10 HEPES, 0.1 EGTA, 10 phosphocreatine, 4 ATP, and 0.3 GTP. Extracellular solution was prepared and bubbled with 95% carbon dioxide, 5% oxygen during experiments. Extracellular solution contained (in mM) 125 NaCl, 25 NaHCO₃, 25 D-glucose, 3 KCl, 2 CaCl₂, 1.25 NaH₂PO₄, and 1 MgCl₂. Experiments were performed at room temperature with constant perfusion. In order to increase the efficiency of brain organoid experiments, we employed pipette cleaning to eliminate the need to manually replace and recalibrate pipettes after each patch attempt (I. Kolb et al., 2016; Ilya Kolb et al., 2019). Pipette cleaning was performed using a custom-made experimental chamber with exterior baths for cleaning and rinsing as well as the two-channel pressure system used for automated

patching. Experiments used 2% w/v Alconox or 2% w/v Tergazyme cleaning solutions and typically involved 8-12 patch clamp attempts per pipette.

3.2.3 *Manual patch clamp methods for intact human brain organoids*

Manual patch clamp recordings were performed in a traditional manner, similar to blind *in vivo* patch clamping in the mouse brain (Figure 13). Briefly, the pipette was positioned directly above the surface of the tissue and the location was noted. Under high positive pressure from a syringe measured with a digital manometer (Dwyer), the pipette was driven into the tissue until the target region for surface (0-10 μm) or subsurface (>10 μm) recordings was reached. High positive pressure was then released, and the pipette was slowly advanced through the tissue until a sharp increase in resistance, indicating contact with a neuronal membrane, was observed (**Fig. 2B**). Once a cell was detected, the pipette was set to atmospheric pressure and gigasealing was attempted. If gigaseal formation was not immediate, suction was applied by syringe or mouth until a gigaseal was achieved (**Fig. 2C**). Once a stable gigaseal state was reached, short pulses of strong suction were applied by mouth or syringe to break into the neuron and achieve the whole cell recording configuration.

3.2.4 *Automated patch clamp methods for intact human brain organoids*

Sequential automated patch clamp recordings were performed using the patcherBot (Figure 13). Automated patching was performed as described previously slices with modifications to allow cell detection and gigaseal formation in intact brain organoids (Ilya Kolb et al., 2019). Critically, neuron hunting was performed at a low positive pressure (+20 mbar) and the cell detection threshold was set at a high level (0.18-0.2 M) (**Fig. 2B**) relative

to iterations of the patcherBot developed for HEK 293T cells and mouse brain slices (Ilya Kolb et al., 2019). To enable semi-blind patching, pipette to camera calibration was performed beside the intact organoid and target regions for neuron hunting were defined relative to the organoid surface.

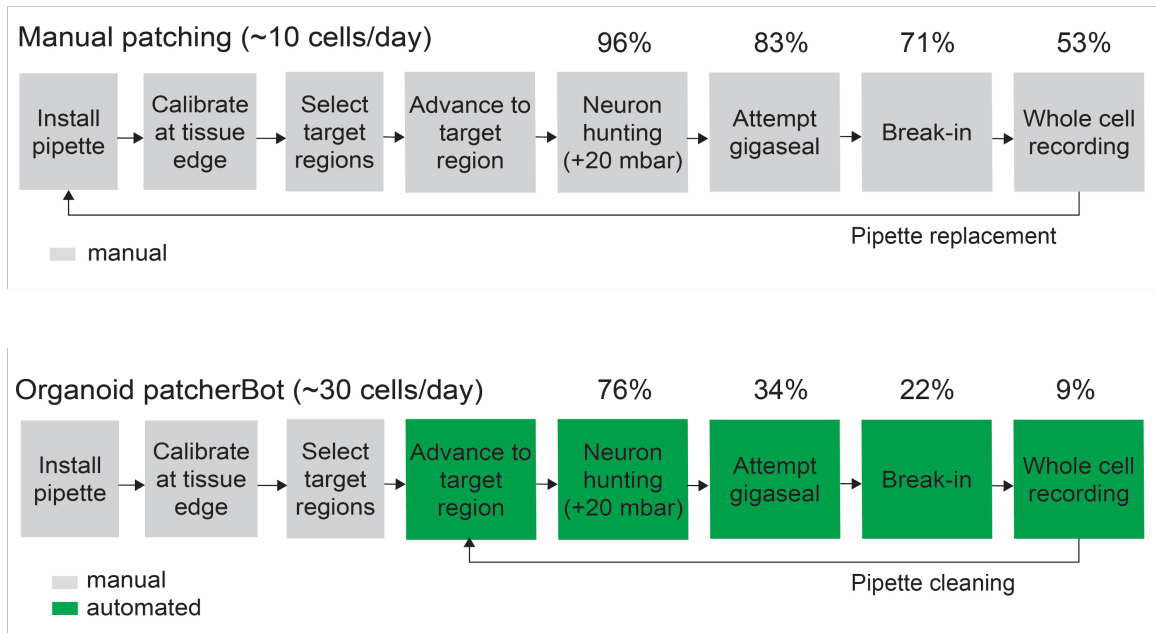


Figure 13. Flow chart showing process and experimental yield from manual and automated patch clamp experiments in intact brain organoids. All recordings were performed on intact control organoids (lines 11C1 and C-3-1) between 80-130 DIV.

3.3 Results and Discussion

3.3.1 Fixturing of intact human brain organoids for patch clamp experiments

We found that for some young organoids (i.e., <90 days *in vitro* (DIV), <1 mm diameter), a weighted harp was sufficient to keep the tissue in place (SHD-42/15, Warner Instruments). These weighted harps, typically a metal ring with nylon fibers stretched across the tissue, are a method of choice for many acute slice experiments (Ting et al., 2018). However, we found that larger brain organoids (~120 DIV, >1 mm diameter) were

either compressed or completely cut by the parallel strings of the harp (Figure 14B,E). Because cutting the tissue or significantly compressing it could cause damage to cells and connections, we developed a method to reduce the strain on large tissues by supporting them with an agarose base. By partially embedding the brain organoid into a 1% agarose slab and then covering the slab with a metal harp, large organoids can be held in place for patch clamp experiments. We found that the harp plus agarose fixturing method held organoids in place while minimizing change in area when compared to traditional weighted harp fixturing (Figure 14). Percent area change for traditional harp fixturing and harp plus agarose fixturing was $30.4 \pm 27.3\%$ and $5.6 \pm 4.5\%$, respectively ($p = .0475$, Student's t-test).

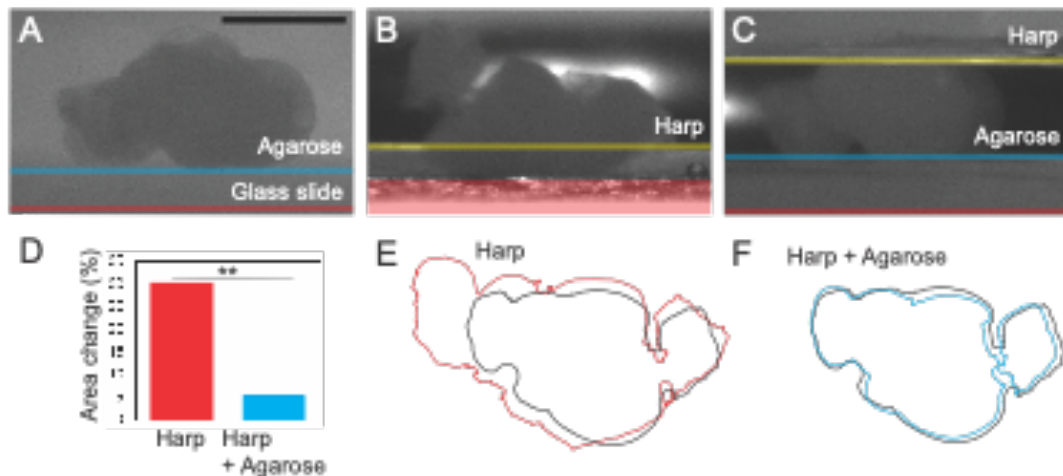


Figure 14. Fixturing methods for intact human brain organoids. (A) Side-view image of a large (1-2 mm) human brain organoid resting on a layer of 1% w/v agarose. (B) Damage caused to human brain organoid by traditional fixturing method of a hard surface and a weighted harp with low clearance. (C) Modified fixturing method preserves shape of intact organoid using a high clearance weighted harp and a layer of 1% w/v agarose to minimize area change in tissue. Scale bar for (A,B,C,E, and F) is 1 mm. (D) Harp and agarose method reduces the area change in organoids compared to harp only method from $30.4 \pm 27.3\%$ to $5.6 \pm 4.5\%$ ($p = .0475$, Student's t-test, $n = 6$ organoids). (E-F) Representative shape outlines show

changes in organoid area for each method (black = unfixtured, red = fixtured with traditional harp, blue = fixtured with harp and agarose).

3.3.2 Performance of manual and automated patch clamp in intact human brain organoids

Next, we applied the practical skills gained from manual experiments with intact brain organoids to our existing automated patch clamp robot, the patcherBot (Figure 13) (Ilya Kolb et al., 2019). Interestingly, we found that even after adjusting system parameters to better match the smaller, younger cells and softer tissue we observed in our manual experiment, the organoid patcherBot performed at a lower yield than manual patching at all stages (neuron hunting – 124/181 attempts, 69%, $p < 0.001$, Fisher’s exact test; gigaseal – 54/181, 54%, $p < 0.001$, Fisher’s exact test; break-in – 32/181 attempts, 18%, $p < 0.001$, Fisher’s exact test; whole cell - 11/181 attempts, 6%, $p < 0.001$, Fisher’s exact test). However, the increases in throughput enabled by automation with pipette cleaning make these experiments more efficient than traditional manual patch clamp experiments in terms of minutes per attempt (manual – 18.8 ± 11.4 minutes per attempt, automated – 10.9 ± 10.0 minutes per attempt, $p < 0.001$, Student’s t-test). The reason for this gain in efficiency is simple – the patcherBot enables time-intensive manual tasks like pipette replacement, filling, and installation to be performed automatically, bringing the downtime between patch clamp attempts to ~60 seconds. Further, the ability to complete patch attempts quickly in an automated fashion enables rapid iteration and improvement of patching methods. We expect that yields for automated patching can be improved further for intact

organoids, as has been done for HEK 293 cells and other preparations (Ilya Kolb et al., 2019).

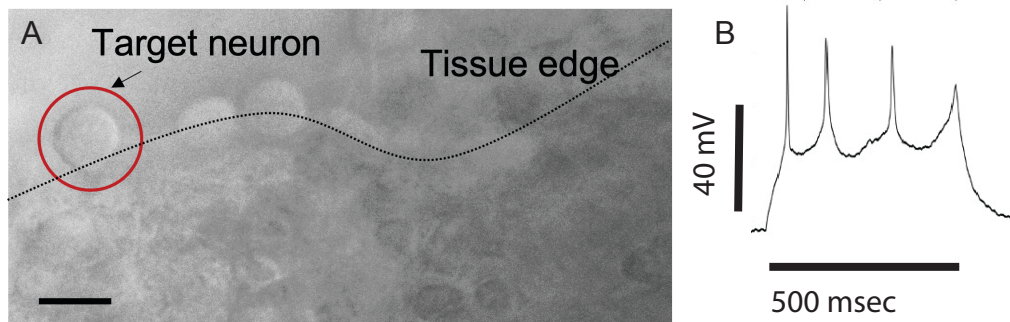


Figure 15. Patching cells on the surface of intact organoids. A) Target organoid cell on the surface of the tissue. Scale bar is 25 μm . B) Representative recording of mature organoid neuron (120 DIV) recorded at the tissue surface firing multiple action potentials.

Building upon previous reports of successful patch clamp recordings being performed on cells that were at the outer edge of an intact organoid, we first attempted manual recordings on the surface (0-10 μm from the surface) under visual guidance (Figure 15). For these experiments, regions of the organoid where light penetrated were chosen for ease of visual targeting. Cells were targeted based on the presence of phase bright edges and location within the first 1-2 layers of cells from the tissue surface. Once a target cell was selected, the pipette was brought near the surface of the target cell and the cell was approached under light positive pressure (0-20 mbar) in order to minimize motion of neurons that were loosely adhered to the organoid surface. For manual surface recordings, small position adjustments were made during gigasealing and recording steps to improve yield and quality. Visual guidance and precise manual control of pipette position enabled high yields in both neuron hunting and gigasealing in surface neurons (neuron hunt – 31/31 attempts, 100%; gigaseal – 30/31 attempts; 97%). Correspondingly, 84% of all patch

attempts achieved break-in and 52 met the criteria for a whole cell recording (break-in – 26/31 attempts, 84%; whole cell - 16/31 attempts, 52%).

Following these experiments, we attempted to determine whether it was possible to obtain whole cell recordings from organoid neurons beneath the tissue surface. From our extensive experience with patching in intact systems (i.e., automated *in vivo* patching in the mouse thalamus (W. A. Stoy et al., 2017; W. M. Stoy et al., 2020)), we hypothesized that this would be readily achievable given that brain organoid tissue does not contain the physical obstructions (i.e., blood vessels) or motion artifacts (i.e., heartbeat and breathing) present *in vivo*. By following the traditional manual approach of descending under low positive pressure to prevent clogging and releasing that pressure when near the region of interest, gigaseals formed readily and whole cell recordings could be obtained (Figure 16). These experiments, like many *in vivo* patching experiments, are “blind” and rely on resistance measurements from the pipette tip in place of visual input. Accordingly, the lack of visual guidance decreased yield in gigaseal stage, but not the neuron hunting stage (neuron hunting – 68/72 attempts, 94%, $p = 0.313$, Fisher’s exact test; gigaseal – 55/72 attempts, 76%, $p = 0.011$, Fisher’s exact test). Differences in break-in and whole cell yields for subsurface manual patching were also nonsignificant (break-in – 48/72 attempts, 67%, $p = 0.096$, Fisher’s exact test; whole cell – 40/72 attempts, 56%, $p = 0.829$, Fisher’s exact test).

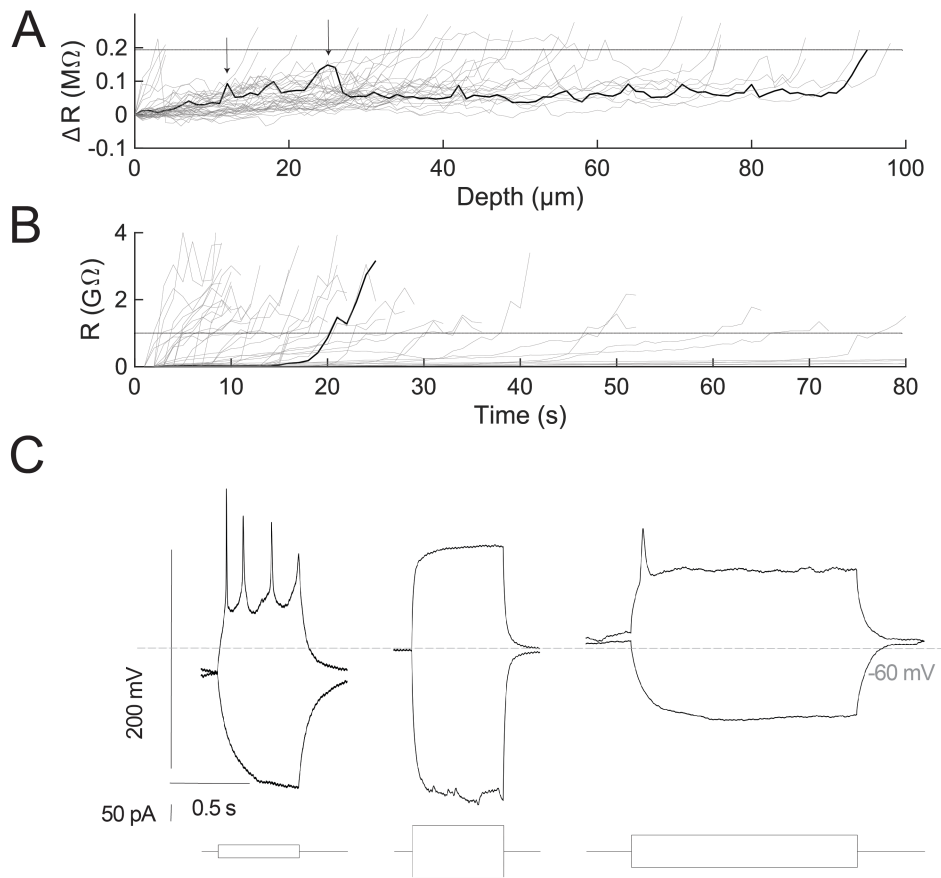


Figure 16. Patch clamp recordings in intact human brain organoids. A) Representative neuron hunt resistance traces as a function of depth (gray) showing cell detection events for blind patching as changes in resistance. Arrows over black trace show potential detections before threshold is crossed. **B)** Representative gigaseal resistance traces (gray) as a function of time from cells in (A). Black trace shows gigaseal formation for cell shown in (A). **C)** Representative current clamp recordings from intact brain organoids showing different levels of action potential activity.

Unlike the *in vivo* rodent brain, human brain organoid tissue lacks the motion (i.e., breathing and heartbeat) and obstructions (i.e., blood vessels) that increase the difficulty of blind patching. The performance of standard, manual patch clamping in organoid tissue does not change as a function of depth (whole cell yield, $p = 0.829$, Fisher's exact test), suggesting that cells below the surface can be readily targeted in intact brain organoids

using the intact organoid fixturing in combination with existing electrophysiology techniques.

3.3.3 *Electrophysiological properties of intact human brain organoid cells*

Intrinsic properties of intact organoid neurons varied with depth and age of neurons (**Fig. 4A-B**). When comparing 90 DIV surface neurons to 90 DIV subsurface neurons, membrane resistance (R_m) decreased from $1.7 \pm 0.6 \text{ G}\Omega$ to $1.1 \pm 0.5 \text{ G}\Omega$ ($p = 0.0065$, t-test). Resting membrane potential also decreased $\sim 3 \text{ mV}$ on average, but this change was not statistically significant. When comparing subsurface organoid neurons at 90 DIV and 120 DIV, membrane resistance increased and resting membrane potential decreased at statistically significant levels ($p = 0.0482$, $p = .0477$, respectively, t-test) (Figure 17D,E).

Of all cells recorded from intact organoids, 73% (49/67 whole cell recordings) fired action potentials, and this rate was consistent across ages and depths (Figure 17B, Figure 18B,C,D). Consistent with surface recordings, subsurface recordings were also largely single action potential firing cells and there was no significant difference in numbers of multiple action potential neurons ($p = 1$, Fisher's exact test). The number of recorded neurons that fired multiple action potentials was low, with no significant difference between groups. Similarly, the number of neurons that expressed rebound action potentials following depolarization was low and did not differ with respect to age or depth. Over all samples, 30.6% expressed rebound action potentials following hyperpolarizing current injections (15/49 action potential expressing cells).

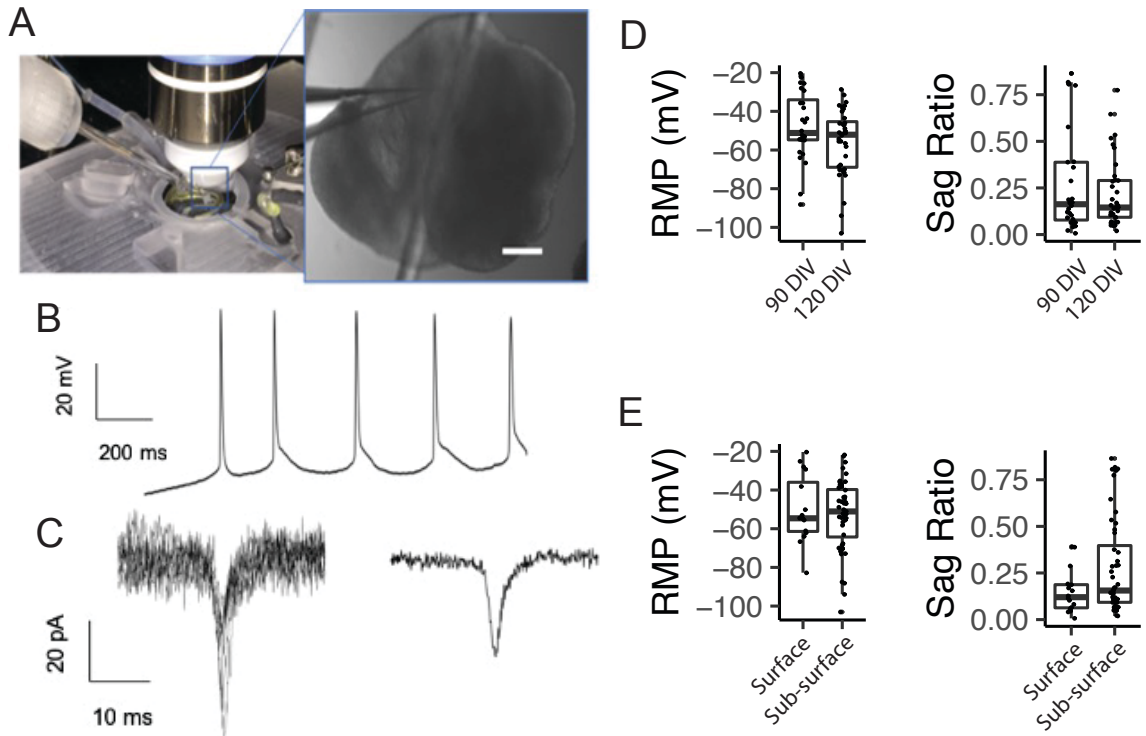


Figure 17. Electrophysiological properties of cells in intact human brain organoids. A) Patch clamp recording rig for recording from intact human brain organoids. Inset shows intact human brain organoid held in place using the harp and agarose method. Scale bar is 100 μ m. B) Representative spontaneous action potentials from organoid neuron. The presence of multiple spontaneous action potentials is a sign of mature neurons. C) Representative voltage clamp recordings showing subthreshold activity in organoid neurons. Trace on the left shows an overlay of many traces, and trace on the right shows the averaged trace. D) Organoid electrophysiological properties vary with age. In recordings of 90 and 120 DIV organoids, resting membrane potential (RMP) decreased slightly in older organoids, but was not significant. Sag ratio decreased significantly in 120 DIV organoids. E) Organoid electrophysiological properties vary with respect to depth of recording. In recordings performed on subsurface cells, RMP increased, but the difference was not significant. Deeper organoid cells express larger sag ratios.

These recordings capture the major classes of action potential activity previously observed in human fetal tissue, the most direct comparison for intact human brain organoid electrophysiology (Figure 18A). Briefly, those classes include 4 types of neurons (Figure 18A,B). First are neurons that fire no action potentials, indicating that they are immature, potentially still in the neural progenitor cell phase of development. Because organoids in

the age range used in these experiments feature the development of astrocytes as well as neurons, it is possible that astrocytes are also included in this category of non-firing cells (Paşca et al., 2015). Second are cells that fire single abortive action potentials. These cells initiate a spike, but the spike is lower amplitude and has different kinetics, corresponding to a lower levels of ion channel expression in these immature neurons. Third are cells that have matured enough to fire full single action potentials, but are not capable of firing trains of action potentials. Finally, mature neurons in organoids are capable of firing multiple, spontaneous action potentials. This electrophysiological diversity in intact human brain organoids reflects the wide range of neuronal cell types present in these tissues (Kang et al., 2021; Qian et al., 2020).

In the course of optimizing recording methods for intact human brain organoids, I gathered a preliminary dataset showing the expression of sag potentials in current clamp recordings. I compared the dimensionless sag ratio, defined as the difference between peak and steady state membrane potential normalized to the peak membrane potential when hyperpolarizing current is applied, from organoids neurons at different depths and ages (Angelo & Margrie, 2011; Moradi Chameh et al., 2019). The presence of sag potential when hyperpolarizing steps are applied in current clamp was significantly different as a function of age ($p = 0.0086$, Student's t-test) and depth ($p = 0.0066$, Student's t-test). These initial results support the observations that sag ratio is larger in human neurons than in mouse neurons (Kalmbach et al., 2018), is more pronounced in pre-term neurons of non-human primates compared to post-term (Kim et al., 2014), and changes as a function of tissue age and layer (Moradi Chameh et al., 2019). In addition, I compared this trend in dimensionless sag ratio to sag ratio data from adult neurons in human brain slices published

by Chameh, et. al., finding that layer 2/3 and layer 5 neurons follow the trend of increasing sag ratio with depth. In addition this comparative dataset supports conclusions from recordings in pre-term and term brain slices from primates that birth tends to reduce sag ratio (Kim et al., 2014). In this dataset, there was a significant reduction in sag ratio between the pool of adult neurons and the pool of organoid neurons ($p = 0.0001$, Student's t-test).

The ability to perform patch clamp studies in intact human brain organoids reliably and to correlate that data to existing datasets from human tissue is a potentially powerful technique for studying neuronal development and modeling diseases in intact human brain organoids. Critically, this technique must be integrated with other neuroscience techniques such as single cell morphology, immunohistochemistry, and gene expression studies to fully capture the processes that influence single cell properties in intact human brain organoids.

3.3.4 *Challenges of interpreting data from intact human brain organoid recordings*

While valuable and informative about the development of electrical activity, interpretation of blind patch clamp recordings alone is difficult. Often, when blind patch clamp methods are used in other model systems, such as the *in vivo* rodent cortex, the types of recorded cells can be narrowed down by the choice of target region. While some information can be collected prior to attempting gigasealing by performing juxtacellular stimulation to measure spiking activity, the population of non-spiking cells could make this type of classification difficult, but useful in some applications of blind patch clamp recordings (Li et al., 2017a). In addition, without confirmatory evidence from

complementary methods, it is difficult to resolve whether changes observed over time and across cell lines are due to neuron-specific effects or can be attributed to glial cell development, spatial heterogeneity, or other factors. Further compounding this problem, no current methods exist for performing histology on patched cells in intact organoids, further limiting the applications of these methods. The ability to label patched cells and re-identify them using histology is essential for the continued development of intact organoid single cell methods.

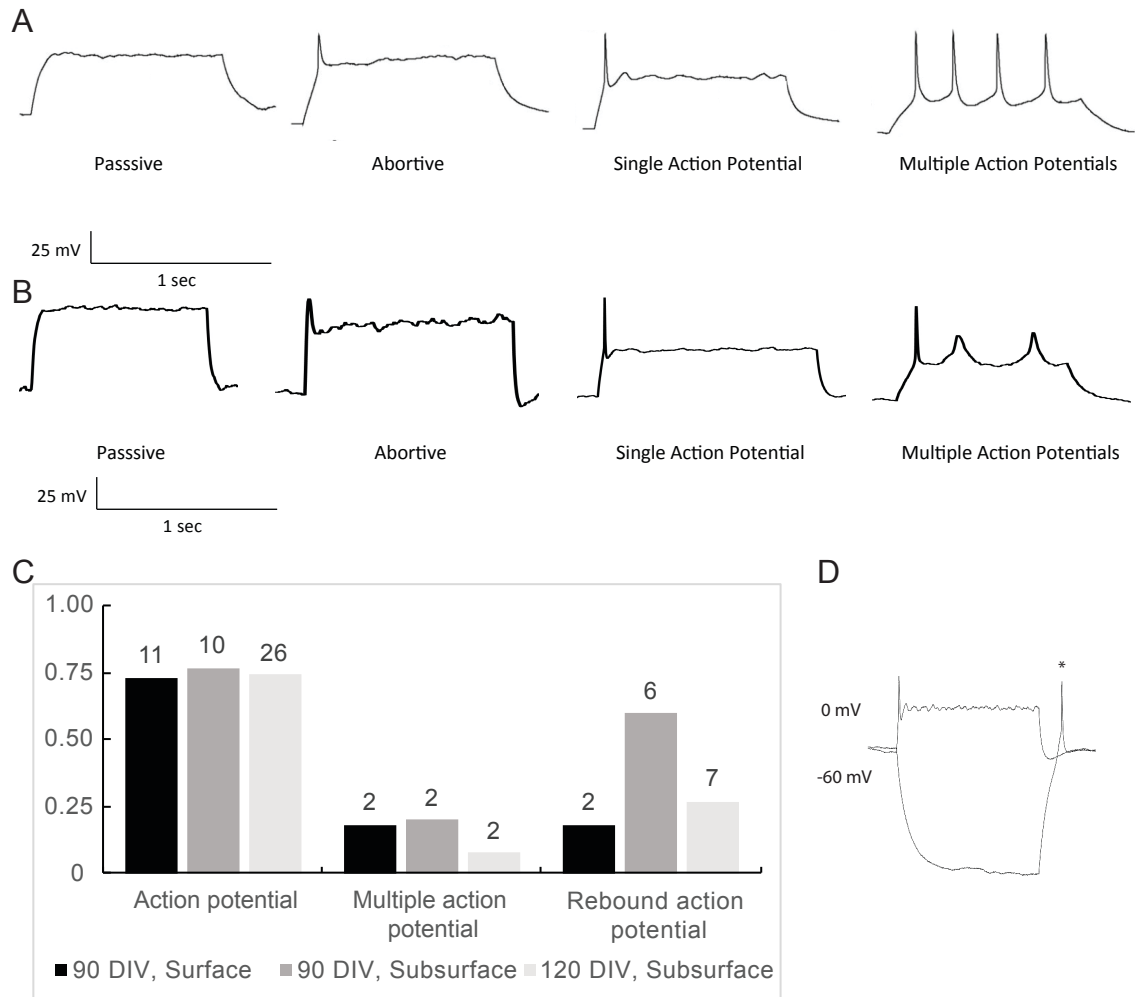


Figure 18. Action potential activity in intact organoid cells show range of developmental stages. A) Developmental stages of action potential development from human fetal brain slices (A. R. Moore et al., 2009). Major stages are passive, abortive action potentials, single action potentials, and multiple action potentials (left to right). B) Cells recorded from intact human brain organoids display these features. All recordings were made from control organoids between 90-120 DIV. C) Across age and depth groups, recordings featured primarily single action potentials, and proportion of cells firing multiple action potentials or rebound action potentials were not statistically significant. D) Representative recording of organoid neuron firing a single action potential and a rebound action potential.

CHAPTER 4. Single Cell Electrophysiology and Morphology in Intact Human Brain Organoids

4.1 Introduction

No existing methods for single cell recording (extracellular or intracellular) in intact human brain organoids provide a means for determining the morphology and spatial location of the recorded cells. The ability to recover the location and morphology of recorded cells in intact organoids enables a variety of single cell studies of intact human brain organoids.

4.1.1 Limitations of blind patch clamp in intact human brain organoids

While blind patching in intact human brain organoids is useful in the sense that it provides single cell electrophysiology from an undisturbed *in situ* tissue sample, there are limitations to the method that preclude its wide adoption. Specifically, the inability to resolve the identity or location of the patched cell with non-electrophysiological data. As the diversity and development of cell types is a critical concern for the broader brain organoid community, it is essential to develop methods to validate the identity of patched cells within the intact organoid to confirm phenotypes suggested by electrophysiology. As discussed previously, whole cell patch clamp provides the experimenter with physical access to the intracellular space. This access is commonly used to deliver dyes that diffuse throughout the cell and reveal fine dendritic and axonal processes. The combination of these methods has been a critical technique for neuroscience and has recently been further

adapted to include extraction of genetic material for RNA sequencing (i.e., PatchSeq) (B. R. Lee et al., 2021).

4.1.2 Neuronal morphology methods

Numerous methods existing for measuring the morphology of single neurons in brain tissue (Livet et al., 2007; Loulier et al., 2014; A. Wertz et al., 2015). These relevant methods differ in terms of their scale and ability to provide non-morphological information about labelled cells (i.e., genetics, electrophysiology, synaptic connectivity, developmental lineage, or cell type). Because of the ability of whole cell patch clamp recordings to deliver intracellular dyes, genetic material, and transsynaptic tracers in combination with intracellular electrophysiology, it remains a key method for a multi-modal characterization of the structure and function of neurons (X. Jiang et al., 2015a; Xiaolong Jiang et al., 2013).

4.1.3 Tissue clearing for imaging of intact tissues

Tissue clearing represents a broad range of chemical treatments that make thick biological tissue samples optically transparent (Richardson & Lichtman, 2015; Kei Takahashi et al., 2020; K. R. Weiss et al., 2021). One of the most widely used and successful of these methods is CUBIC. As a clearing technique, CUBIC, which stands for “clear unobstructed brain imaging cocktails and computational analysis” is in the class of hydrophilic clearing methods (Susaki et al., 2020). While there are many possible clearing techniques, including, but not limited to BABB, CLARITY, and SeeDB, CUBIC was chosen for these experiments because current CUBIC protocols are safe, scalable, and environmentally low-impact, making them ideal for methods development and for batch

processing of samples (Jensen & Berg, 2017; Ke et al., 2016; Richardson & Lichtman, 2015; Susaki et al., 2020; K. R. Weiss et al., 2021).

4.1.4 Classification of neurons using electrophysiology and morphology

Measurement of electrophysiology and morphology from the same cell is a key component of modern morpho-electric cell type classification (Cepeda et al., 2003; Henry Markram et al., 2015). The importance of these methods are reflected in the goals of the BRAIN Initiative as well as the ongoing work of the Allen Institute for Brain Science and other similar groups (Bargmann & Newsome, 2014; Gouwens et al., 2019). In order to facilitate the collection of multidimensional datasets from intact brain organoids, it is necessary to develop optimized methods for recording and morphologically labeling many neurons throughout organoid tissue.

A combination of morpho-electric classification and physiological responses to ligands are critical components of validating the physiological relevance of intact brain organoid data and comparing this data to similar model systems. The ability to collect this sort of data in an automated manner from intact brain organoids will facilitate comparative studies between human brain organoids, adult human brain tissue, and mouse brain tissue (Gouwens et al., 2019; B. R. Lee et al., 2020; Mariani et al., 2015c; Moradi Chameh et al., 2019; Qian et al., 2016b). These studies may help to define the physiological relevance of human brain organoids and provide information for the improvement of organoid generation protocols.

First, by developing methods for integrated measurements of electrophysiology and morphology using “blind” recording techniques, these methods can be implemented by

laboratories without access to complex and expensive two-photon microscopes required to implement visual guidance. Second, by applying automation and optimization to these methods for organoids, the throughput and scalability of single cell analysis in human brain organoids will be increased. Fifth, the collection of morpho-electric and physiological data for subsurface neurons in intact brain organoids will enhance cross-species comparisons of the validity of organoid models.

Because human brain organoids are a new model system for neuroscience, it is of great importance that data from human brain organoids be compared to physiological data from relevant model systems. There is precious little data on the electrophysiology and morphology of neurons from acute slice recordings in human fetal tissue, the most direct comparative source (A. Moore et al., 2011; A. R. Moore et al., 2009). However, large, multidimensional, and increasingly standardized datasets from adult human, adult mouse, and developing mouse represent an important tool for understanding the physiological relevance of brain organoids (Gouwens et al., 2019; B. R. Lee et al., 2020; Tasic et al., 2018). Because the intact human brain organoid methods described in this work are designed for ease of implementation in both manual and automated electrophysiology workflows, it is possible that similar datasets can be generated for human brain organoids to provide a deeper understanding of development and disease in the human brain.

4.2 Methodology

4.2.1 Delivery of intracellular dye during patch clamp experiments

Patch clamp experiments with intracellular dyes were performed according to the methods of Chapter 4 with the addition of intracellular dye in the pipette and increased

recording time to facilitate complete filling of neurons with dye. To maximize yield of these longer recordings, experiments were performed using either fully manual or “push-to-clean” methods (Figure 13). Recordings were performed using Clampex (Molecular Devices). Recording protocols followed the cell types characterization workflow used in the Allen Institute for Brain Science Cell Types database, and were adjusted according to time and recording quality.

Table 2 Compatibility of intracellular dyes with CUBIC L/R

Intracellular dye	Compatibility with CUBIC L/R
Neurobiotin 488	No
Biocytin Alexa Fluor 594	Yes
Alexa Fluor 647	Yes

Fluorescent intracellular dyes evaluated in these experiments were Neurobiotin 488, Biocytin Alexa Fluor 594, and Alexa Fluor 647, as shown in Table 2. Neurobiotin 488, a widely used intracellular dye based on the Alexa Fluor 488 structure, is known to be incompatible with current CUBIC reagents (Kei Takahashi et al., 2020). Because of its similarity to existing biocytin-based intracellular solutions and compatibility with CUBIC L/R clearing, Biocytin Alexa Fluor 594 (0.02 w/v%) was used for the cells in this dataset. Patch clamp recordings were attempted as previously described using manual and semi-automated methods, under DIC guidance for cells near the surface and blind for deeper cells. Recordings were attempted at relatively equal proportions. The presence of fluorescent dye and validation of unobstructed pipette tips were performed using

fluorescent imaging. Once whole cell configuration is obtained, recordings were held for between 5-30 minutes according to existing methods for biocytin filling (Gouwens et al., 2019; X. Jiang et al., 2015a). After recording, pipettes were slowly retracted with the aim of obtaining an outside-out seal, which is indicative of the neuronal membrane re-sealing and promoting full diffusion of the dye throughout the neurites. For cells located near the organoid surface, the presence of fluorescence was used to inform classification and localization of recorded neurons and to monitor steps of the experiment (e.g., cell detection, gigasealing, dye filling, and re-sealing).

4.2.2 *CUBIC tissue clearing of intact human brain organoids*

Intact human brain organoids were cleared following a modified version of the CUBIC protocol (Figure 19) developed by Matsumoto et. al. (Matsumoto et al., 2019). First, organoids were fixed in 4% paraformaldehyde (PFA) in phosphate buffered saline (PBS) for 12-24 hours at room temperature. Next, organoids were washed in PBS 3 times for 10 minutes each with shaking at room temperature to remove any remaining fixative from the tissue. For delipidation, fixed organoids were then placed into 3-5 mL of CUBIC L solution (10% wt/wt N-butyldiethanolamine and 10% wt/wt Triton X-100 in dH₂O) and incubated on a shaker plate for 2 days at room temperature. To preserve the integrity of the tissue and to avoid damage when handling the tissue, organoids were re-fixed in 4% PFA for 2 hours prior to another PBS wash (10 minute wash, repeat 3 times). To match the refractive index (RI) of the delipidated tissue to the imaging media, rendering it transparent, organoids were placed in CUBIC-R overnight. Samples could be stored in CUBIC-R for <1 month at room temperature protected from light.

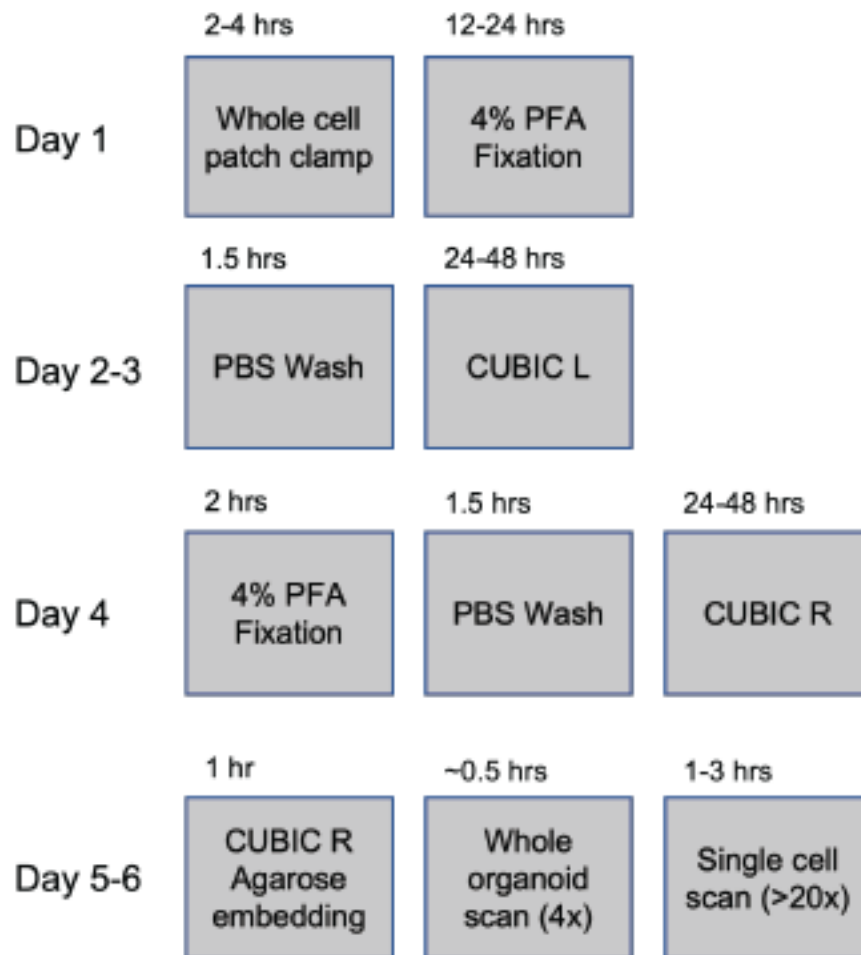


Figure 19 Protocol flowchart for patch clamp and morphological reconstruction using CUBIC tissue clearing. The process is can be performed in one week and is compatible with batch processing and imaging of tissues.

For imaging, cleared organoids were embedded into a solution of 2% w/w agarose in CUBIC-R using a two-step casting method. First, organoids were transferred to a glass bottomed petri dish (Mattek, 1.5 cover glass) using a wide mouth Pasteur pipette. Residual liquid CUBIC-R was carefully aspirated and the organoid was positioned close to the center of the dish using a paintbrush or spatula. The organoid was then coated in a shallow layer of CUBIC-R agarose and allowed to cool at 4° C to prevent motion of the tissue. A second

layer of CUBIC-R agarose was then added to fully embed the cleared organoid. For imaging experiments lasting more than three hours, CUBIC-R could be added on top of the agarose layers to saturate the gel and prevent crystallization of the gel. For storage or reimaging at a different orientation, liquid CUBIC-R could be removed and the gel could be melted by heating briefly in a microwave (<5 seconds) and either transferring the organoid to a tube of liquid CUBIC-R or rotated on the dish using a paintbrush or spatula, respectively.

For these experiments, volumetric imaging of cleared intact human brain organoids was performed on a spinning disk confocal microscope (Nikon W-1, Hamamatsu ORCA-Fusion Gen-III sCMOS camera). Organoids in glass bottom petri dishes were mounted onto an XYZ stage (ASI XY Piezo Z) in a holder that facilitated changing between air and oil objectives without disrupting the sample.

To obtain volumetric images of cleared brain organoids, the whole organoid was imaged using a 4x objective (Nikon CFI Plan Apochromat Lambda 4x Objective Lens, N.A. 0.2, W.D. 20.0mm, F.O.V. 25mm) to identify filled cells and measure their location relative to one another. For well labelled patched cells, the cell body and proximal dendrite were frequently visible under the 4x objective. If the known number of locations of patched cells could be resolved under low magnification, regions of interest were created around each region and those regions were reimaged at higher magnifications. If all cells could not be located under low magnification, whole organoids were imaged using a 10x objective (Nikon CFI Plan Apochromat Lambda 10x Objective Lens, N.A. 0.45, W.D. 4.0mm, DIC, Spring Loaded). Once cells were located under low magnification, regions containing cells

of interest were imaged at 20x magnification (Nikon CFI60 Plan Apochromat Lambda 20x Objective Lens, N.A. 0.75, W.D. 1.0mm, DIC, Spring Loaded).

When using air objectives, optical section thicknesses were oversampled to account for spherical aberration that occurs going from a low RI objective to a high RI imaging media (RI of CUBIC-R = 1.528). Ideal slice interval for imaging 594 nm signal was determined for each objective according to Equation 1 to calculate a correction factor for the median light ray entering the imaging media (Diel et al., 2020).

$$\frac{d'}{d} = \frac{\tan\left(\sin^{-1}\frac{0.5NA}{n_1}\right)}{\tan\left(\sin^{-1}\frac{0.5NA}{n_2}\right)} \quad (1)$$

In Equation 1, d' is the actual focal position, d is the expected focal position, NA is the numerical aperture of the objective, and n_1 and n_2 are the ratios between the refractive indexes of each media calculated for each light path. This model has been implemented as an ImageJ plugin that reconstructs images and provides optimal thicknesses for optical sections. Optimal slice size selection was used to collect z-stack images and reassembled at the correct Z dimensions.

A subset of recorded cells were located near the surface of the organoid and mounted close to the surface of the coverglass. To image these cells using oil immersion objectives, the air objective was retracted and the stage was moved to allow for the application of immersion oil (Nikon Type N immersion oil, RI = 1.51). The stage was then moved to the original location. Because changing refractive indices resulted in shifting the imaging plane in the z axis, focus was adjusted to re-locate the labelled cell. For these high

resolution cells, imaging was performed using a 40x objective (Nikon CFI60 Plan Fluor 40x Oil Immersion Objective Lens, N.A. 1.3, W.D. 0.24mm, DIC) or 60x objective (Nikon CFI60 Plan Apochromat Lambda 60x Oil Immersion Objective Lens, N.A. 1.4, W.D. 0.13mm, DIC).

4.2.3 Correlation of labelled cells with patch clamp recordings

Prior to patch clamp experiment, intact human brain organoids were fixtured using a weighted harp and agarose slab using a 4x objective on an EVOS XL Core microscope. Unique gross features of the organoid (e.g., non-spherical shape, differences in thickness) as well as the orientation of weighted harp strings were recorded (**Error! Reference source not found.**A). The complete experimental chamber was then moved to the patch clamp rig for recordings. The orientation of the experimental chamber was approximately equal to the orientation of the low magnification image. Locations of the targeted regions for patch clamp attempts were recorded based on the pipette location. Locations were recorded when the pipette tip reached the surface of the organoid and then again when the pipette tip attempted to form a gigaseal, creating a depth vector that could be used to match the location of cells relative to the tissue surface.

5 sec

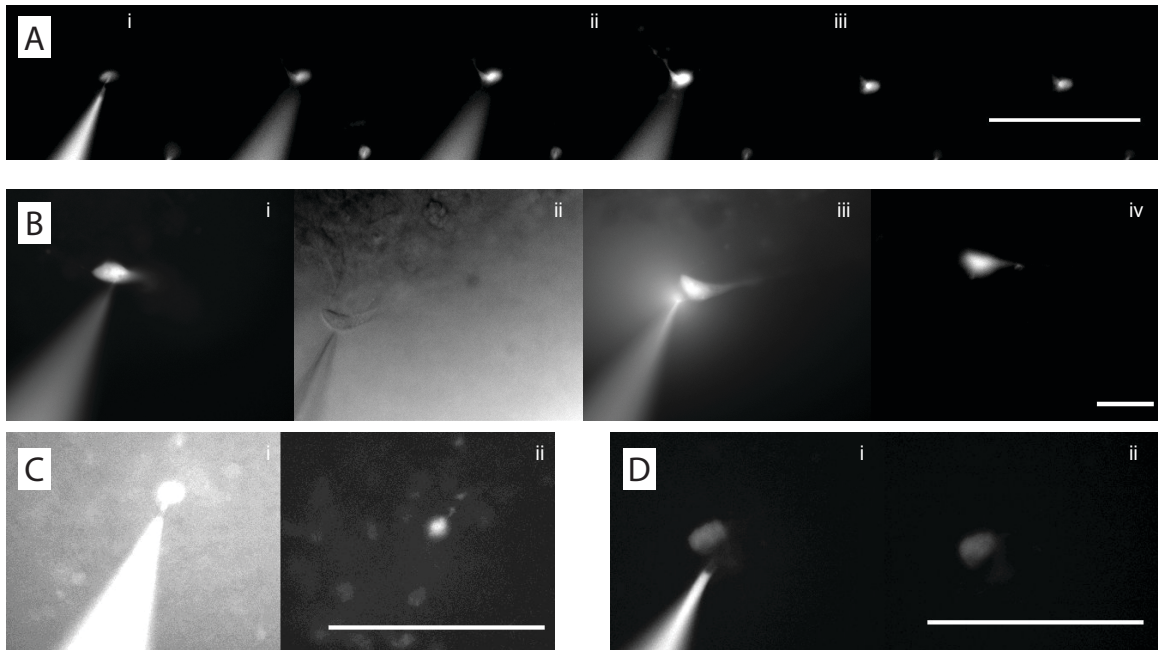


Figure 20. Fluorescence imaging of dye filling in surface cells. A) Sequence of fluorescence images showing dye filling a single cell during patch clamp recordings starting in (i). Cell showed diffusion of dye through visible neurites, indicating successful filling (ii). Cell retained fluorescence signal following retraction of pipette (ii). B) An example of a failure to retract the pipette. This sequence of images shows a filled cell (i) being pulled away from the surface of the cell (ii, iii). The cell retained fluorescence signal briefly after retraction (iv), but was not able to be located in cleared tissue. C) Dye filling showing a patched cell (bright) surrounded by fluorescent cells that have been filled with dye, likely through gap junction coupling, indicative of astrocytes networks. D) Dye filling of a putative neuron, which shows no background dye staining. Scale bar for all images is 25 μm .

During the patch clamp experiment, images were taken under a 40x objective using DIC or fluorescence optics. Cell images were recorded when the cell was close enough to the surface that the fluorescence signal was visible (0-30 micron). These images were helpful in several ways. First, the presence of identifiable cellular features, such as the shape of the soma or large dendrites, made the cells easily identifiable in the cleared tissues (Error! Reference source not found.B,D). Second, using fluorescence imaging during

the patch experiment was useful in estimating the degree of gap junction coupling in the local area, which is indicative that an astrocyte may have been patched (**Error! Reference source not found.**C,D) (Dombeck et al., 2007; Peinado et al., 1993).

Following fixation and clearing, cleared organoids were scanned at low magnification (4x or 10x) to identify likely regions of recorded cells, which often showed high levels of fluorescence above the autofluorescence background due to fluorescent dye ejected from the pipette during neuron hunting and cell detection. In cases where multiple cells were recorded in a single organoid, relative locations were measured in the microscope software (NIS Elements, Nikon) to assign initial cell identifiers. Under low magnification, cells were visible as fluorescent soma and initial segment of proximal dendrites. If cell location and shape could not be resolved under low magnification, cell shape and location in higher magnification were used to assign cell identifications. Cell identification yields were recorded.

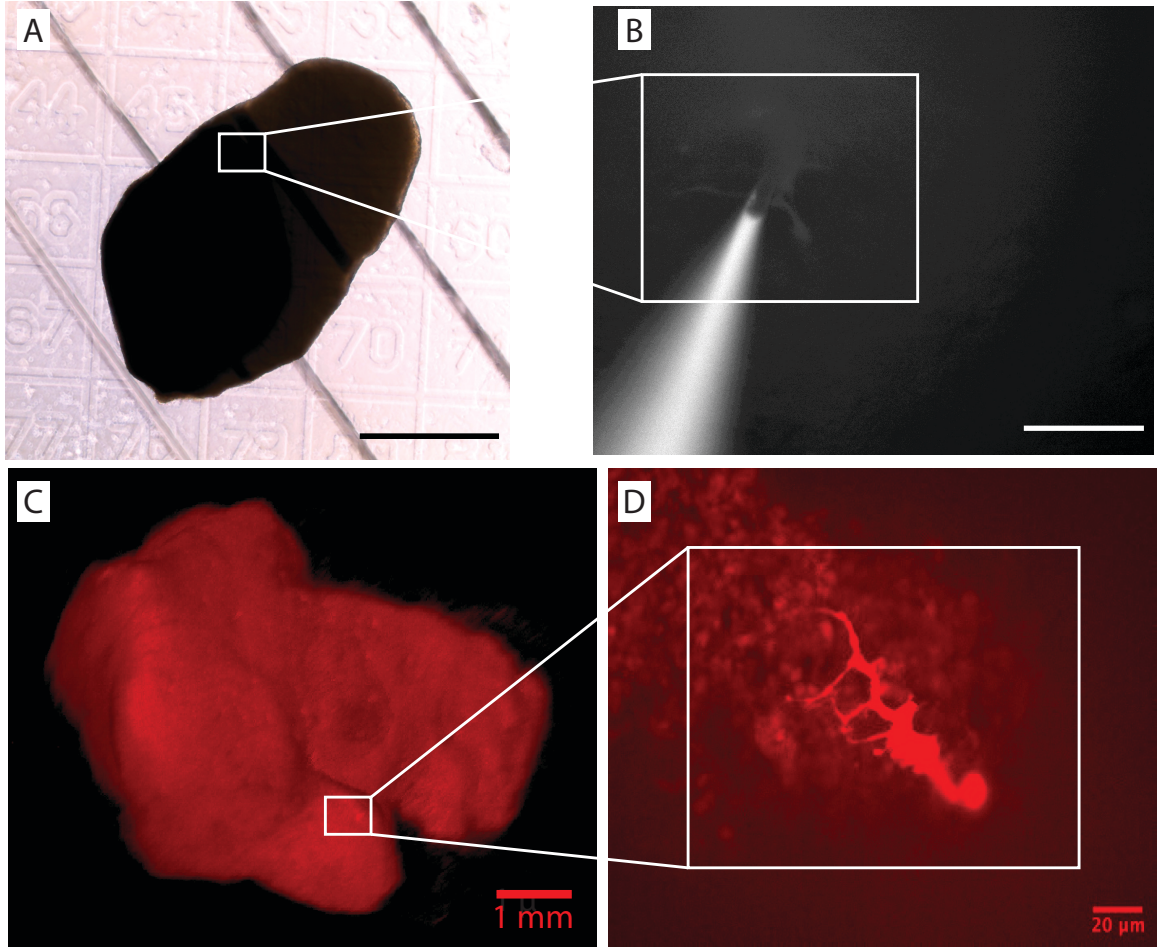


Figure 21. Process of locating patched cells in cleared tissues. A) Organoid fixtured on agarose slab with weighted harp. Shape of the organoid and orientation of the harp strings are critical for locating the cell in the cleared tissue. Scale bar is 1 mm. **B)** Fluorescence image of patched cell in organoid from (A). Note the distinctive branching dendrite feature directly beneath the patch pipette. Scale bar is 10 μm . **C)** Volumetric rendering of the organoid in (A) following clearing showing a visible soma and dendrite. Scale bar is 1 mm. **D)** Relocated patched cell imaged at 20x magnification. Note the dendritic branching pattern observed in (B) is still present. Scale bar is 20 μm .

4.2.4 Morphological tracing of labelled cells

To quantify and visualize morphology of recorded cells, cells were traced manually from cropped image stacks reassembled based on the correction factor from Equation 1. Cell tracing was performed using the Simple Neurite Tracer (SNT) plugin in ImageJ

(National Institutes of Health). Traced cells were analyzed for cable length, average branch length, and number of branches to study quality of reconstructions and development of morphology over time.

4.2.5 Preliminary classification of organoid cells by electrophysiology and morphology

Morphology and electrophysiology of recorded and recovered cells were used to classify cells based on known characteristics of cell types in human brain organoids (Qian et al., 2020). The primary categories examined are immature neurons, mature neurons, and astrocytes. Because these cell types exist on a continuum, only cells that can be definitively classified from electrophysiology and morphology alone will be classified. Integration of these methods with existing immunohistochemistry techniques and genetic techniques can help to resolve complex cell type differences at a larger scale.

4.3 Results and Discussion

4.3.1 Yield and efficacy of detecting filled cells

A total of 32 whole cell recordings were performed with biocytin filling according to this method (Figure 22). Cells were recorded across 15 organoids out of 19 intact human brain organoids attempted (Recording yield = 15/19, 79%), of which 13 produced detectable signal from cells that had been labelled during patch clamp recordings (Detection yield = 13/15, 87%). Organoids were divided between two established control lines, the 11C1 line, which included organoids aged 167-191 DIV, and the C-3-1 line, which included organoids aged 90-100 DIV. Of 8 11C1 organoids, signals from filled cells

were detected from all of them (Detection yield = 8/8, 100%). Of 7 C-3-1 organoids, 5 contained detectable signal from filled cells (Detection yield = 5/7, 71%).

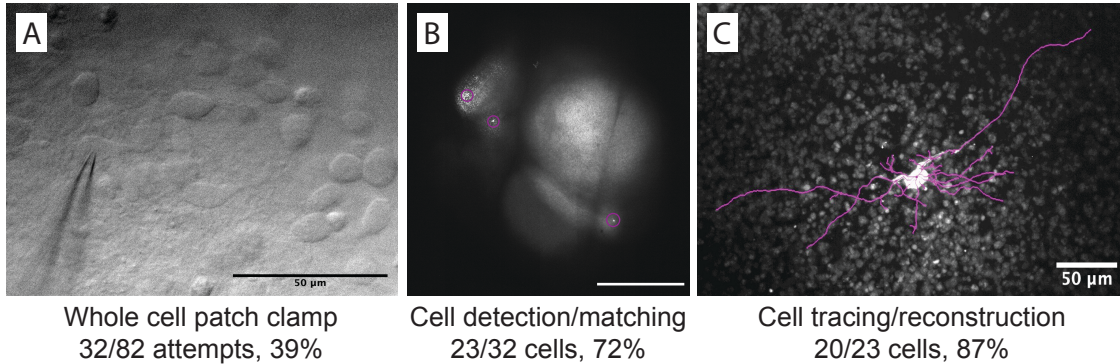


Figure 22. Process yields for patching, relocation, and reconstruction of single cells in intact human brain organoids. A) DIC image of whole cell patch clamp attempt on a surface organoid cell. Scale bar is 50 μm . Whole cell patch clamp yield was 39% for a total of 32 cells recorded from 15 intact human brain organoids. B) Representative slice from a confocal image stack showing localized biocytin Alexa Fluor 594 signal. Cells are manually based on gross organoid features and relative locations of cells. The yield for this process was 72%, with 23/32 total cells being identified by fluorescent signal and assigned to a patch clamp recorded based on location. C) Cell tracing was carried out on recorded and assigned cells to quantify morphological features. Cells that did not feature multiple neurites or significant branching were considered incomplete fills. 20/23 cells (87% yield) passed this stage.

From those 15 intact organoids, a total of 32 whole cell recordings were made at various depths throughout the tissues from a total of 82 patch clamp attempts. For 11C1 organoids, 21 whole cell recordings were obtained, of which 17 could be unambiguously identified from location, shape, and depth information (Cell identification yield = 17/21, 81%). For C-3-1 organoids, a total of 11 whole cell recordings were made, of which 6 could be unambiguously identified from location, shape, and depth information (Cell identification yield = 6/11, 55%). Overall cell identification yield was 23/32 or 72%.

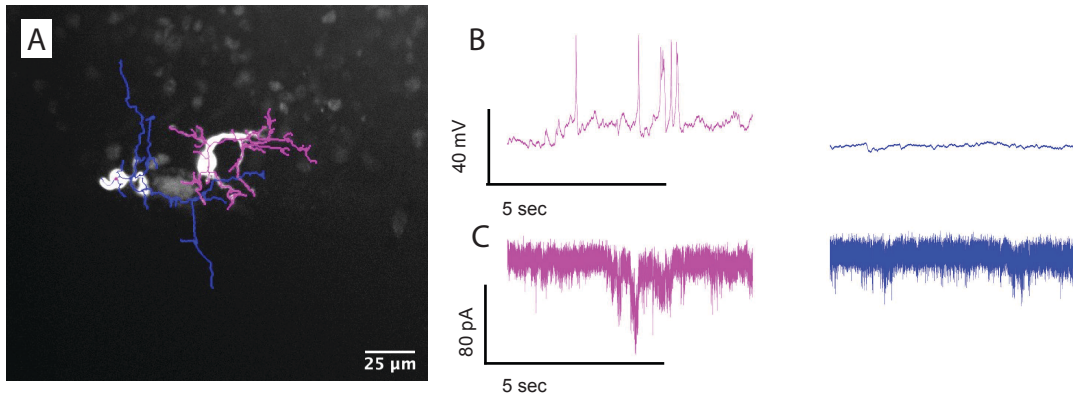


Figure 23. Resolving the morphology and electrophysiology of nearby neurons in intact human brain organoids. A) Neuron tracings overlaid on a maximum intensity z-projection. Scale bar is 25 μm . B) Spontaneous activity recorded in current clamp for both neurons. The blue neuron corresponds to the blue trace and the pink neuron corresponds to the pink trace. Based on the low level of spiking activity (3-5 mV), the blue cell is an immature neuron. Based on spontaneous action potentials, the pink cell is a mature neuron. C) Spontaneous activity recorded in voltage clamp for the pink and blue neurons, respectively.

Of 5 organoids containing only one recorded cell, that cell was detected in 4 organoids (Detection yield = 4/5, 80%). Of the 10 organoids containing more than one recorded cell, the detection yield fell to 70% (19/27 cells). This may be due in part to challenges scanning the entire organoid, poor filling of individual cells, or damage to the tissue during patch clamping or CUBIC processing.

The maximum number of cells recorded from a single organoid in these experiments was 4 ($n = 1$), this limit is more due to the practical concerns associated with performing patch clamp recordings that are long enough to allow for complete filling of cells, which takes 5 minutes or more, in most reported cases. Cells included in this study were recorded for 5-30 minutes. Careful tracking of cell positions as well as correctly

orienting the cleared tissue on the microscope could enable many more cells to be recorded in a single organoid.

4.3.2 Electrophysiology of labelled cells

For whole cell recordings from intact human brain organoids, cells were recorded in current clamp to measure spontaneous changes in membrane potential. These changes in membrane potential are primarily the result of incoming synaptic inputs and the concentration, type, and distribution of ion channels in the cell and reflect the activity and connectivity of intact neuronal tissues (Kodandaramaiah et al., 2012; Margrie et al., 2002). As demonstrated in Chapter 3, action potentials are not expressed in every recorded cell, even in mature organoids (>120 days), making spontaneous and subthreshold properties more informative in an unbiased sample like this one. Spontaneous changes in membrane potential recorded in current clamp mode showed different classes of activity, corresponding to the different levels of maturation expressed in neuronal and glial cells. Spontaneous activity recordings were categorized using the classification model proposed by Moore when studying spontaneous activity in the human fetal cortex (A. R. Moore et al., 2011). Briefly, “Pattern 1” neurons showed no action potentials and very low background variance (<1 mV) (n = 8/20 reconstructed cells), “Pattern 2” cells featured background activity between 1 and 5 mV (n = 8/20 reconstructed cells), “Pattern 3” cells featured high (>5 mV) subthreshold activity and plateaus of depolarization, but not action potentials (n = 3/20 reconstructed cells), and “Pattern 4” cells fired action potentials spontaneously (n = 1/20 reconstructed cells). Other electrophysiological recording protocols in current clamp and voltage clamp were applied to the recorded cells to study

different aspects of the electrophysiology, but are only mentioned briefly in this methods-based analysis (Figure 23C, Figure 24D).

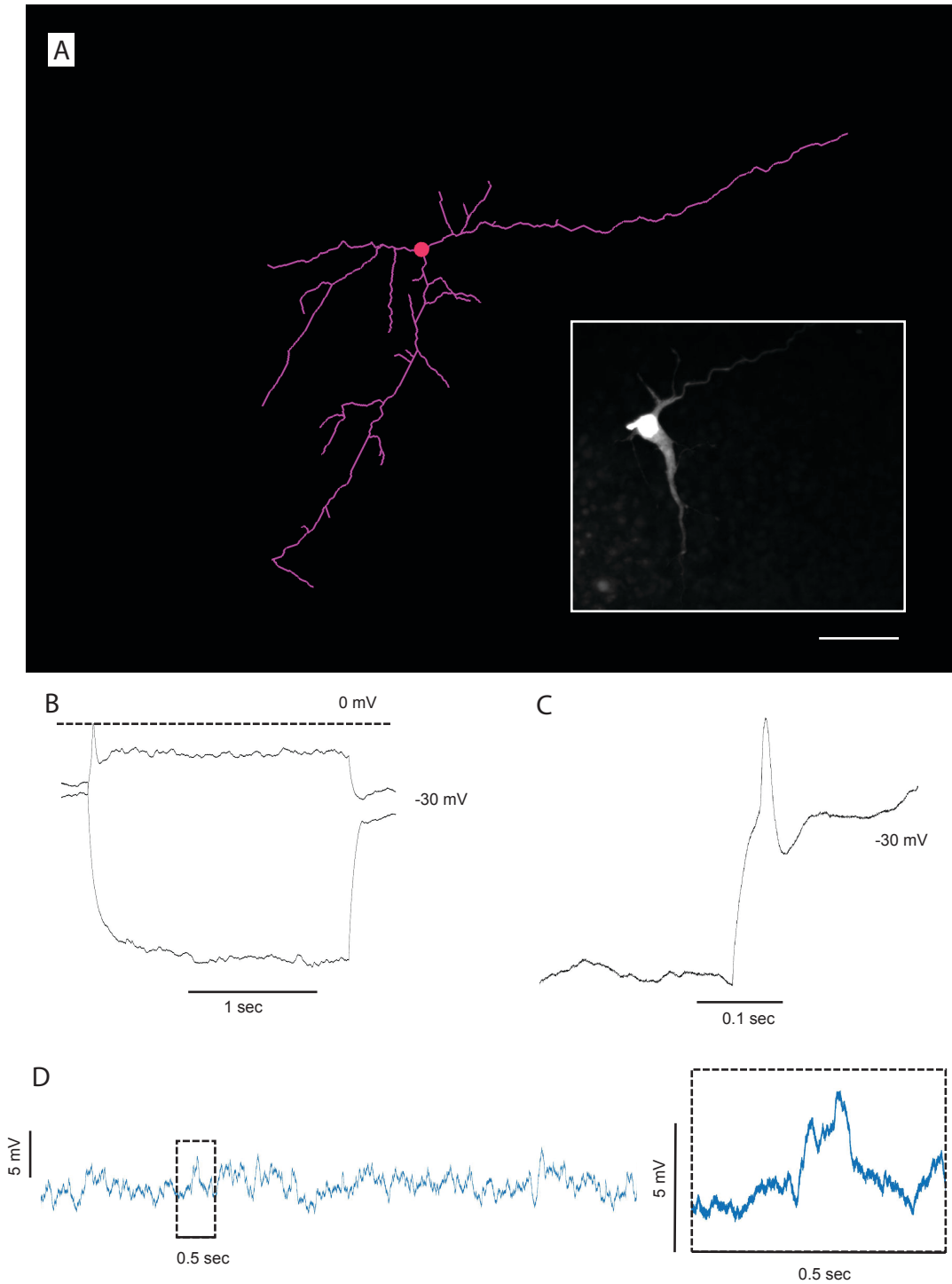


Figure 24. Morphology and electrophysiology of an immature organoid neuron. A) Morphology of a single organoid neuron from manual tracing in ImageJ. Inset image is a maximum intensity z-projection of the raw image stack to show the shape of the soma and proximal dendrites. Scale bar for both images is 50 μm . B) Current clamp

response of the cell recorded in (A) showing strong hyperpolarization response and a single immature action potential. C) Immature rebound spike observed as the cell returns to baseline after hyperpolarization. D) Spontaneous activity recorded in current clamp showing low levels of activity in baseline signal.

4.3.3 Organoid clearing

Autofluorescence signal from the cleared tissue sample is an observable feature in these intact cleared organoids. While imaging at the wavelength required by Biocytin Alexa Fluor 594, different levels of background signal were observed. This level of background signal allows the visualization of structure features of organoids, such as ventricles and rosettes, and has been used similarly in the tissue clearing literature (Renier et al., 2016). The non-labelled cell signals that comprise the background correspond to 3 main scenarios. First, CUBIC cleared tissues are known to have some level of background autofluorescence attributable to biomolecules that have not been fully cleared, especially nucleic acids, and is a feature common to most clearing techniques. This labelling appears typically as low-intensity nuclear signal that overlaps with nuclear labelling dyes such as DAPI. Second, regions of the tissue can uptake dye when exposed to the intracellular solution as the pipette advances through the tissue. This background signal typically appears as diffuse labelling localized to regions of the tissue where the pipette had been inserted. These regions are useful in re-orienting the cleared organoid relative to the recorded locations of cells from the patching experiment (Figure 22B). Third, astrocyte networks may take up Biocytin Alexa Fluor 594 during the patch clamp recording, where it will diffuse throughout the gap-junction coupled network. This was observed in cases where a single patched cell was not visible in the expected region of the tissue.

4.3.4 Morphology of labelled cells

Labelled organoid neurons were traced and analyzed using SNT. Briefly, reconstruction data from organoid neurons collected from different ranges of development showed slight increases in branch length and cable length, but not overall structure, suggesting maturation of existing morphologies during the period studied in these recordings, which ranged from 90 DIV to 190 DIV. Specifically, early stage cells (90-100 DIV, n = 6 reconstructed cells) featured lower overall cable length and average branch length than later stage cells (160-190 DIV, n = 14 reconstructed cells). Differences were not statistically significant and may reflect differences in cell types recorded as well as changes in neuronal maturation.

Organoid cells that were patched and filled with Biocytin Alexa Fluor 594 showed complex branching and long neurite projections (Figure 22C, Figure 23A, Figure 24A). Failed cells appeared to show bright soma and single or shortened neurites. This is likely due to failure of cells to re-seal after patch clamp recording, damage to the neurites near the recording site, or pulling of the cell through the tissue during retraction (Figure 22B). Evidence of damaged dendrites in failed cells could also be observed in the form of punctate spots of fluorescence near, but not connected to the soma.

4.3.5 Preliminary classification of recorded cells from intact human brain organoids

After developing methods for labelling patched cells in intact brain organoids and imaging and reconstructing the morphology of patched cells, assignments of putative cell types to cells that were successfully reconstructed was attempted. At the scale of this study and without secondary confirmation from immunohistochemistry or gene expression, putative cell types was ambiguous in most cases (n = 15/20 reconstructed cells). However,

the following guidelines were developed for assigning putative cell types to guide further methods development with immunohistochemistry. For initial classification, cells in this dataset were divided into four broad categories: mature neurons, immature neurons, neural progenitor cells, and astrocytes. Putative mature neurons featured low background staining, action potentials, and high levels of spontaneous activity, including action potentials. Putative immature neurons featured high levels of spontaneous activity, not including action potentials, and low background staining. Putative neural progenitor cells featured moderate background staining and immature activity in evoked and spontaneous recordings. Putative astrocytes featured high background staining, stellate morphology, no action potentials, and low levels of spontaneous activity.

4.3.6 Putative neurite recordings from intact human brain organoids

Patch clamp recordings in unlabelled cells in intact human brain organoids can be considered an unbiased sampling method, as clear differences in cell morphologies are not readily visible in DIC. Often, the morphology of patched cells is not clear until dye has diffused into the cell. Therefore, it is likely that non-somatic neurite structures such as dendrites and axons represent a portion of intact organoid recordings, as shown in Figure 25. In this recording, the pipette was advanced through the tissue blindly, a gigaseal was formed, and a whole cell recording was obtained. During the recording, fluorescence became visible as dye diffused throughout the cell, revealing that the patch was formed on a neurite near ($<10\ \mu\text{m}$) from the soma. The shape of this neurite was able to be matched to the confocal images from the cleared tissue and is marked on the tracing (Figure 25B).

4.3.7 *Challenges of interpreting data from electrophysiology and morphology in intact human brain organoids*

While powerful, these methods for performing patch clamp and morphology studies in intact organoid cells face challenges in interpretation that point to the complexity of this growing field and suggest a path towards future work in this area. Cell types in the brain and in developing organoids are complex and heterogeneous, rendering the assignment of precisely defined cell types especially challenging. In addition to a similar diversity of cell types in human brain organoids, cell typing studies are confounded by several additional factors specific to the organoid model system. First, organoid cells may mature at different rates compared to *in vivo* human or rodent brains (Maor-Nof et al., 2016; Sloan et al., 2017). Second, organoid cell types may mature at different rates as a function of their developmental program, reliance on glial cells, or expression of ion channels (Oliveira et al., 2019; Squarzoni et al., 2014). Third, brain organoid development appears to be location specific. Because the internal structure of organoids features multiple starting points of growth, commonly called rosettes, it is possible that rosettes mature at different rates within the same organoid (Kelava & Lancaster, 2016b; Knight et al., 2018). These factors combined demonstrate the necessity of integrating the methods discussed here with other techniques to determine cell types conclusively, such as immunohistochemistry. The protocol described here is designed to be directly compatible with commonly used antibody staining protocols for cleared tissues (Susaki et al., 2020).

The ability to record reliably from cells in intact human brain organoids using a series of easy-to-implement methods based on *in vivo* recording protocols could provide new insights into the development of single cells and circuits in the human brain. The

methods discussed in this chapter could be easily implemented using existing equipment, is amenable to batch processing, and can be carried out from start to finish is less than 1 week.

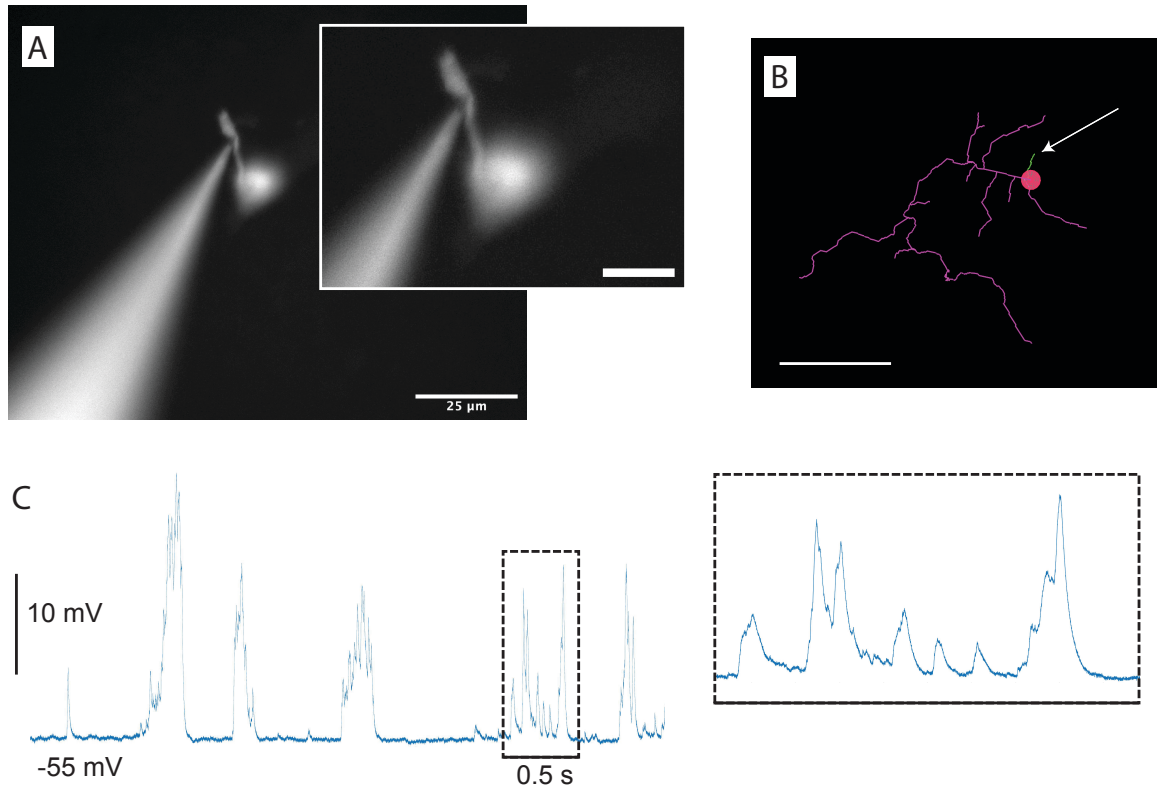


Figure 25. Putative neurite patch clamp recording in intact human brain organoid. A) Fluorescence image during recording showing pipette sealed onto neurite extending outward from soma. Scale bar on main image is 25 μm. Scale bar on inset is 10 μm. B) Trace of recorded neuron. Soma is shown in red and the patched neurite is labelled green and marked with an arrow. Scale bar is 50 μm. C) Spontaneous activity recording in neurite showing stable baseline and complex subthreshold activity.

CHAPTER 5. Conclusion

The further development of brain organoids as a model system will help to generate insight into the mechanisms of brain diseases and to help unravel the general principles of structure and function in the human brain. As with any model system, there will be a myriad of scientific techniques adapted to answer questions at different scales, throughputs, and modalities. Specifically for answering questions regarding the role of synaptic connectivity in physiological networks and for providing “ground truth” data to inform higher throughput experimental and computational work, I believe that intact human brain organoids will play an important role in the broader development of human brain organoids, perhaps analogous to how single cell *in vivo* experiments in mice provide valuable information to guide the use of other models and techniques. To this end, I have worked to demonstrate that these measurements are possible and have made technological innovations to make these methods more accurate, scalable, and easier to implement.

5.1 Major Contributions

In this work, I have made the following specific contributions:

- Validated and characterized the performance of the patcherBot
 - Slice patching in mice
 - Patching in cultured HEK 293 cells
 - Dual patch clamp recordings
- Discover and implement improved pipette cleaning with Tergazyme
 - Conducted first automated single-blind study of patch clamp methods

- Performed the most recordings ever with a single patch clamp pipette (102 whole cells in HEK 293T)
- Developed method for patch clamp recording and morphology reconstruction in intact human brain organoids
 - Perform the first sub-surface patch clamp recordings in intact human brain organoids
 - Perform manual, semi-automated, and fully automated patch clamp recordings in intact human brain organoids
 - Performed the first experiments known to combine electrophysiology and morphology in intact human brain organoids
 - Optimized tissue clearing and imaging protocols to facilitate location, identification, and confirmation of recorded cells in intact brain organoids

5.2 Perspectives

5.2.1 The Future of Automated Patch Clamping

To this date, the patcherBot represents the cumulative effort of 7 PhD students and more than 10 years of innovation. Indeed, since the publication of the patcherBot paper in 2019, we have added new pipette cleaning methods, applied the patcherBot to pharmacological studies, implemented artificial intelligence and machine learning for pipette positioning and cell detection, and continue to work in areas such as multi-pipette patch clamp, high throughput screening, and cell-type specific automated patch clamp in genetically modified mouse brain slices. At this point in the development of the technology, it is worthwhile to reflect and consider the possible future directions of this technology.

Over my years working with automated patch clamp, I have collected data on a wide variety of model systems in different experimental contexts. The following are proposed improvements to the current system that could improve the yield, throughput, and quality of data produced by the patcherBot:

- Faster, more stable micromanipulators
- Optimization and standardization of cell detection, gigasealing, and break-in parameters for each experimental setup using single blind experiments
- Further optimizations of pipette cleaning
- Improved quality and reliability of patch clamp pipettes
- Application of machine learning to monitoring of cell parameters during patch clamp recordings (B. R. Lee et al., 2020)
- Multiplexing of pipettes
- Parallelization of patcherBots

With continue innovation and effort applied to this technology, it is possible that patch clamp electrophysiology could be fully standardized and automated, much like the development of DNA sequencing (Heather & Chain, 2016).

5.3 Future Directions

5.3.1 Improving neuronal yield in intact organoid recordings

Patch clamp and morphology methods for intact human brain organoids are likely to be applied most often to older (>100 DIV) tissues, which presents the challenge of distinguishing mature neurons from other types of cells. As observed in this work using

non-biased sampling, there was a high proportion of cells that were not mature neurons (i.e., astrocytes and neural progenitor cells). For studies where a high proportion of mature neurons is desirable, the following targeting strategies could be used:

- Counter-staining the tissue with a second fluorescent dye prior to attempting patching could preferentially mark areas of the tissue surface with dense astrocyte networks. For example, sulforhodamine 101 can be used for bulk labelling and is taken up primarily by astrocytes (Appaix et al., 2012). By defining astrocyte networks, it is then possible to either target them or avoid them as needed. Alternatively, cells in live tissue could be stained using DiOlistic labelling with lipophilic tracers (O'Brien & Lummis, 2006).
- Testing cells for evoked activity using loose seal cell attached recordings during the period of neuron hunting could identify more mature cells for patching prior to attempting to form a gigaseal. Briefly, when a cell is detected by an increase in tip resistance while still under positive pressure (+10-20 mbar), the experimenter or the automated system could inject a series of short current injections of increasing intensity to determine if the cell will fire action potentials. If the cell does not fire action potentials or show significant evoked activity, the pipette can be retracted and moved to another cell.
- Identifying cell types of interest with fluorescent protein markers is also a variant of this technique that could dramatically improve selectivity. With expression of fluorescent markers in a sub-type of neurons and visual guidance from confocal or two photon microscopes, this method would allow for precise targeting of desired cell types in intact human brain organoids.

5.3.2 Improving Throughput of Imaging and Reconstruction of Organoid Cells

Confocal microscopy provides versatility and speed for switching between objectives, but if this method were to be standardized for higher throughput imaging, I would suggest an imaging technique like light sheet microscopy. The recent increase in volumetric imaging research has provided a wealth of new and rapidly improving computational methods to decrease imaging time and maximize data utility. The methods discussed here for multi-step casting of cleared organoids in CUBIC-R agarose are directly compatible with many setups of light sheet microscopy. Potentially, a custom light sheet microscope could be designed to image multiple organoids embedded in blocks of agarose in a fully automated fashion. Hardware and software tools for large-scale light sheet imaging are currently being developed (Matsumoto et al., 2019).

5.3.3 Integrating Immunohistochemistry Methods in Single Cell Intact Organoid Experiments

A natural and important extension of the CUBIC-based methods presented in this work is the classification of cells in the organoid based on antibody labelling of markers for specific cell types (e.g., neurons, neural progenitor cells, astrocytes, etc.). These methods have been demonstrated before, and with appropriate selection of antibodies and dyes compatible with CUBIC, should be straightforward to implement (Susaki et al., 2020). Some concerns must be addressed before this can be implemented widely. First, considerations of cross-talk between antibody labels could make detection of low levels of fluorescence from labelled dendrites, for example, more difficult. Secondly, incubating large numbers of intact organoids in solutions containing multiple antibodies and then

imaging those tissues with multiple wavelengths will make these experiments increasingly costly. One possible solution comes from an observation made when testing different variants of the CUBIC tissue clearing process prior to the experiments in Chapter 4. In an earlier variant of the CUBIC method, the first clearing solution (typically administered before antibody labelling) produced partially transparent tissue (Susaki et al., 2015). This is due to an overlap between the delipidation and RI-matching chemistries in the earlier versions of the method. While this clearing is not complete, it may be possible to image organoids containing patched and labelled cells prior to antibody staining. This modification to the protocol could provide cost savings in the event that cells were poorly labelled or difficult to register to their original locations in the tissue. More importantly, the ability to analyze the morphology and electrophysiology of targeted cells could inform the selection of antibody targets, providing a more precise determination of cell identity.

5.3.4 Delivery and Extraction of Genetic Material for Multimodal Single Cell Studies

In addition to the delivery of intracellular dyes used in this work, the intracellular access provided to cells in intact human brain organoids could also be used to deliver and extract genetic materials, further extending the utility of these methods. In terms of delivery of genetic material, pipette-based delivery is common in experiments where tracking a single cell over time is desirable, for example, imaging changes in cell morphology. Additionally, the genes delivered could encode for a trans-synaptic tracer, such as rabies virus, which can be delivered to patched cells to discover the network of cells it is connected to within the intact tissue (A. Wertz et al., 2015).

Extraction of genetic material during patch clamp experiments is a rapidly growing area of research. Historically, some labs have applied light suction during whole cell recordings, expelling the contents into a lysis buffer, and performing PCR to detect target genes, but these methods were challenging to implement and not widely adopted. The recent development of the Patch-Seq method has improved the repeatability and accuracy of gene expression studies from whole cell recordings. Implementing this method in intact human brain organoids would require adapting the method to fully blind or low-visibility conditions, something that has not been described in the literature. However, recent work describing optimal methods for Patch-Seq have highlighted the importance of extracting the cell nucleus as an indicator of full removal of the cytosol (B. R. Lee et al., 2021). As this process typically results in an increase of resistance at the pipette tip, which could be detected using an automated resistance monitoring system using the patcherBot. These methods could further extend the utility of patch clamp and morphological reconstruction in intact human brain organoids, producing valuable “ground truth” datasets.

5.3.5 Longitudinal Studies of Disease and Development Using Human Brain Organoids

Because brain organoids are complex, constantly developing tissues, there is broad interest in methods for studying them over time. Such longitudinal studies of intact tissues are typically limited to non-destructive methods where tissues can be maintained in a sterile environment. For many types of experiments, including patch clamping, this means that organoids used for these experiments must be fixed or discarded after the experiment to prevent the possible introduction of contaminants into the cell culture environment.

The ability to use intact organoids over multiple experimental days would provide additional valuable data and could intersect with studies of gene expression and the development of connectivity in brain organoids. In preliminary experiments, I have found that removing the brain organoid from the experimental chamber after patch clamp recordings placing it in a reversible 37 micron cell strainer (StemCell Technologies) prior to a wash series with sterile filtered ACSF (3 washes, 5 mL each) and organoid culture media (3 washes, 5 mL each). In preliminary experiments (n = 3 organoids), this washing step enables organoids to be returned to individual wells in a traditional cell culture incubator without infection for >7 days. After this time, samples of media from these wells were streaked on BHI agar plates and grown for 1 week. No colonies were detected. While promising, this method needs to be tested at a greater scale to fully validate it.

APPENDIX A. Ethical Implications of Brain Organoid Research

Utility of proposed work

Brain organoids represent a novel model system that have significant scientific utility in understanding unique and difficult to study aspects of human neurodevelopment and disease. Beyond this, widespread use of brain organoid technology has the potential to reduce the number of animals required for specific types of neuroscience research. Further, automation of patch clamp methods will make these experiments more efficient, whether they require the use of animals or not. Brain organoids were grown from hiPSC cell cultures either from donors or cell lines according to approved protocols of Emory University. These experiments deal entirely with *in situ* brain organoids, without implantation into animal subjects.

Broader ethical concerns for human brain organoids

Organoid technology enables researchers to explore the stages of human embryonic development in ways that were previously limited by legal restrictions. The “14 day rule” is the typical legal limit during which a researcher can maintain a human embryo *in vitro* (Pera, 2017). After this point, access to human embryonic tissue for research is limited by local laws regarding donation of aborted or stillborn fetuses. Legal restrictions in this area, especially in the United States, have changed dramatically based on political forces, making sustained research programs in this area financially high risk (McCune & Weissman, 2019; D. C. Wertz, 2002). Many critical processes in neurodevelopment occur in this time period where access to tissue is limited by ethical and legal concerns. Organoid

research represents an opportunity to minimize the need for fetal tissue in research if the organoids being used accurately replicate *in vivo* physiology being studied. However, organoid researchers are considering possible situations in which brain organoids may create new ethical concerns. The central concern is that if organoid tissues are or become conscious, research attitudes and practices will change drastically (Lavazza & Massimini, 2018). Both *in situ* brain organoids and animals transplanted with organoid tissue are of concern in this area, but for different reasons. *In situ* brain organoids, like the ones used in this proposal are thought to be unlikely, possibly even unable, to reach consciousness because the modern understanding of consciousness relies on sensory inputs that are largely unavailable to the tissue (Koch et al., 2016). However, there are outstanding questions as to whether or not a sentient *in situ* brain organoid could be detected, because they also lack behavioral output, allowing the possibility that *in situ* brain organoid research could inadvertently create a “locked-in” syndrome. Chimeras, animals implanted with human brain organoid tissue have the theoretical potential to create a “more intelligent” version of that animal, capable of an enhanced ability experience suffering or pain (Mansour et al., 2018; Zhang & Barres, 2013). Despite this possibility being more likely in the near term, it is also somewhat easier to manage ethically, because animals can be measured with behavioral tests to track their potential enhancement (Windrem et al., 2014). It is also a widely accepted scientific norm that animal subjects displaying higher levels of consciousness, especially as it regards pain, should be more protected in research practices (Koch et al., 2016; National Institutes of Health, 2013).

APPENDIX B. Detailed Protocol for Enzymatic Pipette Cleaning

Portions of this protocol have been previously published (Landry et al., 2021)

Materials and reagents

1. Borosilicate pipette glass with filament (Warner Instruments, catalog number: 64-0793)
2. Syringe, 5 ml (VWR, catalog number: BD309646)
3. Syringe filter, 0.2 μm (VWR, catalog number: 10218-486)
4. 23G needle (VWR, catalog number: 89134-098)
5. Tergazyme (Alconox, catalog number: 1304-1)

Equipment

Equipment listed is in addition to standard patch clamp electrophysiology equipment (*e.g.*, amplifier, digitizer, headstage, micromanipulator, microscope, pipette puller, *etc.*). Specific details of the patch clamp rig used in this paper are described in detail elsewhere (Kolb *et al.*, 2016 and 2019).

1. Cleaning dish (3D print or mill according to CAD files in SI, with appropriate changes for microscope stage)
2. Pressure control box (Detailed plans and parts list on autopatcher.org, direct order from Neuromatic Devices, neuromaticdevices.com)

Software

Depending on the level of automation desired, download either (1) and (2) for full automation or only (2) to enable “push-to-clean” for manual patch clamping with cleaning.

1. Autopatcher software (downloadable at autopatcher.org). The autopatcher software enables full automation of the cell detection, gigasealing, and break-in functions.
2. Push-to-clean software (downloadable at [Github](https://github.com/mightenyip/Pipette-Cleaning-Software), <https://github.com/mightenyip/Pipette-Cleaning-Software>). The terminology “push-to-clean” is defined as an otherwise manual electrophysiology rig that includes a button actuated pipette cleaning function. The button initiates a series of pipette position and pressure changes to clean the pipette for reuse.

Procedure

Before first experiment

- A. Manufacture cleaning dish according to plans and microscope stage dimensions (Figure 1C, CAD files in Supplementary Information Appendix B) in-house, using an on-demand production service (*e.g.*, Protolabs, protolabs.com), or purchase from commercial supplier (*e.g.*, Neuromatic Devices).
- B. Install pressure control box on existing patch clamp electrophysiology rig

1. Pressure control box can be built from scratch according to plans presented by Kodandaramaiah *et al.* (2016). Schematics, instructions, and parts lists are also available for download on autopatcher.org.
 2. A cleaning-compatible pressure control box can be purchased directly from Neuromatic Devices (neuromaticdevices.com).
- C. Download and install software from autopatcher.org. Perform initial software setup. Detailed instructions are provided in Supplementary Information Appendix A.
1. Register manipulator according to manufacturer and COM port (see Supplementary Information Figures S1-S2).
 2. Register the pressure control box to the specified COM port (see Supplementary Information Figures S1-S2).

Before each experiment

- A. Prepare biological sample for patch clamp recording. Methods are referenced for experimental preparations in which pipette cleaning has been validated by us or in other published reports.
1. For *in vitro* HEK 293 cells, follow Kolb *et al.* (2016). Pipette cleaning works well with wild-type cells, stably transfected lines, and transient transfections (Kolb *et al.*, 2016 and 2019)

2. For rodent neuron culture recording, follow Kaech and Banker (2006); Kolb *et al.* (2016). Cleaning for this preparation is verified in the following reports (Kolb *et al.*, 2016 and 2019).
 3. For acute brain tissue slices recording, follow Jiang *et al.* (2015). Cleaning for this preparation is verified in the following reports (Kolb *et al.*, 2016 and 2019).
 4. For *in vivo* mouse recording in anaesthetized preparations, follow Bagal *et al.* (2013). Cleaning for this preparation is verified in the following reports (Kolb *et al.*, 2016 and 2019; Stoy *et al.*, 2020).
 5. For acute human brain tissue slices, follow Ting *et al.* (2018); Peng *et al.* (2019). Cleaning for this preparation is verified in the following report (Peng *et al.*, 2019).
 6. For human cerebral organoids, follow Mariani *et al.* (2015); Qian *et al.* (2016). We have verified cleaning in this preparation in unpublished experiments.
- B. Prepare electrophysiology rig for patch clamp experiment and prepare pipettes as appropriate for experiment. Detailed guides for patch clamp rig setup, denoising, and troubleshooting are provided elsewhere (Perin and Markram, 2013; Wang *et al.*, 2015; Kodandaramaiah *et al.*, 2016).
- C. Load software for push-to-clean patch clamp experiment (Supplementary Information Appendix C).
- D. Make 2% w/v Tergazyme cleaning solution.
1. Prepare 2% w/v Tergazyme solution in room temperature deionized water.

2. Mix solution for until all Tergazyme powder is dissolved.

Note: Because Tergazyme is an enzymatic detergent, the enzymatic component degrades over time. The manufacturer recommends making fresh solutions and using them within 8 h for maximum efficacy.

E. Fill cleaning and rinsing bath reservoir with filtered solutions

1. Using a syringe with a 0.2 μm filter and 23G needle, fill the appropriate bath reservoir with freshly made 2% w/v Tergazyme (or extracellular solution for rinsing).
2. Be careful to not overfill the cleaning bath reservoir, as this can cause Tergazyme solution to flow into the experimental chamber, potentially damaging cells.

Note: To ensure there is no fluid exchange between the cleaning bath and the experimental bath, insert the tip of the pipette into the cleaning bath and monitor the square wave pulse in voltage clamp. If there is no electrical contact between the ungrounded cleaning bath and the grounded experimental bath, you will see capacitive transients, similar to when the tip of the pipette is in air. If there is electrical contact, you will see a square wave pulse, similar to when the tip is submerged in the experimental bath. To resolve this, use a task wipe to remove small amount of fluid from the cleaning bath until electrical contact is eliminated.

- F. In the software interface, calibrate manipulators in reference to cells and cleaning baths (Figure 6).

1. Select and save “exp bath location” position above target cell.
2. Select and save “location above baths” position directly above the cleaning bath reservoir.
3. Select and save “cleaning bath location” position with tip safely submerged in cleaning solution.
4. Select and save “wash bath” position with tip safely submerged in rinsing solution (*i.e.*, extracellular solution) if desired.

Patch clamp experiment

- A. Attempt patch clamp recording on target cell
- B. Initiate pipette cleaning using software interface by clicking the “clean” button. The functions performed by the software are as follows:
 1. Pipette retracts from cell to “location above baths” position under light positive pressure (+50 mbar).
 2. Pipette moves from “location above baths” position to “cleaning bath location” position until contact is made between the pipette tip and the cleaning solution.

Note: Touching the pipette to the surface of the cleaning solution can be detected as a change in the capacitance of a square wave pulse at the pipette tip. This can often be observed prior to the pipette visibly touching the surface. Visible confirmation of pipette-fluid contact is also sufficient to begin cleaning.

3. With pipette tip in cleaning bath, suction is applied (-345 mbar) for 5 s.
4. 5 rounds of alternating pulses of suction (-345 mbar for 1 s) and positive pressure (+700 mbar for 1 s) are applied.
5. To expel any residual cleaning solution from pipette tip, positive pressure is applied (+700 mbar) for 5 s.
6. Pipette is retracted from cleaning bath to “location above baths” position and then to either “exp bath location” position or “wash bath” position (optional).

C. Rinse the pipette (optional)

1. Pipette is moved from “cleaning bath location” position to “location above baths” position under positive pressure (+ 200 mbar).
2. Pipette is moved down from “location above baths” position towards “wash bath” position until contact is made between the pipette tip and the cleaning solution.
3. With pipette tip in rinse bath, apply 3 s of suction (-345 mbar) followed by 10 s of positive pressure (+700 mbar).
4. Retract pipette from “wash bath” position to “location above baths” position under positive pressure (+200 mbar).

D. Attempt patch clamp recording on next target cell

- E. Repeat steps A-D until end of experiment or failure of pipette (*e.g.*, tip breakage, clog, evaporation of cleaning solution, or user error).

Note: If pipette appears to be clogged (i.e., visible internal clog observed in pipette tip or increase in resistance) or broken (i.e., visible broken tip or decrease in resistance), then replace the pipette and repeat calibration.

Data analysis

Data from patch clamp experiments using pipette cleaning can be processed in the same way as traditional patch clamp experiments using software tools like pClamp (Molecular Devices) or Matlab (Mathworks). A useful analysis to characterize the efficacy of pipette cleaning is a yield curve, with number of attempts on the x-axis and the gigaseal or whole cell yield on the y-axis (Figure 2A, Figure 3A, Figure 4A, and Figure 5B). By comparing yield curves to ideal yields in which 100% of cells one attempts to patch result in a whole cell patch clamp configuration, it is possible to diagnose problems with cleaning yield, clogs, breaks, or other failure modes (Figure 4A). Methods and experiments can be compared from yield curve data using the Kolmogorov-Smirnov test. In addition, it is important to verify that cleaning does not cause a decrease in patching yield. Success rate plots that show the probability of obtaining a whole cell for a defined number of cleaning attempts are also useful (Figure 1B-C, Figure 5A). Data from these plots can be modeled using linear regression (*e.g.*, the `mnrfit` function in MATLAB). Odds ratios, 95% confidence intervals, and *p*-values test for deviations from initial performance.

Notes

1. How can pipette cleaning be used for multi-pipette experiments? Peng *et al.* (2019) recently demonstrated that multi-pipette connectivity studies in both rodent and human brain slices can be greatly accelerated by using pipette cleaning to both

increase yield and extend the number of connections tested per tissue [see Figures 3 and 5 of ref (Peng *et al.*, 2019)]. These systems rely on routinely achieving simultaneous whole cell recordings with all available pipettes to efficiently test for inter-neuronal connections, but obtaining simultaneous whole cell recordings on all available pipettes is difficult and dependent on experimenter skill (n.b., a study by Perin and Markram (2013) found that with a 12 pipette rig, novice users achieved an average of 4.8 ± 1.7 out of 12 possible whole cell recordings per attempt while experts achieved 9.6 ± 1.4 out of 12 possible whole cells recordings per attempt). Implementing a single round of pipette cleaning with 2% w/v Alconox and no rinsing resulted in significant improvements in success rate (*i.e.*, ratio of actual to possible number of simultaneous whole cell recordings) relative to no cleaning for both 8- and 10-manipulator patch-clamp recording setups, from $85 \pm 13\%$ to $97 \pm 5\%$ and $79 \pm 11\%$ to $92 \pm 6\%$, respectively (Peng *et al.*, 2019). Further, once the first round of simultaneous whole cell recordings was obtained, pipette cleaning allowed for additional surrounding neurons to be patched, increasing the total number of connections that can be tested in a single sample from $140 \pm 24\%$ to $244 \pm 52\%$ with an 8 pipette rig (Peng *et al.*, 2019). Use of this method could enable faster, more efficient collection of large datasets required for understanding neuronal connectivity (Goriounova *et al.*, 2018; Gouwens *et al.*, 2019).

2. How can pipette cleaning be used for high throughput screening? Large-scale efforts are also underway to discover and characterize drug candidates (Dunlop *et al.*, 2008; Bagal *et al.*, 2013), engineer improved genetic tools for neuroscience

(Piatkevich *et al.*, 2018; Yang *et al.*, 2019), and understand human mutations in ion channel proteins (Swanger *et al.*, 2016; Ogden *et al.*, 2017). However, many of these projects are limited by the low throughput of traditional patch clamp experiments (Park *et al.*, 2013; Cho *et al.*, 2019). For most screening experiments, manual patch clamping without cleaning has a throughput of 8-10 whole cell recordings per experimenter per day (Milligan *et al.*, 2009). Using our automated patch clamp system with 2% w/v Tergazyme, we have demonstrated routine throughputs of 10 whole cell recordings per pipette per hour and daily throughputs of up to 100 whole cell recordings (Figure 5) (Kolb *et al.*, 2019). To further show the utility of pipette cleaning for functional screening, we performed a pilot experiment using HEK 293 cells transiently transfected with channelrhodopsin-2 (ChR-2). In this experiment, 46 whole cell recordings were obtained from 51 patch clamp attempts with a single pipette cleaned using 2% w/v Tergazyme (Figure 3).

3. What are expected yields using this method? Our yield and recording quality of patch clamp recordings were comparable to manual pipette replacement. For experiments with HEK 293 cells, whole cell recording yield was consistently 70-90% using the patcherBot. The ability to perform high-yield, high-throughput experiments in a fully automated Tergazyme cleaning system has also enabled us to iteratively improve our automated method in HEK 293 cells. For example, we compared 2% w/v Tergazyme solution to 2% w/v Alconox and saline in a randomized experiment where the operator was blinded to the identity of the cleaning solution (Figure 2). Following that experiment, we then randomly varied

the depth of pipette indentation into the cell membrane and found an optimal range that increased whole cell recording yield to ~90% (Figure 2).

4. How long can cleaned pipettes be used? We have also found that Tergazyme cleaning is effective on single pipettes reused over 100 times, using the patcherBot (Figure 5) (Kolb *et al.*, 2019). Because typical throughput for patch clamp electrophysiology experiments is in the range of 10-30 recordings per day, it is likely that pipettes only need to be replaced once per day, except in cases where pipettes are broken or clogged.
5. How does the cleaning method fail? Using a single pipette cleaned with our improved 2% w/v Tergazyme cleaning solution, we achieved 102 whole cell recordings in 122 patch clamp attempts over a 13 h automated experiment. In our attempts to find the failure point of 2% w/v Tergazyme cleaning, pipette breakage or internal clogs were more likely to cause failure than an inability to clean the pipette. Internal pipette clogs are thought to form from environmental dust of particulates in pipette solution. Clogs tended to form as a function of duration of positive pressure applied, and were more likely to occur over long experiments. Clogs can be diagnosed from flat portions in the yield curve that are unlikely to result from chance. Some clogs are reversible (see representative trace in Figure 4). Pipettes can also fail after a tip breakage, which typically occurs if a target cell is missed. To determine an approximate failure point of cleaning, consider each patch clamp attempt as an independent event with a probability equal to the gigaseal recording failure rate and determine the number of cleaning attempts until the probability is less than or equal to 0.01. For example, with a gigaseal failure

rate of 30% (*i.e.*, gigaseal success rate = 70%), the likelihood of a sequence of 4 failures to gigaseal has a probability of <1%.

6. Does cleaning transfer residual enzyme or detergent to the cells? One concern of patch clamp experimenters interested in implementing cleaning is the possibility of contamination from residual cleaning solution in the pipette after cleaning. Our initial study addressed this concern with two types of experiments (Kolb *et al.*, 2016). First, we performed electrospray ionization mass spectrometry (ESI-MS) on fresh pipettes and pipettes cleaned with 2% w/v Alconox and found that no Alconox residues were detectable. For this experiment, we used 2% w/v Alconox and the limit of detection was 147 ng/ml. Secondly, we performed patch clamp experiments on HEK 293 cells expressing the γ -aminobutyric acid type A Receptor (GABA_AR), which is known to be sensitive to extracellular application of detergents. In these experiments, we did not find any statistically significant differences in GABA_AR electrophysiology between cleaned and fresh pipettes.

7. Is the rinsing step (Procedure Step C. Rinse the pipette) required? Interestingly, recent experiments by Peng *et al.* (2019) (using human brain slices), as well as our lab (using mouse brain slices, Figure 5), have provided evidence that the rinse step (Procedure, Step C. Rinse the pipette (optional)) is unnecessary. Thus in this method description, we label it as “optional”. However, if the possibility of contamination is still a concern in a particular experiment, we suggest rinsing as described in Procedure Step C. Rinse the pipette (optional) with the following modifications as needed to minimize risk:

- a. Add time and cycles to the rinsing step to remove residual Tergazyme by dilution.
- b. Reduce the concentration of Tergazyme in the cleaning solution. A 2% w/v Tergazyme solution is effective at cleaning pipettes up to 100 times with no measurable degradation in yield (Figure 4). This suggests that lower concentrations of Tergazyme will still be effective for pipette cleaning, with a potential trade-off in maximum number of cleans per pipette.
- c. Increase the perfusion rate of external solution so that any residual Tergazyme is removed from the experimental chamber quickly.

REFERENCES

- Angelo, K., & Margrie, T. W. (2011). Population diversity and function of hyperpolarization-activated current in olfactory bulb mitral cells. *Scientific Reports*, *1*, 1–11. <https://doi.org/10.1038/srep00050>
- Appaix, F., Girod, S., Boisseau, S., Römer, J., Vial, J. C., Albrieux, M., Maurin, M., Depaulis, A., Guillemain, I., & van der Sanden, B. (2012). Specific in vivo staining of astrocytes in the whole brain after intravenous injection of sulforhodamine dyes. *PLoS ONE*, *7*(4), 1–13. <https://doi.org/10.1371/journal.pone.0035169>
- Arlotta, P. (2018). Organoids required! A new path to understanding human brain development and disease. *Nature Methods*, *15*(1), 27–29. <https://doi.org/10.1038/nmeth.4557>
- Bargmann, C. I., & Newsome, W. T. (2014). The Brain Research Through Advancing Innovative Neurotechnologies (BRAIN) initiative and neurology. *JAMA Neurology*, *71*(6), 675–676. <https://doi.org/10.1001/jamaneurol.2014.411>
- Barth, A. L., Burkhalter, A., Callaway, E. M., Connors, B. W., Cauli, B., DeFelipe, J., Feldmeyer, D., Freund, T., Kawaguchi, Y., Kisvarday, Z., Kubota, Y., McBain, C., Oberlaender, M., Rossier, J., Rudy, B., Staiger, J. F., Somogyi, P., Tamas, G., & Yuste, R. (2016). Comment on “Principles of connectivity among morphologically defined cell types in adult neocortex.” *Science*, *353*(6304). <http://science.sciencemag.org/content/353/6304/1108.1.long>

- Berg, J., Sorensen, S., Ting, J., Miller, J., Chartrand, T., Buchin, A., Bakken, T., Budzillo, A., Dee, N., Ding, S.-L., Gouwens, N., Hodge, R., Kalmbach, B., Lee, C., Lee, B., Alfiler, L., Baker, K., Barkan, E., Beller, A., ... Ko, A. (2020). *Human cortical expansion involves diversification and specialization of supragranular intratelencephalic-projecting neurons*. <https://doi.org/10.1101/2020.03.31.018820>
- Birey, F., Andersen, J., Makinson, C. D., Islam, S., Wei, W., Huber, N., Fan, H. C., Metzler, K. R. C., Panagiotakos, G., Thom, N., O'Rourke, N. A., Steinmetz, L. M., Bernstein, J. A., Hallmayer, J., Huguenard, J. R., & Pasca, S. P. (2017a). Assembly of functionally integrated human forebrain spheroids. *Nature*, *545*(7652), 54–59. <https://doi.org/10.1038/nature22330>
- Cadwell, C. R., Palasantza, A., Jiang, X., Berens, P., Deng, Q., Yilmaz, M., Reimer, J., Shen, S., Bethge, M., Tolias, K. F., Sandberg, R., & Tolias, A. S. (2015). Electrophysiological, transcriptomic and morphologic profiling of single neurons using Patch-seq. *Nature Biotechnology*, *34*(December), 1–8. <https://doi.org/10.1038/nbt.3445>
- Cadwell, C. R., Scala, F., Fahey, P. G., Kobak, D., Mulherkar, S., Sinz, F. H., Papadopoulos, S., Tan, Z. H., Johnsson, P., Hartmanis, L., Li, S., Cotton, R. J., Tolias, K. F., Sandberg, R., Berens, P., Jiang, X., & Tolias, A. S. (2020). Cell type composition and circuit organization of clonally related excitatory neurons in the juvenile mouse neocortex. *ELife*, *9*, 1–34. <https://doi.org/10.7554/eLife.52951>
- Cepeda, C., Hurst, R. S., Flores-Hernández, J., Hernández-Echeagaray, E., Klapstein, G. J., Boylan, M. K., Calvert, C. R., Jocoy, E. L., Nguyen, O. K., André, V. M., Vinters,

- H. V, Ariano, M. A., Levine, M. S., & Mathern, G. W. (2003). Morphological and electrophysiological characterization of abnormal cell types in pediatric cortical dysplasia. *Journal of Neuroscience Research*, 72(4), 472–486. <https://doi.org/10.1002/jnr.10604>
- Chuong, A. S., Miri, M. L., Busskamp, V., Matthews, G. A. C., Acker, L. C., Sørensen, A. T., Young, A., Klapoetke, N. C., Henninger, M. a, Kodandaramaiah, S. B., Ogawa, M., Ramanlal, S. B., Bandler, R. C., Allen, B. D., Forest, C. R., Chow, B. Y., Han, X., Lin, Y., Tye, K. M., ... Boyden, E. S. (2014). Noninvasive optical inhibition with a red-shifted microbial rhodopsin. *Nature Neuroscience*, 17(8), 1123–1129. <https://doi.org/10.1038/nn.3752>
- Cugola, F. R., Fernandes, I. R., Russo, F. B., Freitas, B. C., Dias, J. L. M., Guimarães, K. P., Benazzato, C., Almeida, N., Pignatari, G. C., Romero, S., Polonio, C. M., Cunha, I., Freitas, C. L., Brandão, W. N., Rossato, C., Andrade, D. G., Faria, D. de P., Garcez, A. T., Buchpigel, C. A., ... Beltrão-Braga, P. C. B. (2016). The Brazilian Zika virus strain causes birth defects in experimental models. *Nature*, 534(7606), 267–271. <https://doi.org/10.1038/nature18296>
- Diel, E. E., Lichtman, J. W., & Richardson, D. S. (2020). Tutorial: avoiding and correcting sample-induced spherical aberration artifacts in 3D fluorescence microscopy. *Nature Protocols*, 15(9), 2773–2784. <https://doi.org/10.1038/s41596-020-0360-2>
- Dombeck, D. A., Khabbaz, A. N., Collman, F., Adelman, T. L., & Tank, D. W. (2007). Imaging large-scale neural activity with cellular resolution in awake, mobile mice. *Neuron*, 56(1), 43–57. <https://doi.org/10.1016/j.neuron.2007.08.003>

- Duan, X., Fu, T. M., Liu, J., & Lieber, C. M. (2013). Nanoelectronics-biology frontier: From nanoscopic probes for action potential recording in live cells to three-dimensional cyborg tissues. In *Nano Today* (Vol. 8, Issue 4, pp. 351–373). <https://doi.org/10.1016/j.nantod.2013.05.001>
- Floch, P. Le, Li, Q., Liu, R., Tasnim, K., Zhao, S., Lin, Z., & Jiang, H. (2021). *A method for three-dimensional single-cell chronic electrophysiology from developing brain organoids*. <https://doi.org/10.1101/2021.06.22.449502>
- Gabriel, E., Albanna, W., Pasquini, G., Ramani, A., Josipovic, N., Mariappan, A., Schinzel, F., Karch, C. M., Bao, G., Gottardo, M., Suren, A. A., Hescheler, J., Nagel-Wolfrum, K., Persico, V., Rizzoli, S. O., Altmüller, J., Riparbelli, M. G., Callaini, G., Goureau, O., ... Gopalakrishnan, J. (2021). Human brain organoids assemble functionally integrated bilateral optic vesicles. *Cell Stem Cell*, 28(10), 1740-1757.e8. <https://doi.org/10.1016/j.stem.2021.07.010>
- Goda, Y., & Davis, G. W. (2003). Mechanisms of synapse assembly and disassembly. In *Neuron* (Vol. 40, Issue 2, pp. 243–264). [https://doi.org/10.1016/S0896-6273\(03\)00608-1](https://doi.org/10.1016/S0896-6273(03)00608-1)
- Gouwens, N. W., Sorensen, S. A., Berg, J., Lee, C., Jarsky, T., Ting, J., Sunkin, S. M., Feng, D., Anastassiou, C. A., Barkan, E., Bickley, K., Blesie, N., Braun, T., Brouner, K., Budzillo, A., Caldejon, S., Casper, T., Castelli, D., Chong, P., ... Koch, C. (2019). Classification of electrophysiological and morphological neuron types in the mouse visual cortex. *Nature Neuroscience*, 22(7), 1182–1195. <https://doi.org/10.1038/s41593-019-0417-0>

- Haider, B., Häusser, M., & Carandini, M. (2013). Inhibition dominates sensory responses in the awake cortex. *Nature*, *493*(7430), 97–102. <https://doi.org/10.1038/nature11665>
- Hamill, O. P., Marty, A., Neher, E., Sakmann, B., & Sigworth, F. J. (1981). Improved patch-clamp techniques for high-resolution current recording from cells and cell-free membrane patches. *Pflügers Archiv European Journal of Physiology*, *391*(2), 85–100. <https://doi.org/10.1007/BF00656997>
- Heather, J. M., & Chain, B. (2016). The sequence of sequencers: The history of sequencing DNA. *Genomics*, *107*(1), 1–8. <https://doi.org/10.1016/j.ygeno.2015.11.003>
- Hodgkin, A. L., & Huxley, A. F. (1952). A quantitative description of membrane current and its application to conduction and excitation in nerve. *The Journal of Physiology*, *117*(4), 500–544. <https://doi.org/10.1113/jphysiol.1952.sp004764>
- Holst, G. L., Stoy, W., Yang, B., Kolb, I., Kodandaramaiah, S. B., Li, L., Knoblich, U., Zeng, H., Haider, B., Boyden, E. S., & Forest, C. R. (2019a). Autonomous patch-clamp robot for functional characterization of neurons in vivo: Development and application to mouse visual cortex. *Journal of Neurophysiology*, *121*(6), 2341–2357. <https://doi.org/10.1152/jn.00738.2018>
- Horikawa, K., & Armstrong, W. (1988). A versatile means of intracellular labeling: injection of biocytin and its detection with avidin conjugates. *Journal of Neuroscience Methods*, *25*(1), 1–11.
- Hunt, D. L., Lai, C., Smith, R. D., Lee, A. K., Harris, T. D., & Barbic, M. (2019). Multimodal in vivo brain electrophysiology with integrated glass microelectrodes.

Nature Biomedical Engineering, 3(9), 741–753. <https://doi.org/10.1038/s41551-019-0373-8>

Jensen, K. H. R., & Berg, R. W. (2017). Advances And Perspectives In Tissue Clearing Using CLARITY. *BioRxiv*. <https://doi.org/10.1016/j.jchemneu.2017.07.005>

Jiang, X., Shen, S., Sinz, F., Reimer, J., Cadwell, C. R., Berens, P., Ecker, A. S., Patel, S., Denfield, G. H., Froudarakis, E., Li, S., Walker, E., & Tolias, A. S. (2016). Response to Comment on “Principles of connectivity among morphologically defined cell types in adult neocortex.” *Science*, 353(6304), 1108–1108. <https://doi.org/10.1126/science.aaf6102>

Jiang, Xiaolong, Shen, S., Cadwell, C. R., Berens, P., Sinz, F., Ecker, A. S., Patel, S., & Tolias, A. S. (2015). Principles of connectivity among morphologically defined cell types in adult neocortex. *Science*, 350(6264), aac9462–aac9462. <https://doi.org/10.1126/science.aac9462>

Jiang, Xiaolong, Wang, G., Lee, A. J., Stornetta, R. L., & Zhu, J. J. (2013). *The organization of two new cortical interneuronal circuits Supplementary Information for The organization of two new cortical interneuronal circuits*. 218(March). <https://doi.org/10.1038/nn.3>

Kalisman, N., Silberberg, G., & Markram, H. (2005). The neocortical microcircuit as a tabula rasa. *Proceedings of the National Academy of Sciences of the United States of America*, 102(3), 880–885. <https://doi.org/10.1073/pnas.0407088102>

Kalmbach, B. E., Buchin, A., Long, B., Close, J., Nandi, A., Miller, J. A., Bakken, T. E.,

- Hodge, R. D., Chong, P., de Frates, R., Dai, K., Maltzer, Z., Nicovich, P. R., Keene, C. D., Silbergeld, D. L., Gwinn, R. P., Cobbs, C., Ko, A. L., Ojemann, J. G., ... Ting, J. T. (2018). h-Channels Contribute to Divergent Intrinsic Membrane Properties of Supragranular Pyramidal Neurons in Human versus Mouse Cerebral Cortex. *Neuron*, *100*(5), 1194-1208.e5. <https://doi.org/10.1016/j.neuron.2018.10.012>
- Kang, Y., Zhou, Y., Li, Y., Han, Y., Xu, J., Niu, W., Li, Z., Liu, S., Feng, H., Huang, W., Duan, R., Xu, T., Raj, N., Zhang, F., Dou, J., Xu, C., Wu, H., Bassell, G. J., Warren, S. T., ... Wen, Z. (2021). A human forebrain organoid model of fragile X syndrome exhibits altered neurogenesis and highlights new treatment strategies. *Nature Neuroscience*, *24*(10), 1377–1391. <https://doi.org/10.1038/s41593-021-00913-6>
- Kao, L., Abuladze, N., Shao, X. M., McKeegan, K., & Kurtz, I. (2012). A new technique for multiple re-use of planar patch clamp chips. *Journal of Neuroscience Methods*, *208*(2), 205–210. <https://doi.org/10.1016/j.jneumeth.2012.05.002>
- Ke, M. T., Nakai, Y., Fujimoto, S., Takayama, R., Yoshida, S., Kitajima, T. S., Sato, M., & Imai, T. (2016). Super-Resolution Mapping of Neuronal Circuitry With an Index-Optimized Clearing Agent. *Cell Reports*, *14*(11), 2718–2732. <https://doi.org/10.1016/j.celrep.2016.02.057>
- Kelava, I., & Lancaster, M. A. (2016a). Dishing out mini-brains: Current progress and future prospects in brain organoid research. *Developmental Biology*. <https://doi.org/10.1016/j.ydbio.2016.06.037>
- Kelava, I., & Lancaster, M. A. (2016b). Stem Cell Models of Human Brain Development.

Cell Stem Cell, 18(6), 736–748. <https://doi.org/10.1016/j.stem.2016.05.022>

Kim, S. E., Lee, S. Y., Blanco, C. L., & Kim, J. H. (2014). Developmental profiles of the intrinsic properties and synaptic function of auditory neurons in preterm and term baboon neonates. *The Journal of Neuroscience : The Official Journal of the Society for Neuroscience*, 34(34), 11399–11404. <https://doi.org/10.1523/JNEUROSCI.4734-13.2014>

Knight, G. T., Lundin, B. F., Iyer, N., Ashton, L. M. T., Sethares, W. A., Willett, R. M., & Ashton, R. S. (2018). Engineering induction of singular neural rosette emergence within hPSC-derived tissues. *ELife*, 7, 1–23. <https://doi.org/10.7554/eLife.37549>

Koch, C., Massimini, M., Boly, M., & Tononi, G. (2016). Neural correlates of consciousness: Progress and problems. *Nature Reviews Neuroscience*, 17(5), 307–321. <https://doi.org/10.1038/nrn.2016.22>

Kodandaramaiah, S. B., Flores, F. J., Holst, G. L., Singer, A. C., Han, X., Brown, E. N., Boyden, E. S., & Forest, C. R. (2018). Multi-neuron intracellular recording in vivo via interacting autopatching robots. *ELife*, 7, 1–19. <https://doi.org/10.7554/eLife.24656>

Kodandaramaiah, S. B., Franzesi, G. T., Chow, B. Y., Boyden, E. S., & Forest, C. R. (2012). Automated whole-cell patch-clamp electrophysiology of neurons in vivo. *Nature Methods*, 9(6), 585–587. <https://doi.org/10.1038/nmeth.1993>

Kodandaramaiah, S. B., Holst, G. L., Wickersham, I. R., Singer, A. C., Franzesi, G. T., McKinnon, M. L., Forest, C. R., & Boyden, E. S. (2016). Assembly and operation of

- the autopatcher for automated intracellular neural recording in vivo. *Nature Protocols*, *11*(4), 634–654. <https://doi.org/10.1038/nprot.2016.007>
- Kolb, I., Stoy, W. A., Rousseau, E. B., Moody, O. A., Jenkins, A., & Forest, C. R. (2016). Cleaning patch-clamp pipettes for immediate reuse. *Scientific Reports*, *6*(1), 35001. <https://doi.org/10.1038/srep35001>
- Kolb, Ilya, Landry, C. R., Yip, M. C., Lewallen, C. F., Stoy, W. A., Lee, J., Felouzis, A., Yang, B., Boyden, E. S., Rozell, C. J., & Forest, C. R. (2019). PatcherBot: A single-cell electrophysiology robot for adherent cells and brain slices. *Journal of Neural Engineering*, *16*(4). <https://doi.org/10.1088/1741-2552/ab1834>
- Krencik, R., Seo, K., van Asperen, J. V., Basu, N., Cvetkovic, C., Barlas, S., Chen, R., Ludwig, C., Wang, C., Ward, M. E., Gan, L., Horner, P. J., Rowitch, D. H., & Ullian, E. M. (2017). Systematic Three-Dimensional Coculture Rapidly Recapitulates Interactions between Human Neurons and Astrocytes. *Stem Cell Reports*, *9*(6), 1745–1753. <https://doi.org/10.1016/j.stemcr.2017.10.026>
- Lancaster, M. A., Corsini, N. S., Wolfinger, S., Gustafson, E. H., Phillips, A. W., Burkard, T. R., Otani, T., Livesey, F. J., & Knoblich, J. A. (2017). Guided self-organization and cortical plate formation in human brain organoids. *Nature Publishing Group*. <https://doi.org/10.1038/nbt.3906>
- Lancaster, M. A., Renner, M., Martin, C.-A., Wenzel, D., Bicknell, L. S., Hurles, M. E., Homfray, T., Penninger, J. M., Jackson, A. P., & Knoblich, J. A. (2013). Cerebral organoids model human brain development and microcephaly. *Nature*, *501*(7467),

373–379. <https://doi.org/10.1038/nature12517>

Lancaster, M. a, Renner, M., Martin, C., Wenzel, D., Bicknell, S., Hurles, M. E., Homfray, T., Penninger, J. M., & Andrew, P. (2014). Cerebral organoids model human brain development and microcephaly. *Nature*, *501*(7467). <https://doi.org/10.1038/nature12517>. Cerebral

Landry, C. R., Yip, M. C., Kolb, I., Stoy, W. A., Gonzalez, M. M., & Forest, C. R. (2021). Method for Rapid Enzymatic Cleaning for Reuse of Patch Clamp Pipettes: Increasing Throughput by Eliminating Manual Pipette Replacement between Patch Clamp Attempts. *Bio-Protocol*, *11*(14), e4085. <https://doi.org/10.21769/BioProtoc.4085>

Lavazza, A., & Massimini, M. (2018). Cerebral organoids: Ethical issues and consciousness assessment. *Journal of Medical Ethics*, *44*(9), 606–610. <https://doi.org/10.1136/medethics-2017-104555>

Lee, B. R., Budzillo, A., Hadley, K., Miller, J. A., Jarsky, T., Baker, K., Hill, D., Kim, L., Mann, R., Ng, L., Oldre, A., Rajanbabu, R., Trinh, J., Braun, T., Dalley, R., Gouwens, N. W., Kim, T. K., Smith, K., Soler-Llavina, G., ... Berg, J. (2020). High fidelity electrophysiological, morphological, and transcriptomic cell characterization using a refined Patch-seq protocol. *BioRxiv*, 2020.11.04.369082. <http://biorxiv.org/content/early/2020/11/05/2020.11.04.369082.abstract>

Lee, B. R., Budzillo, A., Hadley, K., Miller, J. A., Jarsky, T., Baker, K., Hill, D., Kim, L., Mann, R., Ng, L., Oldre, A., Rajanbabu, R., Trinh, J., Vargas, S., Braun, T., Dalley, R., Gouwens, N. W., Kalmbach, B. E., Kim, T. K., ... Berg, J. (2021). Scaled, high

- fidelity electrophysiological, morphological, and transcriptomic cell characterization. *ELife*, 10, 1–30. <https://doi.org/10.7554/eLife.65482>
- Lee, C. T., Bendriem, R. M., Wu, W. W., & Shen, R. F. (2017). 3D brain Organoids derived from pluripotent stem cells: Promising experimental models for brain development and neurodegenerative disorders Julie Y.H. Chan. *Journal of Biomedical Science*, 24(1), 1–12. <https://doi.org/10.1186/s12929-017-0362-8>
- Lee, J., Kolb, I., Forest, C. R., & Rozell, C. J. (2018). Cell Membrane Tracking in Living Brain Tissue Using Differential Interference Contrast Microscopy. *IEEE Transactions on Image Processing*, 27(4), 1847–1861. <https://doi.org/10.1109/TIP.2017.2787625>
- Li, L., Ouellette, B., Stoy, W. A., Garren, E. J., Daigle, T. L., Forest, C. R., Koch, C., & Zeng, H. (2017a). A robot for high yield electrophysiology and morphology of single neurons in vivo. *Nature Communications*, 8. <https://doi.org/10.1038/ncomms15604>
- Livet, J., Weissman, T. A., Kang, H., Draft, R. W., Lu, J., Bennis, R. A., Sanes, J. R., & Lichtman, J. W. (2007). Transgenic strategies for combinatorial expression of fluorescent proteins in the nervous system. *Nature*, 450(7166), 56–62. <https://doi.org/10.1038/nature06293>
- Loulier, K., Barry, R., Mahou, P., Le Franc, Y., Supatto, W., Matho, K. S., Ieng, S., Fouquet, S., Dupin, E., Benosman, R., Chédotal, A., Beaupaire, E., Morin, X., & Livet, J. (2014). Multiplex cell and lineage tracking with combinatorial labels. *Neuron*, 81(3), 505–520. <https://doi.org/10.1016/j.neuron.2013.12.016>

Mansour, A. A., Gonçalves, J. T., Bloyd, C. W., Li, H., Fernandes, S., Quang, D., Johnston, S., Parylak, S. L., Jin, X., & Gage, F. H. (2018). An in vivo model of functional and vascularized human brain organoids. *Nature Biotechnology*, *36*(5), 432–441. <https://doi.org/10.1038/nbt.4127>

Maor-Nof, M., Romi, E., Shalom, H. S., Ulisse, V., Raanan, C., Nof, A., Leshkowitz, D., Lang, R., & Yaron, A. (2016). Axonal Degeneration Is Regulated by a Transcriptional Program that Coordinates Expression of Pro- and Anti-degenerative Factors. *Neuron*, *92*(5), 991–1006. <https://doi.org/10.1016/j.neuron.2016.10.061>

Margrie, T. W., Brecht, M., & Sakmann, B. (2002). In vivo, low-resistance, whole-cell recordings from neurons in the anaesthetized and awake mammalian brain. *Pflügers Archiv: European Journal of Physiology*, *444*(4), 491–498. <https://doi.org/10.1007/s00424-002-0831-z>

Mariani, J., Coppola, G., Zhang, P., Abyzov, A., Provini, L., Tomasini, L., Amenduni, M., Szekely, A., Palejev, D., Wilson, M., Gerstein, M., Grigorenko, E. L., Chawarska, K., Pelphrey, K. A., Howe, J. R., & Vaccarino, F. M. (2015a). FOXP1-Dependent Dysregulation of GABA/Glutamate Neuron Differentiation in Autism Spectrum Disorders. *Cell*, *162*(2), 375–390. <https://doi.org/10.1016/j.cell.2015.06.034>

4

Markram, H, Lübke, J., Frotscher, M., Roth, A., & Sakmann, B. (1997). Physiology and anatomy of synaptic connections between thick tufted pyramidal neurones in the developing rat neocortex. *The Journal of Physiology*, *500* (Pt 2, 409–440.

<https://doi.org/10.1126/science.275.5297.213>

Markram, Henry. (1997). A network of tufted layer 5 pyramidal neurons. *Cerebral Cortex*, 7(6), 523–533. <https://doi.org/10.1093/cercor/7.6.523>

Markram, Henry. (2008). Fixing the location and dimensions of functional neocortical columns. *HFSP Journal*, 2(3), 132–135. <https://doi.org/10.2976/1.2919545>

Markram, Henry, Muller, E., Ramaswamy, S., Reimann, M. W., Abdellah, M., Sanchez, C. A., Ailamaki, A., Alonso-Nanclares, L., Antille, N., Arsever, S., Kahou, G. A. A., Berger, T. K., Bilgili, A., Buncic, N., Chalimourda, A., Chindemi, G., Courcol, J. D., Delalondre, F., Delattre, V., ... Schürmann, F. (2015). Reconstruction and Simulation of Neocortical Microcircuitry. *Cell*, 163(2), 456–492. <https://doi.org/10.1016/j.cell.2015.09.029>

Marx, M., Günter, R. H., Hucko, W., Radnikow, G., & Feldmeyer, D. (2012). Improved biocytin labeling and neuronal 3D reconstruction. *Nature Protocols*, 7(2), 394–407. <https://doi.org/10.1038/nprot.2011.449>

Matsui, T. K., Matsubayashi, M., Sakaguchi, Y. M., Hayashi, R. K., Zheng, C., Sugie, K., Hasegawa, M., Nakagawa, T., & Mori, E. (2018). Six-month cultured cerebral organoids from human ES cells contain matured neural cells. *Neuroscience Letters*, 670(November 2017), 75–82. <https://doi.org/10.1016/j.neulet.2018.01.040>

Matsumoto, K., Mitani, T. T., Horiguchi, S. A., Kaneshiro, J., Murakami, T. C., Mano, T., Fujishima, H., Konno, A., Watanabe, T. M., Hirai, H., & Ueda, H. R. (2019). Advanced CUBIC tissue clearing for whole-organ cell profiling. *Nature Protocols*,

14(12), 3506–3537. <https://doi.org/10.1038/s41596-019-0240-9>

McCune, J. M., & Weissman, I. L. (2019). The Ban on US Government Funding Research Using Human Fetal Tissues: How Does This Fit with the NIH Mission to Advance Medical Science for the Benefit of the Citizenry? *Stem Cell Reports*, 13(5), 777–786. <https://doi.org/10.1016/j.stemcr.2019.10.003>

Moore, A. R., Filipovic, R., Mo, Z., Rasband, M. N., Zecevic, N., & Antic, S. D. (2009). Electrical excitability of early neurons in the human cerebral cortex during the second trimester of gestation. *Cerebral Cortex*, 19(8), 1795–1805. <https://doi.org/10.1093/cercor/bhn206>

Moore, A. R., Zhou, W.-L., Jakovcevski, I., Zecevic, N., & Antic, S. D. (2011). Spontaneous Electrical Activity in the Human Fetal Cortex In Vitro. *Journal of Neuroscience*, 31(7), 2391–2398. <https://doi.org/10.1523/JNEUROSCI.3886-10.2011>

Moradi Chameh, H., Wang, L., Rich, S., Zhang, L., Carlen, P., Tripathy, S., & Valiante, T. (2019). Sag currents are a major contributor to human pyramidal cell intrinsic differences across cortical layers and between individuals. 1–26. <https://doi.org/10.1101/748988>

National Institutes of Health. (2013). Public Health Service Policy on Humane Care and Use of Laboratory Animals. *Office of Laboratory Animal Welfare*, 2002.

Neher, E., & Sakmann, B. (1976). Single-channel currents recorded from membrane of denervated frog muscle fibres. *Nature*, 260(5554), 799–802.

<https://doi.org/10.1038/260799a0>

O'Brien, J. A., & Lummis, S. C. R. (2006). Diolistic labeling of neuronal cultures and intact tissue using a hand-held gene gun. *Nature Protocols*, *1*(3), 1517–1521. <https://doi.org/10.1038/nprot.2006.258>

Oliveira, B., Çerağ Yahya, A., & Novarino, G. (2019). Modeling cell-cell interactions in the brain using cerebral organoids. *Brain Research*, *1724*(September). <https://doi.org/10.1016/j.brainres.2019.146458>

Otani, T., Marchetto, M. C., Gage, F. H., Simons, B. D., & Livesey, F. J. (2016). 2D and 3D Stem Cell Models of Primate Cortical Development Identify Species-Specific Differences in Progenitor Behavior Contributing to Brain Size. *Cell Stem Cell*, *18*(4), 467–480. <https://doi.org/10.1016/j.stem.2016.03.003>

Ozden, I., Wang, J., Lu, Y., May, T., Lee, J., Goo, W., O'Shea, D. J., Kalanithi, P., Diester, I., Diagne, M., Deisseroth, K., Shenoy, K. V., & Nurmikko, A. V. (2013). A coaxial optrode as multifunction write-read probe for optogenetic studies in non-human primates. *Journal of Neuroscience Methods*, *219*(1), 142–154. <https://doi.org/10.1016/j.jneumeth.2013.06.011>

Paşca, A. M., Sloan, S. A., Clarke, L. E., Tian, Y., Makinson, C. D., Huber, N., Kim, C. H., Park, J.-Y., O'Rourke, N. A., Nguyen, K. D., Smith, S. J., Huguenard, J. R., Geschwind, D. H., Barres, B. A., & Paşca, S. P. (2015). Functional cortical neurons and astrocytes from human pluripotent stem cells in 3D culture. *Nat Methods*, *12*(7), 671–678. <https://doi.org/10.1038/nmeth.3415>

- Peinado, a, Yuste, R., & Katz, L. C. (1993). Extensive Dye-Coupling Between Rat Neocortical Neurons During the Period of Circuit Formation. *Neuron*, *10*, 103–114. [https://doi.org/10.1016/0896-6273\(93\)90246-N](https://doi.org/10.1016/0896-6273(93)90246-N)
- Peng, H., Xie, P., Liu, L., Kuang, X., Wang, Y., Qu, L., Gong, H., Jiang, S., Li, A., Ruan, Z., Ding, L., Yao, Z., Chen, C., Chen, M., Daigle, T. L., Dalley, R., Ding, Z., Duan, Y., Feiner, A., ... Zeng, H. (2021). Morphological diversity of single neurons in molecularly defined cell types. *Nature*, *598*(7879), 174–181. <https://doi.org/10.1038/s41586-021-03941-1>
- Peng, Y., Mittermaier, F. X., Planert, H., Schneider, U. C., Alle, H., & Geiger, J. R. P. (2019). High-throughput microcircuit analysis of individual human brains through next-generation multineuron patch-clamp. *ELife*, *8*, 1–52. <https://doi.org/10.7554/eLife.48178>
- Pera, M. F. (2017). Human embryo research and the 14-day rule. *Development (Cambridge)*, *144*(11), 1923–1925. <https://doi.org/10.1242/dev.151191>
- Perin, R., & Markram, H. (2013). A Computer-assisted Multi-electrode Patch-clamp System. *Journal of Visualized Experiments*, *80*, 1–13. <https://doi.org/10.3791/50630>
- Petersen, C. C. H. (2017). Whole-Cell Recording of Neuronal Membrane Potential during Behavior. *Neuron*, *95*(6), 1266–1281. <https://doi.org/10.1016/j.neuron.2017.06.049>
- Piatkevich, K. D., Jung, E. E., Straub, C., Linghu, C., Park, D., Suk, H. J., Hochbaum, D. R., Goodwin, D., Pnevmatikakis, E., Pak, N., Kawashima, T., Yang, C. T., Rhoades, J. L., Shemesh, O., Asano, S., Yoon, Y. G., Freifeld, L., Saulnier, J. L., Riegler, C.,

- ... Boyden, E. S. (2018). A robotic multidimensional directed evolution approach applied to fluorescent voltage reporters article. *Nature Chemical Biology*, *14*(4), 352–360. <https://doi.org/10.1038/s41589-018-0004-9>
- Qian, X., Nguyen, H. N., Song, M. M., Hadiono, C., Ogden, S. C., Hammack, C., Yao, B., Hamersky, G. R., Jacob, F., Zhong, C., Yoon, K.-J., Jeang, W., Lin, L., Li, Y., Thakor, J., Berg, D. A., Zhang, C., Kang, E., Chickering, M., ... Ming, G.-L. (2016a). Brain-Region-Specific Organoids Using Mini-bioreactors for Modeling ZIKV Exposure. *Cell*, *165*(5), 1238–1254. <https://doi.org/10.1016/j.cell.2016.04.032>
- Qian, X., Su, Y., Adam, C. D., Deutschmann, A. U., Pather, S. R., Goldberg, E. M., Su, K., Li, S., Lu, L., Jacob, F., Nguyen, P. T. T., Huh, S., Hoke, A., Swinford-Jackson, S. E., Wen, Z., Gu, X., Pierce, R. C., Wu, H., Briand, L. A., ... Ming, G. li. (2020). Sliced Human Cortical Organoids for Modeling Distinct Cortical Layer Formation. *Cell Stem Cell*, *26*(5), 766-781.e9. <https://doi.org/10.1016/j.stem.2020.02.002>
- Quadrato, G., Nguyen, T., Macosko, E. Z., Sherwood, J. L., Min Yang, S., Berger, D. R., Maria, N., Scholvin, J., Goldman, M., Kinney, J. P., Boyden, E. S., Lichtman, J. W., Williams, Z. M., McCarroll, S. A., & Arlotta, P. (2017). Cell diversity and network dynamics in photosensitive human brain organoids. *Nature*, *545*(7652), 48–53. <https://doi.org/10.1038/nature22047>
- Ransohoff, R. M., & Stevens, B. (2011). How Many Cell Types Does It Take to Wire a Brain? *Science*, *333*(6048), 1391–1392. <https://doi.org/10.1126/science.1212112>
- Renier, N., Adams, E. L., Kirst, C., Wu, Z., Azevedo, R., Kohl, J., Autry, A. E., Kadiri, L.,

- Umadevi Venkataraju, K., Zhou, Y., Wang, V. X., Tang, C. Y., Olsen, O., Dulac, C., Osten, P., & Tessier-Lavigne, M. (2016). Mapping of Brain Activity by Automated Volume Analysis of Immediate Early Genes. *Cell*, *165*(7), 1789–1802. <https://doi.org/10.1016/j.cell.2016.05.007>
- Renner, H., Grabos, M., Becker, K. J., Kagermeier, T. E., Wu, J., Otto, M., Peischard, S., Zeuschner, D., TsyTsyura, Y., Disse, P., Klingauf, J., Leidel, S. A., Seebohm, G., Schöler, H. R., & Bruder, J. M. (2020). A fully automated high-throughput workflow for 3D-based chemical screening in human midbrain organoids. *ELife*, *9*, 1–39. <https://elifesciences.org/articles/52904>
- Richardson, D. S., & Lichtman, J. W. (2015). Clarifying Tissue Clearing. *Cell*, *162*(2), 246–257. <https://doi.org/10.1016/j.cell.2015.06.067>
- Sakmann, B, & Neher, E. (1984). Patch clamp techniques for studying ionic channels in excitable membranes. *Annual Review of Physiology*, *46*, 455–472. <https://doi.org/10.1146/annurev.physiol.46.1.455>
- Sakmann, Bert, & Stuart, G. J. (1994). Active propagation of somatic action potentials into neocortical pyramidal cell dendrites. *Nature*, *367*(January), 69–72.
- Sasai, Y., Eiraku, M., & Suga, H. (2012). In vitro organogenesis in three dimensions: self-organising stem cells. *Development*, *139*(22), 4111–4121. <https://doi.org/10.1242/dev.079590>
- Sasai, Yoshiki. (2013). Next-generation regenerative medicine: Organogenesis from stem cells in 3D culture. *Cell Stem Cell*, *12*(5), 520–530.

<https://doi.org/10.1016/j.stem.2013.04.009>

Sato, T., & Clevers, H. (2013). Growing Self-Organizing Mini-Guts from a Single Intestinal Stem Cell: Mechanism and Applications. *Science*, *340*(6137), 1190–1194.

<https://doi.org/10.1126/science.1234852>

Schröter, M., Paulsen, O., & Bullmore, E. T. (2017). Micro-connectomics: probing the organization of neuronal networks at the cellular scale. *Nature Reviews Neuroscience*,

18(3), 131–146. <https://doi.org/10.1038/nrn.2016.182>

Schwiening, C. J. (2012). A brief historical perspective: Hodgkin and Huxley. *Journal of Physiology*, *590*(11), 2571–2575. <https://doi.org/10.1113/jphysiol.2012.230458>

Segev, A., Garcia-Oscos, F., & Kourrich, S. (2016). Whole-cell Patch-clamp Recordings in Brain Slices. *JoVE*, *112*, e54024. <https://doi.org/doi:10.3791/54024>

Sloan, S. A., Darmanis, S., Huber, N., Khan, T. A., Birey, F., Caneda, C., Reimer, R., Quake, S. R., Barres, B. A., & Pasca, S. P. (2017). Human Astrocyte Maturation

Captured in 3D Cerebral Cortical Spheroids Derived from Pluripotent Stem Cells.

Neuron, *95*(4), 779-790.e6. <https://doi.org/10.1016/j.neuron.2017.07.035>

Sotelo, C. (2003). Viewing the brain through the master hand of Ramon y Cajal. *Nature Reviews Neuroscience*, *4*(1), 71–77. <https://doi.org/10.1038/nrn1010>

Squarzoni, P., Oller, G., Hoeffel, G., Pont-Lezica, L., Rostaing, P., Low, D., Bessis, A., Ginhoux, F., & Garel, S. (2014). Microglia Modulate Wiring of the Embryonic

Forebrain. *Cell Reports*, *8*(5), 1271–1279.

<https://doi.org/10.1016/j.celrep.2014.07.042>

Stoy, W. A., Kolb, I., Holst, G. L., Liew, Y., Pala, A., Yang, B., Boyden, E. S., Stanley, G. B., & Forest, C. R. (2017). Robotic navigation to subcortical neural tissue for intracellular electrophysiology in vivo. *Journal of Neurophysiology*, *118*(2), 1141–1150. <https://doi.org/10.1152/jn.00117.2017>

Stoy, W., Yang, B., Kight, A., Wright, N., Borden, P., Stanley, G., & Forest, C. (2020). Compensation of physiological motion enables high-yield whole-cell recording in vivo. *Journal of Neuroscience Methods*, *November 2020*, 109008. <https://doi.org/10.1101/2020.06.09.143008>

Suk, H. J., van Welie, I., Kodandaramaiah, S. B., Allen, B., Forest, C. R., & Boyden, E. S. (2017). Closed-Loop Real-Time Imaging Enables Fully Automated Cell-Targeted Patch-Clamp Neural Recording In Vivo. *Neuron*, *95*(5), 1037-1047.e11. <https://doi.org/10.1016/j.neuron.2017.08.011>

Susaki, E. A., Shimizu, C., Kuno, A., Tainaka, K., Li, X., Nishi, K., Morishima, K., Ono, H., Ode, K. L., Saeki, Y., Miyamichi, K., Isa, K., Yokoyama, C., Kitaura, H., Ikemura, M., Ushiku, T., Shimizu, Y., Saito, T., Saido, T. C., ... Ueda, H. R. (2020). Versatile whole-organ/body staining and imaging based on electrolyte-gel properties of biological tissues. *Nature Communications*, *11*(1), 1982. <https://doi.org/10.1038/s41467-020-15906-5>

Susaki, E. A., Tainaka, K., Perrin, D., Yukinaga, H., Kuno, A., & Ueda, H. R. (2015). Advanced CUBIC protocols for whole-brain and whole-body clearing and imaging.

Nature Protocols, 10(11), 1709–1727. <https://doi.org/10.1038/nprot.2015.085>

Takahashi, Kazutoshi, Tanabe, K., Ohnuki, M., Narita, M., Ichisaka, T., Tomoda, K., & Yamanaka, S. (2007). Induction of pluripotent stem cells from adult human fibroblasts by defined factors. *Cell*, 131(5), 861–872. <https://doi.org/10.1016/j.cell.2007.11.019>

Takahashi, Kazutoshi, & Yamanaka, S. (2006). Induction of pluripotent stem cells from mouse embryonic and adult fibroblast cultures by defined factors. *Cell*, 126(4), 663–676. <https://doi.org/10.1016/j.cell.2006.07.024>

Takahashi, Kei, Kubota, S. I., Ehata, S., Ueda, H. R., & Miyazono, K. (2020). Protocol for Imaging and Analysis of Mouse Tumor Models with CUBIC Tissue Clearing. *STAR Protocols*, 1(3), 100191. <https://doi.org/10.1016/j.xpro.2020.100191>

Tasic, B., Yao, Z., Graybuck, L. T., Smith, K. A., Nguyen, T. N., Bertagnolli, D., Goldy, J., Garren, E., Economo, M. N., Viswanathan, S., Penn, O., Bakken, T., Menon, V., Miller, J., Fong, O., Hirokawa, K. E., Lathia, K., Rimorin, C., Tieu, M., ... Zeng, H. (2018). Shared and distinct transcriptomic cell types across neocortical areas. *Nature*, 563(7729), 72–78. <https://doi.org/10.1038/s41586-018-0654-5>

Ting, J. T., Lee, B. R., Chong, P., Soler-Llavina, G., Cobbs, C., Koch, C., Zeng, H., & Lein, E. (2018). Preparation of Acute Brain Slices Using an Optimized N-Methyl-D-glucamine Protective Recovery Method. *Journal of Visualized Experiments : JoVE*, 132, 1–13. <https://doi.org/10.3791/53825>

Trujillo, C. A., Gao, R., Negraes, P. D., Chaim, I. A., Domissy, A., Vandenberghe, M., Devor, A., Yeo, G. W., Voytek, B., & Muotri, A. R. (2018). Nested oscillatory

dynamics in cortical organoids model early human brain network development. *BioRxiv*, 358622. <https://doi.org/10.1101/358622>

Trujillo, C. A., Gao, R., Negraes, P. D., Gu, J., Buchanan, J., Preissl, S., Wang, A., Wu, W., Haddad, G. G., Chaim, I. A., Domissy, A., Vandenberghe, M., Devor, A., Yeo, G. W., Voytek, B., & Muotri, A. R. (2019). Complex Oscillatory Waves Emerging from Cortical Organoids Model Early Human Brain Network Development. *Cell Stem Cell*, 25(4), 558-569.e7. <https://doi.org/10.1016/j.stem.2019.08.002>

Trujillo, C. A., & Muotri, A. R. (2018). Brain Organoids and the Study of Neurodevelopment. *Trends in Molecular Medicine*, 24(12), 982–990. <https://doi.org/10.1016/j.molmed.2018.09.005>

Velasco, S., Kedaigle, A. J., Simmons, S. K., Nash, A., Rocha, M., Quadrato, G., Paulsen, B., Nguyen, L., Adiconis, X., Regev, A., Levin, J. Z., & Arlotta, P. (2019a). Individual brain organoids reproducibly form cell diversity of the human cerebral cortex. In *Nature* (Vol. 570, Issue 7762, pp. 523–527). <https://doi.org/10.1038/s41586-019-1289-x>

Weiss, K. R., Voigt, F. F., Shepherd, D. P., & Huisken, J. (2021). Tutorial: practical considerations for tissue clearing and imaging. *Nature Protocols*, 16(6), 2732–2748. <https://doi.org/10.1038/s41596-021-00502-8>

Weiss, P., & Taylor, A. C. (1960). Reconstitution of Complete Organs From Single-Cell Suspensions of Chick Embryos in Advanced Stages of Differentiation. *Proceedings of the National Academy of Sciences of the United States of America*, 46(9), 1177–

1185.

<http://www.pubmedcentral.nih.gov/articlerender.fcgi?artid=223021&tool=pmcentrez&rendertype=abstract>

Wertz, A., Trenholm, S., Yonehara, K., Hillier, D., Raics, Z., Leinweber, M., Szalay, G., Ghanem, A., Keller, G., Rozsa, B., Conzelmann, K.-K., & Roska, B. (2015). Single-cell-initiated monosynaptic tracing reveals layer-specific cortical network modules. *Science*, *349*(6243), 70–74. <https://doi.org/10.1126/science.aab1687>

Wertz, D. C. (2002). Embryo and stem cell research in the United States: History and politics. *Gene Therapy*, *9*(11), 674–678. <https://doi.org/10.1038/sj.gt.3301744>

Whalley, K. (2016). Techniques: Spinning organoids shed light on Zika. *Nature Reviews Neuroscience*, *17*(6), 334–335. <https://doi.org/10.1038/nrn.2016.66>

Wilson, H. V. (1907). On some phenomena of coalescence and regeneration in sponges. *Journal of Experimental Zoology*, *5*(2), 245–258. <https://doi.org/10.1002/jez.1400050204>

Windrem, M. S., Schanz, S. J., Morrow, C., Munir, J., Chandler-Militello, D., Wang, S., & Goldman, S. A. (2014). A competitive advantage by neonatally engrafted human glial progenitors yields mice whose brains are chimeric for human glia. *Journal of Neuroscience*, *34*(48), 16153–16161. <https://doi.org/10.1523/JNEUROSCI.1510-14.2014>

Winter, J., Ilbert, M., Graf, P. C. F., Özcelik, D., & Jakob, U. (2008). Bleach Activates a Redox-Regulated Chaperone by Oxidative Protein Unfolding. *Cell*, *135*(4), 691–701.

<https://doi.org/10.1016/j.cell.2008.09.024>

Yang, L., & Ng, H. H. (2017). Lab-grown mini-brains upgraded. *Nature Cell Biology*, *19*(9), 1010–1012. <https://doi.org/10.1038/ncb3601>

Yin, X., Mead, B. E., Safaei, H., Langer, R., Karp, J. M., & Levy, O. (2016). Engineering Stem Cell Organoids. *Cell Stem Cell*, *18*(1), 25–38. <https://doi.org/10.1016/j.stem.2015.12.005>

Yuste, R. (2015). The discovery of dendritic spines by Cajal. *Frontiers in Neuroanatomy*, *9*(APR), 1–6. <https://doi.org/10.3389/fnana.2015.00018>

Zeng, H., & Sanes, J. R. (2017). Neuronal cell-type classification: challenges, opportunities and the path forward. *Nature Reviews Neuroscience*, *18*(9), 530–546. <https://doi.org/10.1038/nrn.2017.85>

Zhang, Y., & Barres, B. A. (2013). A smarter mouse with human astrocytes. *BioEssays*, *35*(10), 876–880. <https://doi.org/10.1002/bies.201300070>